40822R03

IMPROVED IRON CATALYSTS FOR SLURRY PHASE FISCHER–TROPSCH SYNTHESIS

Final Report

Period: 09/01/2000-12/31/2003

Submitted by

Dr. Dragomir B. Bukur (Professor, PI)

Contributors:

Victor Carreto–Vazquez (Graduate Student)
Dr. Wen–Ping Ma (Postdoctoral fellow)
Department of Chemical Engineering
Texas A&M University
College Station, TX 77843-3122

January 29, 2004

Grant No. DE-FG26-00NT40822
Period: 09/01/2000-08/31/2003

to

Texas A&M University
318 Administrative Building
College Station, TX 77843-3121

Prepared for

The U.S. Department of Energy
University Coal Research Program
National Energy Technology Laboratory
Project Officer: Donald Krastman

Disclaimer

Abstract

This report describes research conducted to support the DOE program in development of improved (attrition resistant) catalysts for converting coal-derived synthesis gas to liquid fuels via slurry phase Fischer–Tropsch (F–T) synthesis. The primary objective of this research program is to develop highly active and selective attrition resistant iron F–T catalysts by spray drying.

Attrition strength of various types of iron F–T catalysts was studied under reaction conditions in a stirred tank slurry reactor (STSR). The attrition behavior was evaluated on the basis of observed changes in morphological properties (via SEM), and changes in particle size distribution after F–T synthesis in the STSR.

Three spray-dried catalysts (100 Fe/3 Cu/5 K/16 SiO_2 in parts by weight) prepared from wet precursors at Texas A&M University had excellent sphericity and smooth external surfaces. Their particle size distribution was rather broad ranging from 5 μm to 40 μm in diameter, regardless of the source of silica (colloidal silica, TEOS, or potassium silicate) employed in their preparation. The catalyst prepared from colloidal silica had the highest attrition strength among all catalysts studied during the course of this project. After 345 h of testing in the STSR its morphology remained practically unchanged, and it experienced small reductions in the volume mean diameter (5.4 %) and generation of particles smaller than 10 μm in diameter was very small (0.7 %). Catalytic performance of these catalysts was excellent. Syngas conversion was between 71 and 76 %, whereas methane selectivity was between 2.2 and 3.5 % and that of C_5^+ hydrocarbons was 78 % to 86 % (all selectivities are on C–atom basis).

Spray-dried catalysts, synthesized at Hampton University, with compositions 100 Fe/5 Cu/4.2 K/11 SiO_2 and 100 Fe/5 Cu/4.2 K/1.1 SiO_2 had excellent selectivity characteristics (methane selectivity of 2 %, and C_5^+ selectivity of about 85 %) but their activity and stability (deactivation rate) need to be improved. Spray-dried HU1112 catalyst (100 Fe/3 Cu/4 K/16 SiO_2 produced more methane (3.5 %) and less C_5^+ hydrocarbons (77 %) than the other two spray-dried catalysts. The attrition strength of catalysts containing 1.1 and 16 parts of silica per 100 parts of iron was found to be adequate for use in a slurry bubble column reactor (SBCR).

The primary objective of this project of synthesizing spray-dried iron F–T catalysts with adequate attrition strength and desirable F–T activity and selectivity for use in a SBCR for converting coal-derived synthesis into liquid fuels, has been achieved.

TABLE OF CONTENTS Page

Introduction

Fischer–Tropsch (F–T) synthesis in a slurry bubble column reactor (SBCR) is considered to be an attractive route for converting coal- or natural gas-derived synthesis gas into transportation fuels and valuable chemicals. The main advantages of the slurry-phase operation relative to fixed-bed reactors include the following: lower capital and operating costs, better temperature control, and capability of on-line catalyst addition and removal [1–3].

Iron (Fe) is the preferred catalyst for F–T synthesis with coal-derived synthesis gas, due to its high water-gas-shift activity. However, attrition of Fe F–T catalysts has been identified as a major problem in commercial implementation of SBCRs [2–4]. Researchers from Sasol in South Africa [2,3] stated that precipitated Fe F–T catalyst, used in fixed bed reactors at Sasol, was structurally too weak for use in the SBCR. Attrition resistant catalysts for use in the SBCR were prepared by precipitation followed by spray drying to produce micro-spherical particles. Operational difficulties, caused by catalyst breakup, were encountered during F–T demonstration run in a SBCR at LaPorte Texas [4]. Filtering system was plugged after one day of operation, and the external catalyst/wax separation in a settling tank was inefficient, resulting in gradual loss of catalyst from the reactor. The catalyst used in this run was a precipitated Fe prepared by spray drying at United Catalysts Inc (UCI).

These findings have led to studies directed at developing suitable techniques for evaluation of attrition resistance and at understanding and improving the attrition resistance of catalysts for slurry phase F–T synthesis [5–16]. In several of these studies it was found that precipitated Fe catalysts (both irregularly shaped and spherical particles) are not attrition resistant [5–8,10,11], whereas some researchers [10,12,13,15] were successful in preparing Fe F–T catalysts with adequate attrition strength using spray drying method to produce nearly spherical particles. Attrition and agglomerate strength are complex phenomena that are not well understood. Several factors (e.g. silica type and concentration, and morphology of primary particles formed during catalyst synthesis) have been identified as important in determining the attrition resistance of Fe F–T catalysts [10,12,13]. Pietsch [17] has provided a more general overview of various binding mechanisms that may play a role in agglomerate strength.

Most of attrition studies were conducted with catalysts in either oxide or pre-reduced form, as well as under hydrodynamic conditions that were not representative of those encountered in a SBCR or in a stirred tank slurry reactor (STSR). Attrition tests under these conditions provide information on relative physical attrition resistance (strength) of different materials. However, it is known [5,6] that Fe catalysts also undergo "chemical" attrition under reaction conditions due to volume changes and/or carbon formation that accompany phase transformation of oxide precursor into reduced Fe species. There have been only a few studies of attrition properties in a SBCR and/or STSR under F–T reaction conditions. Zhao et al. [9] and Wei et al. [14] studied attrition properties of supported cobalt-based F–T catalysts in a SBCR, whereas O'Brien et al. [11] conducted a similar study with supported Fe catalysts in a STSR.

In recent years, several precipitated Fe F–T catalysts ($Fe/Cu/K/SiO_2$) synthesized and tested at Texas A&M University (TAMU) in a STSR, have demonstrated high activity, excellent stability

with time, and high selectivity to liquid and wax hydrocarbons [18–20]. Even though the catalytic performance of these catalysts was excellent, there is a concern that they may be structurally too weak for use in SBCRs. The objectives of the present study are to study attrition properties of precipitated Fe F–T catalysts prepared by both conventional procedures and spray-drying, and to synthesize attrition resistant catalysts of high activity and selectivity towards high molecular weight hydrocarbons (high-alpha catalysts) that would be suitable for use in SBCRs.

In order to achieve these objectives the project has been divided into the following tasks:

Task 1. Literature Review and Equipment Testing
Task 2. Catalyst Synthesis and Spray Drying
Task 3. Attrition Resistance Tests
Task 4. Catalyst Testing and Data Analysis

A brief description of each task and its original goals is as follows.

In task 1, research personnel will become familiar with the existing equipment for catalyst synthesis, operation of fixed-bed and slurry reactors, and gas chromatographs for product analysis. Shakedown runs with reactors will be conducted, and standard mixtures representative of F-T products (aqueous phase, organic phase and wax) will also be analyzed.

In task 2, synthesis and spray drying of precipitated Fe catalysts will be performed at TAMU and Hampton University (HU). Spray-dried catalysts will be characterized by scanning electron microscopy.

In task 3, attrition tests will be performed in a stirred tank slurry reactor (STSR). Particle size distributions will be measured by a Coulter® counter particle size analyzer or by Malvern 2600 particle analyzer after separation of hydrocarbon wax (or initial slurry medium) from the catalyst. Scanning electron microscope (SEM) will be used to study particle morphology and the mechanism of attrition (erosion vs. fracture).

In task 4, selected synthesized catalysts will be tested in a STSR (up to 21 days on stream). Slurry samples from the STSR runs will be periodically withdrawn from the reactor for particle size distribution measurements. Several catalysts synthesized at Hampton University will be tested in our laboratory.

Executive Summary

This report covers a three-year period of research grant under the University Coal Research program. The primary objectives of the present study have been to study attrition properties of precipitated iron Fischer–Tropsch (F–T) catalysts prepared by both conventional procedures and spray drying, and to synthesize attrition resistant catalysts of high activity and selectivity towards high molecular weight hydrocarbons (high-alpha catalysts) that would be suitable for use in slurry bubble column reactors.

Attrition behavior of catalysts tested in this work was evaluated on the basis of observed changes in morphological properties (via SEM), and changes in particle size distribution after testing in a stirred tank slurry reactor (STSR). In the latter case, particle size distribution (PSD) measurements were performed using the Coulter® Counter Multisizer. From PSD results, one can obtain several parameters that can be used to quantify attrition. These are: changes in Sauter mean diameter ($d_{3,2}$) and volume moment diameter ($d_{4,3}$), and change in fraction of fine particles (particles less than 10 μm in diameter) after testing in the STSR. Sauter mean diameter and the volume moment diameter are weighted toward large particles, since they occupy most of the catalyst volume. Generation of fines is important to assess the attrition behavior of iron F–T catalysts, because difficulties with catalyst/wax separation and product contamination are caused by fine particles.

The catalysts used in this study can be classified in the following four groups: (1) precipitated (not spray-dried) catalysts; (2) spray-dried catalysts prepared from vacuum dried precursors; (3) spray-dried catalysts prepared from wet precursors at Texas A&M University (TAMU); and (4) spray-dried catalysts synthesized at Hampton University (HU). First we'll summarize our findings on the attrition strength of these four groups of catalysts, followed by remarks on their catalytic performance.

The attrition properties of precipitated catalysts with nominal compositions 100 Fe/3 Cu/5 K/16 SiO_2 (catalysts PPS3516–1 and PPS3516–2) and 100 Fe/5 Cu/4.2 K/25 SiO_2 (commercial Ruhrchemie catalyst) were evaluated in STSR tests SB–19102, SB–04803 and SB–32901. In all three tests the particle size reduction due to fracture was moderate, whereas attrition by erosion was small. All three precipitated Fe F–T catalysts have had relatively high attrition strength, under reaction conditions in the STSR reactor after 364–497 h of testing. The observed reductions in the volume moment diameter were 14.3–18.6 %, whereas the increase in fraction of particles smaller than 10 μm was between 2.6 and 7.8 %. It is obvious that precipitated silica, which was used as a binder, provides strong interlocking forces between the primary particles. The observed increase in fraction of fine particles is similar to that observed in tests with spray dried catalysts (HU1112 and HU3471) synthesized at Hampton University (Table 2).

Spray-dried catalyst particles, prepared from vacuum dried Fe/Cu/K/SiO_2 precursors, were largely of irregular shape (SEM micrographs) except for small particles, which were nearly spherical (Figure 4). Particle morphology and attrition strength of spray-dried DPS5624–2 catalyst (100 Fe/5 Cu/6 K/24 SiO_2) tested in run SB–16502 were similar to those of precipitated (not spray-dried). After 295 h of testing, the observed reduction in the volume moment was 16.1

%, whereas the increase in fraction of fine particles was 2.3 % (Table 2). Thus, pray drying of dry precursors did not impart any additional strength, at least not under conditions employed in the present study.

Spray-dried catalysts prepared from wet precursors at TAMU had excellent sphericity and smooth external surfaces (Figures 5 and 6). The particle size distribution was rather broad ranging from 5 μm to 40 μm in diameter, regardless of the source of silica used. The observed morphology of spray-dried catalysts (APV Anhydro Lab S1 unit; 1 m diameter, 2.4 m high) is ideally suited for use in slurry reactors, but the particles were smaller than intended (30–70 μm) due to limitations of small-scale equipment used for spray drying. Catalysts WCS3516–1, WTO3516–1 and WPS3516–4 were spray-dried from wet slurries having the same composition (100 Fe/3 Cu/16 SiO_2) but were prepared from different silica sources. Colloidal silica, TEOS and potassium silicate, respectively, were used as sources of silica in preparation of these three catalysts. All three catalysts were impregnated with potassium by incipient wetness impregnation after spray drying, and were tested in STSR runs SB–30702, SB–33802 and SB–09703 (300–364 h on stream).

WCS3516–1 catalysts (prepared from colloidal silica) had the highest attrition strength among all catalysts studied during the course of this project. After 345 h of testing in the STSR the catalyst morphology remained practically unchanged (Fig. 20) and PSD measurements showed small reductions in the volume mean diameter (5.4 %) and very small increase in the fraction of fine particles (0.7 %). After testing in the STSR WTO3516–1 and WPS3516–4 catalysts lost their sphericity due to attrition and agglomeration effects (Figures 23 and 26). The presence of large irregularly shaped particles has been attributed to micro-spherical particle breakup and encapsulation by residual wax. The attempts to remove the wax through multiple washings with hot Varsol 18, CS_2, n-hexane followed by Soxhlet extraction (with xylenes for 48 h, followed by 48 h of extraction with MEK) were only partially successful. In spite of the absence of reliable results from PSD measurements with WTO3516–1 and WPS3516–4 catalysts, it is clear that the spray dried WCS3516–1 was more attrition resistant than the other two spray-dried catalysts.

Three spray-dried catalysts prepared at HU were tested in the STSR for 380–450 hours. Catalysts HU2061 and HU1112 contain 11 and 16 parts of precipitated silica (from TEOS), respectively, whereas catalyst HU3471 contains 1.1 parts of silica binder per 100 parts of Fe. Mechanical integrity of catalysts HU2061, HU1112 and HU3471 was markedly dependent upon their morphological features. The attrition strength of catalysts made out of largely spherical particles (HU1112 and HU3471) was considerably higher than that of the HU2061 catalyst consisting of irregularly shaped particles (i.e. plate-like particles). The latter catalyst experienced large changes in Sauter mean and volume moment diameters (85 and 65.7 %, respectively) after 380 h of testing in the STSR. The inferior attrition strength of this catalyst is also reflected in considerable generation of fine particles (less than10 μm in diameter) during the STSR test (62.5 %). Both HU1112 and HU3471 catalysts lost their sphericity after ~450 hours in the STSR (Figures 8b and 9b). However, the generation of fine particles was relatively small (6.7 and 3.7 %). HU1112 and HU3471 had similar reductions in their Sauter mean diameters (32.7 and 40.1 %, respectively) after testing in the STSR. On the other hand, the change in volume moment diameter for these two catalysts showed an unexpected behavior. The volume moment diameter of HU1112 catalyst decreased by 5.7 % only (Table 2), whereas that of

HU3471 catalyst increased by 2.2 % (listed as -2.2 % in Table 2). This has been attributed to agglomeration of particles in the presence of residual wax, which was not completely removed during washing with hot Varsol 18 solvent.

In order to assess catalytic performance of the catalysts tested in this study, we have used TAMU's precipitated catalysts of similar compositions as benchmarks. TAMU's precipitated catalyst PPS3416–4 (100 Fe/3 Cu/4 K/16 SiO_2) was found to have the highest intrinsic activity and catalyst productivity, among high alpha iron F–T catalysts, as well as excellent selectivity (low methane and high yield of C_5^+ hydrocarbons) as reported earlier [19,20,31].

Catalytic performance of precipitated (not spray-dried) TAMU's catalyst PPS3516–2 at baseline process conditions (260 °C, 1.5 MPa, 4 Nl/g-Fe/h and H_2/CO = 2/3) was excellent (syngas conversion of 81 %, methane selectivity of 2.7 %, and C_5^+ selectivity of 82 %). This is quite similar to the performance of PPS3416–4 catalyst (Figs. 35 and 36). Catalytic performance of the other precipitated catalysts (PPS3516–1, Ruhrchemie catalyst) and spray-dried catalysts prepared from dry precursors (DPS3616 and DPS5624–2) was very good, but their productivity was lower and their selectivity less favorable (more light hydrocarbon products) in comparison to that of the PPS3416–4 catalyst.

Spray-dried catalysts, synthesized at Hampton University, with compositions 100 Fe/5 Cu/4.2 K/11 (P) SiO_2 and 100 Fe/5 Cu/4.2 K/1.1 (B) SiO_2 had excellent selectivity characteristics (methane selectivity of 2 %, and C_5^+ selectivity of about 85 %) but their activity and stability (deactivation rate) need to be improved significantly. Spray-dried HU1112 catalyst (100 Fe/3 Cu/4 K/16 (P) SiO_2) produced more methane (3.5 %) and less C_5^+ hydrocarbons (77 %) than the other two spray-dried catalysts and the TAMU's precipitated catalyst of the same composition. Its productivity and stability were better than those of the other two spray-dried catalysts synthesized at HU, but inferior in comparison to the PPS3416–4 catalyst (Table 4 and Figure 31).

Catalytic performance of catalysts WCS3516–1, WTO3516–1 and WPS3516–4, prepared by spray drying from wet slurries of the same composition (100 Fe/3 Cu/4 K/16 SiO_2), at the baseline process conditions was excellent (Figs. 41 and 42). Syngas conversion was between 71 and 76 %, whereas methane selectivity was between 2.2 and 3.5 % and that of C_5^+ hydrocarbons was between 78 and 86 % (all selectivities are on C–atom basis). Catalyst productivities were 5–12 % lower than that of precipitated (not spray-dried) PPS3516–2 catalyst of the same composition, whereas hydrocarbon selectivities were similar. Spray-dried WCS3516–1 catalyst (run SB–30702) had the most superior strength but it produced more light hydrocarbons than the other two spray-dried catalysts.

The main project objectives have been accomplished. We were successful in synthesizing both precipitated and spray-dried iron F–T catalysts with adequate attrition strength and desirable F–T activity and selectivity for use in SBCR for converting coal-derived synthesis into liquid fuels.

Experimental

Catalyst Synthesis Procedure – TAMU

(a) Precipitated Iron Catalysts

Synthesis of a precipitated iron F–T catalyst (100 Fe/x Cu/y K/z SiO_2 in parts by weight) was described in detail in our publications [21,22]. Catalyst preparation consists of three distinct steps: preparation of the iron-copper precursor, incorporation of silica binder (Fe/Cu/SiO_2 precursor), and impregnation by potassium.

An aqueous solution containing Fe $(NO_3)_3$ (~ 0.6 M) and Cu $(NO_3)_2$ corresponding to the desired Fe/Cu ratio in the final catalyst, and a second solution containing aqueous NH_3 (~2.7 M) are maintained in stirred vessels at 84 ± 2°C. The two solutions are separately conveyed by fluid pumps to a stirred tubular reaction vessel that is maintained at 82 ± 2°C. Precipitation (to form FeOOH and Cu $(OH)_2$) occurs continuously as the two solutions are pumped upward through the vessel, while an in-line pH electrode is used to monitor the pH of the reactor effluent, which is maintained at 6.0 ± 0.2. Collection of the slurried precipitate is made in ice-cooled vessels and is continued until one of the two solutions is consumed. The precipitate is then thoroughly washed by vacuum filtration to remove excess NH_3 and NO_3^-. The washed precipitate is then used for the preparation of final catalysts.

The wet Fe/Cu precipitate is mixed with deionized and distilled water to make uniform slurry. Dilute potassium silicate solution containing a desired amount of silica (SiO_2) is added to the slurry very slowly. During potassium silicate addition the pH is maintained at about 9.0. Once the addition of potassium silicate is over and the pH stabilized, a 10% dilute nitric acid is added drop by drop until the pH reaches ~ 6.0 – 6.5 with constant stirring. Stirring is continued for additional four hours after the addition of nitric acid. Immediately after completing the stirring procedure the resulting silica containing slurry is filtered, washed (to remove the K^+ ions) and vacuum oven dried at 50°C for 48 h and then at 120°C for 24 h.

After a vacuum drying step, the potassium promoter is added as aqueous $KHCO_3$ solution via an incipient wetness impregnation (IWI) pore filling technique. The final step is to dry catalyst at 120°C for 16 hours in a vacuum oven.

(b) Spray-dried Catalysts

Synthesis of spray-dried catalysts was done in several different ways. One approach that was employed was to start with a precipitated iron catalyst in its final form (vacuum dried Fe/Cu/K/SiO_2 catalyst). The catalyst was first sieved and the fraction, which passed through a 325-mesh sieve (particles less than 45 μm in diameter), was collected and placed in a cylindrical can (0.15 m in diameter and 0.20 m in height) filled with 30 metal balls (~6 mm in diameter). The can was placed in a tumbler for 5 h to reduce the catalyst particle size, due to friction and collision with walls and spherical balls. The resulting powder was mixed with water to form slurry, which was sonicated for 60 minutes in an ultrasonic bath to break up any agglomerates, and then spray-dried as described below.

A slight modification of this procedure was used to prepare a catalyst containing both precipitated SiO_2 (from K_2SiO_3) and a binder SiO_2. A silica binder (Bindzil 30/360 from Akzo Nobel) was added to slurry of precipitated catalyst 100 Fe/3 Cu/4 K/16 SiO_2 (prepared as described above). The slurry was sonicated for 60 minutes in an ultrasonic bath to break up any agglomerates. The resulting slurry was then spray-dried in a spray dryer. The additional amount of silica added (in the form of binder) was 3 wt% of total catalyst weight, and the total silica content in the final catalyst was about 12.5 wt% (9.5 wt% precipitated SiO_2 from K_2SiO_3 and 3 wt% of binder SiO_2).

The other procedures employed utilize a wet catalyst precursor (Fe/Cu or Fe/Cu/SiO_2) prepared as described in section (a). For example if one uses K_2SiO_3 as a source of precipitated SiO_2, one would start with the wet Fe/Cu/SiO_2 precursor (after washing to remove excess K^+ and NO_3^- ions). This precursor is reslurried using deionized water and the desired amount of K promoter is added (drop wise) using an aqueous solution of potassium bicarbonate ($KHCO_3$). After sonication in the ultrasonic bath, the resulting slurry is spray-dried in a spray dryer. Alternatively, K promoter may be added after spray drying step, utilizing incipient wetness impregnation, followed by vacuum drying. Catalysts containing both precipitated and binder SiO_2 can be prepared using this procedure. Binder silica may be added before or after K addition to washed Fe/Cu/SiO_2 precursor.

Also, colloidal silica can be used as a source of SiO_2 (instead of K_2SiO_3). In this case one starts with a Fe/Cu precursor prepared according to the procedure described above (section (a)). The washed co-precipitate is reslurried and desired amount of SiO_2 is added using a commercial colloidal silica suspension. In one preparation 100 Fe/3 Cu/16 SiO_2 was divided in two fractions (B_1 and B_2). Potassium promoter was added drop wise to the fraction B_1 (in wet form) from an aqueous solution of $KHCO_3$. Both fractions, B_1 and B_2, were sonicated for 60 minutes in an ultrasonic bath before spray drying step. Subsequently, fractions B_1 and B_2 were spray-dried. Finally, after the spray-drying step, fraction B_2 was impregnated with potassium by incipient wetness impregnation method, and then dried in a vacuum oven (overnight) at 110 ºC.

Spray Drying Procedure - TAMU

Spray drying was conducted in two large spray dryer units manufactured by APV and located in Food and Protein Research Center at Texas A&M University. Most experiments were conducted in a smaller unit (APV Anhydro Lab S1), 1 m in diameter and 2.4 m in height. A limited number of experiments were made in a larger unit (APV Anhydro), 2.1 m in diameter and 2.4 m in height. In both units the centrifugal atomization system consists of a feed pump (Cole Parmer Instruments – Masterflex) and a spinning disk system mounted at the top of the spray dryer. The inlet air temperature (210–300°C) is controlled electrically. The atomized droplets evaporate during their fall through a conically shaped chamber, and dried particles carried in air stream pass through a cyclone. Larger particles are collected in a cyclone, whereas the small ones are either vented into atmosphere, or collected in a bag filter downstream from the spray dryer. A typical run is initiated by feeding water at a desired flow rate, adjusting power input to electric heaters to achieve a desired inlet air temperature, and adjusting the wheel (disk) speed by controlling applied voltage to an electrical motor. After the desired conditions are established, the system is allowed to run for about 10–15 minutes before switching to slurry feed. Slurry of a

material to be spray-dried was kept suspended with a stirrer throughout the entire test. The slurry is fed to a spinning disk using a pump with a maximum capacity of 6.5 kg/h (small unit) or 29 kg/h (large unit). The run is terminated, when the slurry is consumed (in our case 8–30 minutes) and particles collected at the bottom of the cyclone are removed.

Catalyst Synthesis – Hampton University

We received three spray-dried iron F–T catalysts from Professor Adeyinka Adeyiga of Hampton University, with nominal compositions 100 Fe/5 Cu/4.2 K/ z SiO_2 (z= 1.1 and 11) and 100 Fe/3 Cu/4 K/16 SiO_2. Two of these catalysts were prepared from precipitated silica (z = 11 and 16) and one from binder silica (z = 1.1). Details of preparation procedure were not provided to us. However, descriptions of synthesis of catalysts of similar compositions were provided in the literature [23,24] and are reproduced here.

Catalyst preparation involved four steps: preparation of the iron, copper, and silica (if added) precursor; incorporation of potassium; addition of binder silica (if added) and finally spray drying. The constant pH precipitation technique was used to prepare Fe/Cu/Si precursor. The catalyst precursor was continuously precipitated from a flowing aqueous solution containing iron nitrate, copper nitrate, and tetraethyl orthosilicate – TEOS (when added) at the desired Fe/Cu/Si ratio using aqueous NH_3. The precipitate was then thoroughly washed with distilled water by vacuum filtration. The potassium promoter was added as aqueous $KHCO_3$ solution to undried, reslurried Fe/Cu/Si co-precipitate. This is referred as a precipitated silica catalyst.

Catalysts containing binder silica were prepared in the same way as above (with the omission of tetraethyl orthosilicate during the co-precipitation step). The binder silica preparation and addition method is proprietary.

Spray drying and calcination methods for both precipitated and binder silica catalysts is the same. Precursor slurry (Fe/Cu/Si/K) was spray-dried at 250°C using a large bench-scale Niro spray drier (0.9 m in diameter and 1.8 m in height). Finally, the spray-dried catalyst was calcined at 300°C for 5 h in a muffle furnace.

Particle Size Distribution (PSD) Measurements

Particle size distributions measurements were made employing two different techniques. Initially we used instrument manufactured by Malvern Company (Malvern 2600) located in Mechanical Engineering Department at TAMU, which is based on Fraunhoffer's diffraction principle. This method is based on optical principles. It is fast and does not need calibration. It is suitable for particles larger than 1–2 μm, and can be used for solid particles as well as for liquid droplets. The measurement is not intrusive, and there is no probe to disturb the flow and to introduce sampling errors.
Most measurements were made in Civil Engineering Department at TAMU, using a Coulter Counter Multisizer I analyzer. This instrument employs the Coulter electrical impedance method to provide a particle size distribution analysis within the overall range 0.4 μm to 1200 μm. Each result is displayed graphically as a percentage of channel content, which can be selected to represent volume (weight), number (population) or surface area, in either differential or

cumulative form. The Coulter Multisizer employs changes in electrical impedance as particles are swept through a small cylindrical aperture (electro zone sensing) of known diameter and length to determine the particle size distribution. The measurable particle size range is from about 0.4 μm to 1200 μm depending on the aperture tube selected. For our samples, we used aperture tubes of 280 μm and 50 μm, which cover the particle size range of 1–168 μm.

Raw sample was prepared using 20 ml of distilled/deionized water, and ~0.014 g of the sample powder to be analyzed in a glass vial (diameter: 20 mm, height: 80 mm). To this dilute suspension 2–3 droplets of Nonionic Dispersant, type IB, was added, and the vial was shaken gently until complete homogenization was achieved. Finally, 4 ml of this raw sample was diluted in a sample jar containing Isoton solution to 250 ml, and this solution was used for PSD measurements.

Scanning Electron Microscopy (SEM) Measurements

Particle morphology information (shape, smoothness) was obtained for each sample by using a JEOL JSM-6400 Scanning Electron Microscope at an acceleration voltage of 15 kV and a working distance of 39 mm. The specimens were observed at different magnifications to get topographic details of the surface of the catalysts.

In order to prepare the catalyst sample, a double-stick adhesive carbon tape, previously mounted on SEM specimen stubs, was used. Then the catalyst particles were transferred to the carbon tape by a spatula. The excess particles (loose particles) were removed by applying a gentle air stream to minimize charging effects. SEM specimen was coated with an Au/Pd layer using a Hummer Sputter Coater at 10 mA for 8 minutes (in a vacuum/He environment). This coating was performed to provide an ample supply of conductive surface for the SEM analysis.

Slurry Reactor Tests

All tests were conducted in a 1 dm^3 stirred tank slurry reactor (Autoclave Engineers). The feed gas flow rate was adjusted with a mass flow controller and passed through a series of oxygen removal, alumina and activated charcoal traps to remove trace impurities. After leaving the reactor, the exit gas passed through a series of high and low (ambient) pressure traps to condense liquid products. High molecular weight hydrocarbons (wax), withdrawn from a slurry reactor through a porous cylindrical sintered metal filter, and liquid products, collected in the high and low pressure traps, were analyzed by capillary gas chromatography. The reactants and noncondensible products leaving the ice traps were analyzed on an on-line GC (Carle AGC 400) with multiple columns using both flame ionization and thermal conductivity detectors. Further details on the experimental set up, operating procedures and product quantification can be found elsewhere [18,25,26].

Catalyst/Wax Separation

Catalyst suspended in hydrocarbon wax (or initial startup fluid) was withdrawn from the reactor through a dipleg connected to a sampling cylinder. All tubing and the sampling cylinder were purged with nitrogen prior to slurry withdrawals. Then the sampling cylinder was heated and

slurry collected in a glass beaker. The sampling cylinder was rinsed with a commercial solvent (a mineral spirit-Varsol) to remove residual slurry from the sampling cylinder. Collected slurry was diluted with heated Varsol (~100°C) and filtered (under vacuum) through a glass frit covered with a paper filter (pore size of 2.5 μm). Hot Varsol was used to rinse the catalyst coated with wax, and this procedure was repeated several times. Catalyst collected on the paper filter, and the filter paper, were transferred into a beaker filled with ~ 100 ml of hot Varsol. The filter paper free of any solid residue was removed from the beaker, followed by evaporation of Varsol and recovery of wax-free catalyst. This material was used for PSD and SEM measurements.

Results and Discussion

Catalyst Synthesis and Characterization

Catalysts synthesized at TAMU and at Hampton University are listed in Table 1, together with information on preparation procedure employed. Catalysts 1–3 were synthesized and spray-dried at Hampton University. Identification label for catalysts prepared at Hampton University consists of capital letters HU (for Hampton University) and a 4–digit number that is related to slurry reactor test designation. Identification label for catalysts prepared at TAMU consists of 3 capital letters, which indicate the preparation procedure employed, and a 4-digit number that shows catalyst composition. The specific meanings for these letters and numerals are as follows. First capital letter (P, D or W) designates type of preparation: P = precipitated catalyst (not spray-dried); D = spray-dried catalyst from a dry precursor; W = spray-dried catalyst from a wet precursor. The second and third capital letters designate the main source of silica used in preparation: PS = potassium silicate; CS = colloidal silica; TO = Tetraethyl orthosilicate (TEOS). The 4-digit number shows the catalyst composition in parts by weight (pbw) relative to 100 pbw of Fe, and batch number (if applicable). The first digit stands for Cu, the second one for K, and the third and fourth for SiO_2. For catalysts of the same composition prepared by the same method more than once, the batch number is given as the fifth digit after a hyphen. For example, designation WCS3516–1 means that the catalyst of composition 100 Fe/3 Cu/5 K/16 SiO_2 (batch 1) was prepared by spray drying from wet precursor using colloidal silica.

Precipitated catalyst precursors for catalysts 4 and 5 were synthesized previously at TAMU during DOE Contract DE–AC22–94PC93069 [27]. These two catalysts (100 Fe/5 Cu/6 K/24 SiO_2 – batch 5, and 100 Fe/3 Cu/6 K/16 SiO_2 – batch 3) were sieved and particles that passed through 325-mesh sieve (less than 45 μm in diameter) were collected. These particles were reduced in size by placing them in a rotating tumbler filled with metal balls (~6 mm in diameter) for 5 h, and then mixed with water. The resulting slurries were spray-dried at TAMU. Catalyst containing 24 parts of SiO_2 (DPS5624–2) was spray-dried at 250 °C in a large APV Anhydro Spray Dryer (2.1 m in diameter and 2.4 m in height). Catalyst containing 16 SiO_2 (DPS3616) was mixed with a silica binder (Bindzil 30/360) prior to spray drying in APV Anhydro Spray Dryer S1 (1 m in diameter, 2.4 m in height) at 210 °C. The additional amount of silica added through the binder was 3wt% of the total mass of the catalyst. Catalysts 6–9 were prepared from the same wet precursor (Fe/Cu/K/SiO_2). A portion of this precursor was spray-dried after

addition of small amount of silica binder (Bindzil 30/360) under different conditions (6–8), whereas the remainder was vacuum dried (Catalyst No. 9).

Table 1. Catalyst compositions and preparation methods employed.

No.	Catalyst ID	Catalyst composition 100 Fe/x Cu/y K/z SiO_2	Silica source	Potassium Addition	Spray dryed
1	HU2061	5/4.2/11	TEOS	Wet slurry	Yes
2	HU1112	3/4/16	TEOS	Wet slurry	Yes
3	HU3471	5/4.2/1.1	Binder	Wet slurry	Yes
4	DPS5624–2	5/6/24	K_2SiO_3	IWI (BSD)	Yes
5	DPS3616	3/6/16 + 3 wt% SiO_2 (Bindzil 30/360)	K_2SiO_3 + Bindzil	IWI (BSD)	Yes
6	WPS3516–1	3/5/16 + 3 wt% SiO_2 (Bindzil 30/360)	K_2SiO_3 + Bindzil	Drop-wise (wet slurry)	Yes
7	WPS3516–2	3/5/16 + 3 wt% SiO_2 (Bindzil 30/360)	K_2SiO_3 + Bindzil	Drop-wise (wet slurry)	Yes
8	WPS3516–3	3/5/16 + 3 wt% SiO_2 (Bindzil 30/360)	K_2SiO_3 + Bindzil	Drop-wise (wet slurry)	Yes
9	PPS3516–1	3/5/16	K_2SiO_3	Drop-wise (wet slurry)	No
10	PPS3516–2	3/5/16	K_2SiO_3	IWI	No
11	WPS3516–4	3/5/16	K_2SiO_3	IWI (ASD)	Yes
12	WCS3516–1	3/5/16	CS	IWI (ASD)	Yes
13	WCS3516–2	3/5/16	CS	Drop-wise (wet slurry)	Yes
14	WTO3516–1	3/5/16	TEOS	IWI (ASD)	Yes
15	WTO3516–2	3/5/16	TEOS	Drop-wise (wet slurry)	Yes

Abbreviations: TEOS = Tetraethyl orthosilicate; IWI = Incipient Wetness Impregnation; BSD = before spray drying; Bindzil (silica binder from Akzo Nobel); ASD = after spray drying; CS = colloidal silica.

Catalyst No. 10 (PPS3516–2) was prepared by our usual procedure for precipitated iron catalysts [21,22]. Catalyst No. 11 (WPS3516–4) was prepared from the same wet Fe/Cu/SiO_2 precursor as the catalyst No. 10, and then this precursor was spray-dried. Potassium was added after spray drying by IWI method. Catalysts 12 and 13 (WCS3516–1 and WCS3516–2) were prepared from the same wet Fe/Cu/SiO_2 precursor (using colloidal silica), but potassium was added either before spray drying (wet slurry) or after spray drying by IWI (catalyst No. 12). Similarly, catalysts 14 and 15 were prepared in the same way (same precursor, but different method of K addition), using TEOS as a silica source.

SEM Images of Spray-dried Catalysts and Model Powder Systems

Several spray-drying experiments were made using two model powder systems. Iron oxide (Fe_2O_3) powder from Bayer (Bayferrox 105 M) with average particle size of 0.25 μm in diameter was mixed with water to form slurries containing 20–40 wt% of solid, and then spray-dried in small spray drier unit (APV Anhydro Lab S1) at 220–300°C. In another set of experiments the Bayferrox iron oxide was mixed with commercial silica binder obtained from Akzo Nobel (Bindzil 30/360) and water to form slurries, and then spray-dried in the APV Anhydro Lab S1 spray drier under the same conditions used with pure Bayferrox iron oxide. The amount of Bindzil added was chosen to give 11 wt% of silica, based on the total weight of solid. This is similar to the amount of silica in TAMU's iron F–T catalysts (9–14 wt% of SiO_2 based on total weight of the catalyst in oxide form). The objectives of experiments with model systems were to gain experience with operation of the APV Anhydro spray dryer and investigate the effect of slurry concentration and/or inlet temperature on size and morphology of spray-dried particles.

Representative SEM micrographs are shown in Fig. 1. Pure iron oxide (Bayferrox) did not agglomerate well, regardless of chosen operating conditions. The resulting powder consisted of small irregularly shaped agglomerates (Fig. 1a). Addition of silica binder resulted in formation of largely spherical agglomerates with smooth external surface (Fig. 1b). Particle size and morphology were not markedly dependent on operating conditions.

SEM micrographs of as received (no sieving or calcination) spray-dried catalysts prepared at Hampton University are shown in Figures 2 and 3. Particle size distribution of spray-dried 100 Fe/5 Cu/4.2 K/11 (P) SiO_2 catalyst is very broad (Fig. 2). Smaller particles (5–10 μm) are nearly spherical, whereas larger particles are of irregular shape, including some plate-like particles. Some of the larger particles have smaller ones attached to its external surface. Spray-dried catalysts 100 Fe/5 Cu/4.2 K/16 (P) SiO_2 and 100 Fe/5 Cu/4.2 K/1.1 (B) SiO_2 have similar morphologies and size distributions (Figs. 3a and 3b). Majority of particles are nearly spherical, but external surfaces are relatively rough and smaller particles are attached to the surface.

TAMU catalysts prepared from vacuum dried precursors (Nos. 4 and 5 in Table 1) have a significant number of irregularly shaped particles (large particles) whereas smaller particles are nearly spherical (Fig. 4). Catalyst containing 16 parts of precipitated SiO_2 and 3-wt% of SiO_2 (from silica binder) was spray-dried in a smaller unit (APV Anhydro Lab S1) and the particles are markedly smaller in comparison to the catalyst containing 24 parts of SiO_2 (Fig. 4b). The latter was spray-dried in the larger diameter spray dryer unit (APV Anhydro). SEM image of this catalyst shows the presence of large (>50 μm) irregularly shaped particles with relatively smooth edges. Also several aggregates, which consist of primary grains of smaller size particles, can be seen in this image.

Spray-dried TAMU catalysts prepared from wet precursors have excellent sphericity and smooth external surfaces (Figs. 5 and 6). The particle size distribution is rather broad ranging from 5 μm to 40 μm in diameter, regardless of the source of silica used. It should be noted that SEM micrographs have a bias towards smaller particles, since larger particles are preferentially blown away during the sample preparation (see above). The observed morphology of spray-dried catalysts (APV Anhydro Lab S1 unit) is ideally suited for use in slurry reactors.

Attrition Resistance Tests

Attrition resistance and performance of spray-dried catalysts and precipitated catalysts were determined simultaneously during F–T reaction tests conducted in a stirred tank slurry reactor (STSR). Attrition was measured by following the particle size distribution of catalysts as a function of time in the STSR. This provides a direct measure of changes in particle size distribution in the STSR after activation and during synthesis, and accounts for both physical and chemical effects. Slurry samples were withdrawn from the reactor before the catalyst activation (oxide form of catalyst) and at the end of the test. Catalysts were separated from slurry by washing and filtration as described previously in this report. PSD was determined by particle size analyzer manufactured by Coulter (Multisizer I). SEM micrographs (images) were obtained to investigate the mechanism of attrition – erosion vs. fracture, and to obtain morphological characteristics of catalysts at various stages of use.

(a) *Attrition strength of spray-dried catalysts synthesized at Hampton University*

SEM images of catalysts withdrawn from the reactor before activation (TOS = 0 h) are shown in Figures 7a–9a. As expected, they are similar to the corresponding micrographs (Figs. 2 and 3) of as-received catalysts. Particle size distribution is very broad for all three catalysts. Small particles are nearly spherical, whereas larger ones have irregular shape. Some particles clearly represent aggregates of smaller particles. Catalyst with nominal composition 100 Fe/5 Cu/4.2 K/11 (P) SiO_2 (HU2061), which was used in run SB–20601, is characterized by presence of a number of large flat particles with sharp edges (plate-like particles).

Images of catalyst particles withdrawn at the end of F–T tests (380–450 h on stream) are shown in Figures 7b–9b. PSD distribution at the end of run SB–20601 (TOS = 380 h) is still very broad, however, large particles broke into smaller fragments (fracture) and their morphology has changed. All particles have irregular surface structure due to chipping and erosion.

Comparison of SEM images of particles from run SB–34701 (100 Fe/5 Cu/4.2 K/1.1 (B) SiO_2; HU3471 catalyst) at TOS = 0 (Fig. 8a) and TOS = 449 h (Fig. 8b) reveals the presence of significantly larger number of particles at the end of the run. Overall it appears that the average particle size is smaller, and less spherical after F–T synthesis, and that primary mechanism of attrition is fragmentation (breakup of large aggregates into smaller ones). The image at the end of the test also shows the presence of a few irregularly shaped large particles. This is probably due to agglomeration caused by incomplete removal of wax, i.e. the residual wax acts like glue holding smaller aggregates together.

After 450 h of testing in STSR (SB–11102) 100 Fe/3 Cu/5 K/16 (P) SiO_2 catalyst (HU1112) had an irregular morphology, and the total number of particles was larger compared to TOS = 0 h (Fig. 9a). This image was obtained after multiple washings with a solvent to remove residual wax. However, one can still notice a number of large irregularly shaped particles, which are believed to be due to the presence of residual wax.

Quantitative information on particle size distribution (PSD) was obtained using Coulter Counter Multisizer and representative results are shown in Fig. 10. These plots show the volumetric

percent of the sample that is greater than a given (volumetric) diameter. For run SB–20601 (HU2061 catalyst) the PSD at the end of the run (TOS = 380 h) is shifted to the left from the PSD at 0 h, reflecting reduction in the particle size as the result of physical and chemical attrition. For example, the median particle size at TOS = 0 h was 54 μm, whereas at TOS = 380 the median size was only 7 μm (significant reduction in the particle size). On the other hand HU3471 catalyst (run SB–34701) showed much smaller reduction in the median particle size (52 μm at 0 h, 47 μm at 449 h). The PSD lines for cumulative distributions at TOS = 0 h and TOS = 449 h are crossing at about 55 mm (Fig. 10b), indicating increase in fraction of both smaller and larger particles at 449 h (relative to 0 h). The increase in fraction of smaller particles is the result of attrition, whereas the increase in fraction of larger particles is an artifact caused by incomplete removal of hydrocarbon wax resulting in formation of larger agglomerates. The PSD of HU1112 catalyst (run SB–11102) was qualitatively similar to that of HU3471 catalyst (not shown).

(b) *Attrition strength of precipitated catalysts and spray-dried catalysts prepared from dry precursors*

Attrition properties of three precipitated (not spray-dried) F–T catalysts and of DPS5624–2 catalyst (No. 4 in Table 1) prepared by spray drying from a vacuum dried precursor were determined under reaction conditions in a STSR. One of the catalysts used in these tests was a commercial precipitated catalyst with nominal composition 100 Fe/5 Cu/4.2 K/25 SiO_2, which was obtained from Ruhrchemie AG (Oberhausen-Holten, Germany). This catalyst was used in commercial fixed bed reactors at Sasol during mid 50's.

SEM micrograph of catalyst PPS3516–1 particles (after separation from Durasyn-164 oil) withdrawn from the STSR before CO activation (TOS = 0 h) is shown in Figure 11a. Catalyst particles are irregularly shaped with sharp edges. SEM micrograph of the catalyst particles separated from hydrocarbon wax after 497 h on stream (run SB–19102) is shown in Figure 11b. As can be seen the particle morphology and size have changed relative to that at TOS = 0 h. The particle edges are more rounded (large particles) due to erosion, and the number of small particles has increased.

The PSDs of catalyst samples withdrawn from the STSR are shown in Figure 12. The PSD after 497 h of F–T synthesis at 260°C, 1.5–2.2 MPa and 4–5.9 Nl/g-Fe/h, is shifted to the left from the PSD at 0 h, reflecting reduction in the particle size as the result of physical and chemical attrition. For example the median particle size at TOS = 0 h was 56 μm, whereas at TOS = 497 h the median size was 47 μm.

SEM micrographs of catalyst PPS3516–2 (no. 10 in Table 1) are shown in Figure 13. Majority of particles withdrawn from the STSR before CO activation (TOS = 0 h), are irregularly shaped with sharp edges. Some of the smaller particles are attached to the surface of the larger ones (Figure 13a). SEM micrograph of the catalyst particles separated from hydrocarbon wax after 364 h on stream (run SB–04803) is shown in Figure 13b. As can be seen, both the particle morphology and size have changed relative to that at TOS = 0 h. The particle edges are more rounded and the number of smaller particles attached to the surface of larger ones has decreased due to erosion.

PSDs of PPS3516−2 catalyst are shown in Figure 14. Shift in PSD distribution to the left is due to reduction in particle size by fracture and erosion. The median particle size at TOS = 0 h was 39 μm, whereas at TOS = 364 h the median size was 29 μm.

SEM micrographs of Ruhrchemie catalyst show a broad particle size distribution (Fig. 15). Catalyst morphologies before and after the reaction test (428 hours of F−T synthesis at 260°C, 1.5−2.2 MPa, 2.4−4 Nl/g-Fe/h) are similar, and it is hard to draw any conclusions about the extent of attrition from these images. Particles are irregularly shaped, and the texture of particles after F−T synthesis is a bit smoother (Fig. 15b) in comparison to that before the reaction. Morphology of the fresh Ruhrchemie catalyst (Fig. 15a) is similar to that of PPS3516−1 catalyst (Fig. 11a).

PSDs of the Ruhrchemie catalyst are shown in Figure 16. The shift in PSD distribution to the left is due to reduction in particle size primarily by fracture. Significant differences in PSDs occur for particles between 20 and 50 μm in diameter, whereas they are much smaller for particles outside this range.

SEM images of spray-dried DPS5624−2 catalyst are shown in Figures 17 and 18. Figure 17 represents image of particles after crushing in a tumbler and ultrasonication, i.e. before spray drying. As can be seen from Fig. 17 there are two groups of agglomerates: larger ones (5−10 μm) and smaller ones (less than 1 μm). After spray drying and few hours of stirring in nitrogen in the STSR the particles are much larger, but are not spherical (Fig. 18a). Some have a smooth texture, but also there are large agglomerates, which are clearly formed from smaller particles. After 295 hours of F−T synthesis (run SB−16502) at 260°C, 1.5−2.2 MPa and 4−5.8 Nl/g-Fe/h, the attrition effects are visible in Fig. 18b. Some of the large agglomerates have disintegrated into smaller fragments, and the number of small particles has increased. Shift in PSD towards smaller particles is clearly seen in Fig. 19.

(c) *Attrition strength of spray-dried catalysts prepared from wet precursors*

Three catalysts (Nos. 11, 12 and 14 in Table 1) of the same nominal composition (100 Fe/3 Cu/5 K/16 SiO_2) prepared by spray drying using three different sources of silica were tested in a STSR and their attrition properties were determined by SEM and PSD measurements.

SEM images of catalysts withdrawn from the reactor before activation (TOS = 0 h) are shown in Figures 20a, 22a and 25a. They are similar to the corresponding micrographs (Figs. 5 and 6) of these catalysts after spray drying.

A SEM micrograph of the WCS3516−1 catalyst (SiO_2 from colloidal silica) at TOS = 0 h is shown in Fig. 20a. The catalyst consists of micro-spherical particles with smooth external surfaces. Larger particles are around 30 μm, whereas smaller ones are about 5 μm in diameter. Figure 20b shows the same catalyst after 345 h of testing at 4−6 Nl/g-Fe/h, 260 °C and 1.5−2.2 MPa (run SB−30702). From this figure it appears that this catalyst has high attrition strength, because its morphology is practically unchanged, except for a reduction in the smoothness of the

external surfaces. Cumulative PSD (Fig. 21) shows only a small shift to smaller particles (i.e., high attrition strength).

SEM images of the WTO3516−1 catalyst (TEOS as the silica source), used in STSR test SB−33802, are shown in Figures 22 and 23. A sample withdrawn from the reactor at TOS = 0 h consists of micro-spherical particles, but cracks are visible on some of the particles (Fig. 22a). A SEM micrograph of this sample obtained at a higher magnification (Fig. 22b) shows evidence of the particle disintegration, including the presence of a significant number of particles smaller than about 2 μm. This indicates that this catalyst does not have high attrition strength. Surface cracks and particle disintegration took place during sieving and/or stirring in the STSR. SEM micrographs of this catalyst after 299 h of F−T synthesis in the STSR at 4−6 Nl/g-Fe/h, 260 °C and 1.5−2.2 MPa are shown in Figure 23. The particle morphology (after a regular washing procedure with Varsol 18 solvent) has changed dramatically; there are hardly any spherical particles, and large irregularly shaped particles represent agglomerates of smaller particles (Fig. 23a). The presence of large irregularly shaped particles is attributed to the micro-spherical particle breakup and their encapsulation by residual hydrocarbon wax. A SEM image of the catalyst sample after multiple washings with Varsol 18 solvent, CS_2, n-hehane and soxhlet extraction with a mixture of xylenes for 48 h, followed by extraction with MEK (methyl ethyl ketone) for 48 hours is shown in Fig. 23 b. This image shows the presence of some micro-spherical particles (with rough surfaces) as well as of large agglomerates (up to 100 μm) with smoother surfaces compared to those shown in Fig. 23a. We suspect that large particles represent agglomerates of irregularly shaped smaller particles that are held together by hydrocarbon wax, which acts like a glue. This hydrocarbon wax is extremely difficult to remove through the use of common organic solvents.

The PSDs of the WTO3516−1 catalyst are shown in Figure 24. The PSD at 299 h was obtained using the catalyst sample after the first washing with Varsol 18. It can be seen that the entire PSD of the sample at TOS = 299 h is shifted to the right from that of the catalyst sample at TOS = 0 h, indicating particle aggregation, which is consistent with SEM results shown in Figures 22a and 23a.

SEM micrographs of the WPS3516−4 catalyst (K_2SiO_3 as the source of silica), used in the STSR test SB−09703, are shown in Figures 25 and 26. The results are qualitatively similar to the ones obtained with the WTO3516−1 catalyst. A sample withdrawn from the STSR at TOS = 0 h consists of micro-spherical particles (~5−40 μm in diameter) with generally smooth external surfaces (Fig. 25a). SEM micrographs of this catalyst after 364 h of F−T synthesis in the STSR at 4−6 Nl/g-Fe/h, 260 °C and 1.5−2.2 MPa have completely different morphology; the majority of particles are irregularly shaped and there is a significant number of large aggregates (> 50 μm in size). The presence of large irregularly shaped particles is attributed to the micro-spherical particle breakup and their encapsulation by residual hydrocarbon wax. A SEM micrograph of a sample after multiple washings with Varsol 18 solvent, and warm CS_2 and n-hexane (Fig. 26a) is similar to that obtained after the first washing with Varsol 18 (Fig. 25b), which indicates that both CS_2 and n-hehane are not effective solvents under our standard washing procedure. The Soxhlet extraction (48 h with xylenes followed by 48 h with MEK) was only partially successful in removing the residual wax (Fig. 26b). In this micrograph one can see a much larger number

of small (nearly spherical) particles in comparison to Figs. 25b and 26a. However, even this procedure was not completely effective in removing all residual wax, and overall the particles appear to be larger at the end of F–T run (comparing Fig. 26b with Fig. 25a).

Comparison of attrition behavior of iron F–T catalysts

From PSD measurements one can obtain several parameters, which can be used to quantify reduction in particle size due to attrition. These include: (a) reduction in Sauter mean diameter ($d_{3,2}$); (b) reduction in volume moment diameter ($d_{4,3}$); and (c) increase in fraction of fine particles (particles less than 10 μm in diameter). The first two attrition indicators reflect the particle size reduction in general, and are weighted toward larger particles. On the other hand the increase in fraction of fines generated is a critical parameter for slurry-phase reactor applications, because difficulties with catalyst/wax separation and product contamination are caused by small particles. The Sauter mean diameter and volume moment diameter were calculated from the following definitions:

$$d_{3,2} = \frac{\sum d_i^3 N_i}{\sum d_i^2 N_i} \qquad\qquad d_{4,3} = \frac{\sum d_i^4 N_i}{\sum d_i^3 N_i}$$

where, d_i is the particle diameter, and N_i is the number of particles of size d_i.

Reduction in the Sauter mean diameter or the volume moment diameter was expressed as percentage of the initial value, i.e.:

$$\Delta Y\ (\%) = [(Y\ (0\ h) - Y\ (EOR))/Y\ (0\ h)] * 100$$

where: Y = $d_{3,2}$ or $d_{4,3}$; EOR = end of the run (i.e., time on stream at the end of a STSR test). Increase in fraction of particles smaller than 10 μm, was calculated as: $\Delta F = F\ (EOR) - F\ (0\ h)$, where F represents a fraction of particles less than 10 μm in diameter.

The results from all STSR tests are summarized in Table 2. Before we discuss these results the following cautionary remarks and observations are in order. From SEM results we know that we were not successful in removing all residual wax, and this resulted in particle agglomeration. This has an impact on the results in two ways: (1) the actual extent of attrition is underestimated; and (2) quantitative comparison of the attrition strength of different catalysts is more difficult, since the extent of particle agglomeration was not the same with all catalysts. The results, which were affected to a large extent by particle agglomeration, are given in bold font.

It appears that precipitated (not spray-dried) catalysts were less affected by particle agglomeration, then the spray-dried catalysts synthesized at HU and TAMU. For all catalysts the reduction in the volume mean diameter was smaller than the corresponding reduction in the Sauter mean diameter, because the former is more weighted toward larger particles.

Table 2. Results from attrition resistance measurements in the STSR under reaction conditions.

Catalyst ID/ EOR (h)	TOS = 0 h			TOS = EOR (h)			% change		
	$d_{3,2}$ (μm)	$d_{4,3}$ (μm)	F (<10 μm)	$d_{3,2}$ (μm)	$d_{4,3}$ (μm)	F (<10 μm)	$\Delta d_{3,2}$	$\Delta d_{4,3}$	ΔF
HU2061/ 380	48.0	52.8	0.4	6.2	18.1	62.9	87.0	65.7	62.5
HU1112/ 450	40.1	49.6	0.7	27.0	**46.8**	7.4	32.7	**5.6**	6.7
HU3471/ 449	37.3	46.4	0.5	22.4	**47.4**	4.2	40.1	**(-2.2)**	3.7
Ruhrchemie/ 429	34.1	46.9	3.3	25.8	40.2	5.9	24.3	14.3	2.6
PPS3516–1/ 497	47.1	53.1	0.3	30.8	43.2	3.0	34.6	18.6	2.7
PPS3516–2/ 364	26.1	39.7	3.3	18.3	33.9	5.9	29.9	14.6	7.8
DPS5624–2/ 295	48.3	57.3	1.0	33.1	48.1	3.3	31.5	16.1	2.3
WCS3516–1/ 345	20.6	24.1	4.1	19.2	22.8	4.8	6.8	5.4	0.7
WTO3516–1/ 299	15.6	17.4	7.0	**29.0**	**41.0**	**3.6**	**(-85.9)**	**(-135.6)**	**(-3.4)**

EOR = time on stream at the end of the run.

Three spray-dried catalysts prepared at HU were tested in the STSR for 380–450 hours. Catalysts HU2061 and HU1112 contain 11 and 16 parts of precipitated silica (from TEOS), respectively, whereas HU3471 catalyst contains 1.1 parts of silica binder per 100 parts of Fe. Morphological analyses of catalysts samples collected at TOS= 0 h showed that catalyst HU2061 had a large number of plate-like particles (Fig. 7a), whereas HU1112 and HU3471 catalysts had similar morphologies (Figures 8a and 9a). These two catalysts had a relatively large number of spherical particles with rough surfaces. After testing in the STSR for 380–450 hours, their morphologies changed. Catalyst HU2061 disintegrated into a significant number of small pieces due to fracture (Fig. 7b). Both HU1112 and HU3471 catalysts lost their sphericity after ~450 hours in the STSR (Figures 8b and 9b). The results from PSD measurements show that HU1112 and HU3471 catalysts had similar reductions in their Sauter mean diameters (32.7 and 40.1 %, respectively) after testing in the STSR. Changes in fraction of fine particles (diameter less than 10 μm) for these two catalysts were also similar (6.7 and 3.7 %, respectively). On the other hand, the change in volume moment diameter for these two catalysts showed an unexpected behavior. The volume moment diameter of the HU1112 catalyst decreased by 5.6 % only, whereas that of the HU3471 catalyst increased by 2.2 % (listed as -2.2 % in Table 2). As stated above, the volume moment diameter has bias towards large particles. Therefore, the increase in the volume moment diameter of the HU3471 catalyst, and a small reduction observed with the HU1112 catalyst may have been caused by agglomeration of particles due to residual wax, and loss of small particles during washing procedure to obtain "wax-free" catalyst samples.

The HU2061 catalyst had much lower attrition resistance relative to catalysts HU1112 and HU3471. This catalyst experienced large reductions in the Sauter mean and volume moment diameters (87 and 65.7 %, respectively) after 380 h of testing in the STSR. The inferior attrition strength of this catalyst is also reflected in considerable generation of particles < 10 μm in diameter during the STSR test (62.5 %).

It can be concluded that mechanical integrity of catalysts HU2061, HU1112 and HU3471 was markedly dependent upon their morphological features. The attrition strength of catalysts made out of largely spherical particles was considerably higher than that of the catalyst consisting of irregularly shaped particles (i.e. plate-like particles).

Three precipitated catalysts (PPS3516–1, PPS3516–2 and the Ruhrchemie catalyst) containing 16 or 25 parts of silica per 100 parts of Fe, and a spray-dried catalyst prepared from a vacuum-dried precursor (DPS5624–2 containing 24 parts of precipitated silica) were tested in the STSR for 295–497 hours. SEM micrographs (Figures 11a, 13a and 15a) of precipitated catalysts at TOS= 0 h show that they were formed of irregularly shaped particles with sharp edges and relatively smooth surfaces. After testing in the STSR the Ruhrchemie's catalyst morphology did not change much (Fig. 15). At the end of the test, the catalyst had slightly smoother edges and surfaces. A similar behavior was observed with the other two precipitated catalysts synthesized at TAMU. On the other hand, catalyst DPS5624–2 collected at TOS= 0 h (Fig. 18a) was formed of large irregularly shaped particles, some of which are aggregates of smaller particles. After 295 h of F–T synthesis in the STSR, the morphological changes of this catalyst were similar to those observed with precipitated catalysts.

The attrition results from PSD measurements (Table 2) show that the three precipitated catalysts have similar mechanical strength, as spray-dried DPS5624−2 catalyst prepared from the vacuum-dry precursor. Changes in the volume moment and Sauter mean diameters for these four catalysts were 14.3−18.6 % and 24.3−34.6 %, respectively. Changes in fraction of fine particles after 295−497 h in the STSR, also demonstrated similarities in the attrition behavior of these four catalysts. Therefore, from PSD results it can be concluded that spray drying of the vacuum-dry precursor did not result in improvement of the attrition strength relative to precipitated iron catalysts, which were not spray dried. This is consistent with SEM results, which showed that the spray-dried catalyst had similar morphology as the three precipitated catalysts.

Catalysts WCS3516−1, WTO3516−1 and WPS3516−4 were spray-dried at TAMU from wet slurries having the same composition (100 Fe/3 Cu/5 K/16 SiO_2) but were prepared using different sources of silica. SEM micrographs of catalyst samples at TOS= 0 h (Figures 20a, 22a and 25a) showed that all three catalysts are formed of mostly spherical particles. However, catalyst WTO3516−1 showed the presence of cracks and surface irregularities, which had an adverse effect on its attrition resistance. After 299−449 h of testing in the STSR WTO3516−1 and WPS3516−4 catalysts lost their sphericity due to attrition effects (Figures 23 and 26). Also, the formation of large agglomerates was observed after reaction tests. In contrast, the WCS3516−1 catalyst had an excellent attrition resistance. After 345 hours of testing in the STSR the catalyst's morphology remained practically unchanged relative to catalysts sample at TOS= 0 h (Figure 20).

Results from PSD measurements with catalyst WCS3516−1 confirmed its excellent attrition resistance. Reductions in the volume moment and Sauter mean diameters (5.4 and 6.8 %, respectively) were the smallest among all catalysts used in this study. A small increase in the fraction of fine particles (0.7 %) shows that this catalyst also did not experience a significant attrition by erosion.

PSD results from the STSR test of WTO3516−1 catalyst (Figure 24 and Table 2) showed increase in the average particle size. This phenomenon is attributed to the presence of residual wax. However, it is not clear why this catalyst, as well as WPS3516−4, HU1112 and HU3471 catalysts, had this problem. In spite of the absence of reliable results from PSD measurements with WTO3516−1 and WPS3516−4 catalysts, it is clear from SEM images that the spray-dried WCS3516−1 catalyst prepared with colloidal silica is more attrition resistant than the other two catalysts.

Attrition properties of catalysts evaluated in this study will be now compared with those of other F−T catalysts, which were tested in slurry reactors and/or devices intended to simulate the slurry reactor environment. Srinivasan et al. [7] studied attrition behavior of a spray-dried CO pretreated unsupported (Fe/Cu/K) F−T catalyst (prepared by UCI) by placing the catalyst/oil slurry on a rotating mill and following the PSD as a function of time. They found that particles retained their spherical shape, but their average diameter decreased with time. Pertinent to the present study the authors stated that this catalyst rapidly disintegrated to 1−3 μm particles during stirring in STSR in nitrogen atmosphere. Similarly, O'Brien et al. [11] reported that spray-dried and calcined Fe/Cu/K/SiO_2 catalyst particles in the 30−50 μm range disintegrated to 1−3 μm

particles during 24 h of stirring under inert gas as well as under synthesis conditions. Apparently, these catalysts, even though of spherical shape, are much weaker than catalysts used in the present study.

O'Brien et al. [11] also studied the attrition behavior of several supported Fe F–T catalysts in the STSR under reactive conditions. After 120–288 h of operation in the STSR the alumina and magnesium aluminate particles showed size reduction due to fracture, whereas magnesium silicate and silica supported catalysts showed no evidence of attrition. These observations were made on the basis of qualitative examination of SEM images before and after F–T synthesis. However, as stated earlier, it is difficult to draw conclusions about the extent of attrition from SEM images alone.

Goodwin and co-workers [9,14] studied attrition behavior under F–T synthesis conditions of several supported Co F–T catalysts in a small scale (1-in in diameter) SBCR. Changes in PSD were determined using a laser beam techniques, which measures a volumetric particle diameter. Zhao et al. [9] reported 8.1 % reduction in the volume moment diameter after 240 h of F–T synthesis with silica-supported (spray-dried Davison 952) Co catalyst. Changes in fraction of particles smaller than 10 μm were not reported, due to a loss of small particles through a filter with openings greater than 10 μm. Wei et al. [14] conducted additional SBCR tests under F–T conditions (240 h on stream). Reductions in the volume moment diameter ranging from 1.6–8.4 % were reported for experiments with alumina-supported catalysts (Catapal-B alumina from Condea/Vista), and 10.2–14.2 % for silica supported (Davison 952) Co catalysts. The attrition strength of silica and alumina supported Co catalysts was considered to be adequate for use in SBCRs [12,13].

The Ruhrchemie catalyst and precipitated Fe catalysts (PPS3516–1 and PPS3516–2), synthesized at TAMU, had experienced higher reductions in the volume moment (14.3–18.6 %) than the silica supported Co catalysts (8.1–14.2 %) in the SBCR tests [9,14]. However, precipitated Fe catalysts were tested in a STSR, where hydrodynamic conditions leading to physical attrition are expected to be more severe than in a SBCR. Another factor, which may have contributed to larger reductions in particle size during STSR tests, is that test durations (295–497 h) were longer than in the SBCR tests (240 h). The observed extent of attrition with Fe catalysts is the result of both chemical attrition, due to phase transformations in the Fe catalyst and carbon deposition [5,6], and physical attrition, whereas chemical attrition is not considered to be important with Co based F–T catalysts. As noted previously, generation of fine particles in the STSR tests with precipitated Fe catalysts was small (2.3–7.8 %) whereas there is no information on attrition by erosion in SBCR tests of Co supported catalysts. Spray-dried catalysts synthesized at TAMU and at HU (except for the HU20601) had similar reductions in the volume moment (5.4–16.1 %) and generation of fine particles was small (0.7–6.7 %).

Recently, Pham et al. [16] studied attrition properties of two aluminas (Vista HP 14 and Vista B 965) and two silicas (Davison 948 and 952) in the STSR under nonreactive conditions. These commercial supports are either the same or of a similar type as those used in attrition resistance studies of supported Co F–T catalysts [9,14]. Vista B alumina support had the highest attrition strength among all supports tested, characterized by small extent of fracture and moderate

erosion (after 168 h of testing in the STSR). We have shown elsewhere [28] that TAMU's precipitated Fe catalyst (100 Fe/3 Cu/4 K/16 SiO_2), of similar composition as catalysts used in this study, had similar physical attrition resistance as the Vista B 965 alumina. This catalyst and Vista B 965 alumina were tested under the same conditions (260 °C, 1.5 MPa and 3 Nl/g-cat/h using N_2 as the feed gas) in the STSR.

Contrary to several previous reports [2–8, 10,11] that precipitated unsupported Fe catalysts are structurally very weak, we have found that precipitated Fe catalysts have adequate attrition strength even when subjected to severe hydrodynamic conditions of a STSR and chemical stresses induced by phase transformations during F–T synthesis. Attrition is a very complex phenomenon, and various binding mechanisms may play role in agglomerate strength [17]. Pham et al. [10] stated that the shape of primary iron oxide precursor particles is important in determining the attrition resistance of the Fe F–T catalysts. Spray-dried iron oxide catalyst (Fe/Cu/K) and a similar catalyst containing kaolin binder, both prepared by United Catalyst (UCI), disintegrated easily during ultrasound fragmentation tests [5,6]. Both catalysts were found to have plate-like morphology that was not conducive to creating strong interlocking forces between primary particles. They synthesized precipitated Fe/Cu precursor (under similar conditions used to prepare TAMU's catalysts), which consisted of roughly spherical primary particles, and found significant improvement in the attrition strength [10]. Further improvement in attrition strength was obtained upon addition of precipitated silica followed by spray drying. According to them precipitated silica provides very irregular structures, which are more conducive to creating strong interlocking forces to keep agglomerates together. Since the catalysts used in this study were prepared in a similar manner, this may explain their good attrition resistance under F–T conditions in a STSR.

Slurry Reactor Tests

Twelve slurry reactor tests were completed during this project. Test designations, catalysts employed and process conditions are summarized in Table 3. The following coding system was used to designate experimental tests. Two-letter prefix (SB) refers to the reactor unit used for the test (S = slurry reactor; B = reactor unit). The first three digits refer to the day of the year corresponding to the start of the run, whereas the next two digits correspond to the last two digits in the year of the start date (e.g. 01 for 2001).

As received or sieved catalyst (14–15 g) and 320–350 g of Durasyn 164 oil (a hydrogenated 1-decene homopolymer, ~ C_{30} obtained from Albemarle Co.) were loaded into the reactor. The catalysts were pretreated in CO at 280 °C, 0.8 MPa (100 psig), 3 Nl/g-cat/h for 8 hours (12 hours in runs SB–20601 and SB–34701). In run SB–32901 (Ruhrchemie catalyst) the syngas (H_2/CO = 2/3) was used as reductant instead of CO. Slurry samples (containing ~1 g of catalyst) were withdrawn from the reactor before the pretreatment and at the end of the run for particle size distribution measurements.

Table 3. Catalysts tested and reaction conditions.

Test ID/ Catalyst ID	Catalyst details/Size	Process conditions [(a)] /(Hours)
SB–20601 HU2061	100 Fe/5 Cu/4.2 K/11 (P) SiO_2 (Spray dried – HU) Not determined	3.3 Nl/g-Fe/h, 2.1 MPa (0–224; 334–380 h) 5 Nl/g-Fe/h, 2.1 MPa (224–334 h)
SB–32901 Ruhrchemie	100 Fe/5 Cu/4 K/25 (P) SiO_2 (Ruhrchemie – commercial) 140–325 mesh	3.8 Nl/g-Fe/h, 1.5 MPa (0–209 h) 2.3 Nl/g-Fe/h, 1.5 MPa (210–325 h) 2.3 Nl/g-Fe/h, 2.2 MPa (326–429 h)
SB–34701 HU3471	100 Fe/5 Cu/4.2 K/1.1 (B) SiO_2 (Spray dried – HU) Not determined	3.1 Nl/g-Fe/h, 2.1 MPa (0–449 h)
SB-11102 HU1112	100 Fe/3 Cu/4 K/16 (P) SiO_2 (Spray dried – HU) Not determined	3.9 Nl/g-Fe/h, 1.5 MPa (0–210 h) 5.8 Nl/g-Fe/h, 2.2 MPa (215–450)
SB–16502 DPS5624–2	100 Fe/5 Cu/6 K/24 (P) SiO_2 (Spray dried-dry form/ TAMU) 140–325 mesh	4 Nl/g-Fe/h, 1.5 MPa (0–160 h) 5.8 Nl/g-Fe/h, 2.2 MPa (161–295 h)
SB–19102 PPS3516–1	100 Fe/3 Cu/5 K/16 (P) SiO_2 (Precipitated – TAMU) 170–325 mesh	4 Nl/g-Fe/h, 1.5 MPa (0–197; 312–500 h) 4 Nl/g-Fe/h, 2.2 MPa (198–311 h) 355–380 h (H_2 reg.); 404–428 h (CO reg.)
SB–22102 DPS3616	100 Fe/3 Cu/6 K/16 (P) SiO_2 (Spray dried-dry form/ TAMU) 170–325 mesh	4 Nl/g-Fe/h, 1.5 MPa (0–57 h)
SB–28402 DPS3616	100 Fe/3 Cu/6 K/16 (P) SiO_2 (Spray dried-dry form/ TAMU) 170–325 mesh	4 Nl/g-Fe/h, 1.5 MPa (0–170 h)
SB–30702 WCS3516–1	100 Fe/3 Cu/5 K/16 (B) SiO_2 (Spray dried–wet form/TAMU) As received (< 325 mesh)	4 Nl/g-Fe/h, 1.5 MPa (0–165 h) 5.9 Nl/g-Fe/h, 2.2 MPa (166–345 h)
SB–33802 WTO3516–1	100 Fe/3 Cu/5 K/16 (P) SiO_2 (Spray dried–wet form/TAMU) As received (< 325 mesh)	4 Nl/g-Fe/h, 1.5 MPa (0–178 h) 5.9 Nl/g-Fe/h, 2.2 MPa (179–300 h)
SB–04803 PPS3516–2	100 Fe/3 Cu/5 K/16 (P) SiO_2 (Precipitated – TAMU) 170–325 mesh	4 Nl/g-Fe/h, 1.5 MPa (0–202 h) 5.9 Nl/g-Fe/h, 2.2 MPa (203–364 h)
SB–09703 WPS3516–4	100 Fe/3 Cu/5 K/16 (P) SiO_2 (Spray dried–wet form/TAMU) As received (< 325 mesh)	4 Nl/g-Fe/h, 1.5 MPa (0–240 h) 5.9 Nl/g-Fe/h, 2.2 MPa (241–364 h)

[(a)] T= 260 °C, H_2/CO = 2/3 in all tests
(P) = Precipitated silica; (B) = Binder silica

Test of the Ruhrchemie Catalyst (Run SB−32901)

The primary objectives of this test were to provide training for a new operator (Dr. Wen-Ping Ma) in the use of equipment, instruments and software for data reduction, and to obtain information on the attrition strength of this catalyst. Ruhrchemie catalyst was used extensively in our laboratory during previous DOE contracts, and performance results from these tests can be found elsewhere [25,26,29,30]. This is a robust catalyst with good performance, and in mid 1950's it was used in fixed bed reactor plants at Sasol in South Africa.

After a pretreatment with syngas (H_2/CO = 2/3) at 280 °C, 0.8 MPa, 3 Nl/g-cat/h for 8 hours, the catalyst was tested initially at 260 °C, 1.5 MPa, 3.8 Nl/g-Fe/h using syngas feed with H_2/CO molar feed ratio of 0.67. Syngas conversion as a function of time and/or process conditions is shown in Figure 27a. After initial decrease with time, the conversion reached a stable value of 46 % at about 100 h on stream. Upon decreasing the gas space velocity to 2.3 Nl/g-Fe/h while maintaining all other process conditions unchanged the syngas conversion quickly reached a new steady state value of 62 %. The conversion was stable during 115 hours of testing at these process conditions. Upon increasing reaction pressure to 2.2 MPa at 326 h, the syngas conversion increased further to 68−70 %, and remained fairly stable during another 100 h of testing.

Figure 27b shows changes of carbon dioxide selectivity (defined as a fraction of CO converted to CO_2) with time. Carbon dioxide selectivity is a measure of the extent of water-gas-shift (WGS) reaction, and 50 % selectivity represents the maximum possible value corresponding to complete conversion of water produced during hydrocarbon formation reaction. Carbon dioxide selectivity increased with time and reached a stable value of about 44 % at 40 h on stream. During testing at a lower gas space velocity, the CO_2 selectivity increased to 46 % (220−325 h). During testing at 2.2 MPa (325−429 h) the CO_2 selectivity was about 42 % (lower WGS activity).

Selected aspects of catalyst's hydrocarbon selectivity are shown in Figure 28. Methane selectivity, calculated as 100 x (moles of CO converted to CH_4)/ (total moles of CO converted - moles of CO converted to CO_2), was about 3 % up to 150 h, and then started to increase reaching 4 % at 209 h. During testing at lower gas space velocity (220−325 h) methane selectivity was about 4 %, and then it decreased to 3.5 % during testing at 2.2 MPa (330−420 h). Selectivity of C_5^+ hydrocarbons (liquids and wax) was high throughout the entire test. C_5+ selectivity decreased from about 87 % to 80 % during the first 200 hours of testing (Figure 28b), and then remained fairly stable until the end of the test.

Overview

A precipitated iron F−T catalyst (100 Fe/5 Cu/4 K/25 SiO_2) synthesized by Ruhrchemie was tested in the STSR for 429 hours. Catalyst selectivity was excellent (low methane and high C_5^+ hydrocarbon selectivity), whereas the activity was stable at different process conditions. These results are consistent with previous studies conducted in our laboratory with this catalyst. The attrition resistance of this catalyst was high (Table 2). Catalyst breakup by fracture was

moderate (14.3 % reduction in the volume moment) and erosion was small (2.6 % increase in fine particles).

STSR tests with spray-dried catalysts synthesized at Hampton University

Three iron F–T catalysts synthesized at Hampton University (HU) were evaluated in the STSR. These catalysts were prepared as a part of an on-going project at HU supported by DOE. The catalysts were tested in a slurry reactor at TAMU to provide information on activity, stability and selectivity over a long period of time, and on attrition strength under the reaction conditions.

Results from tests SB–20601 and SB–34701 are shown in Figures 29 and 30. The catalysts were pretreated under the same conditions, and the process conditions were similar in both tests except for a 110 h time period (224–334 h) in run SB–20601 when a significantly higher gas space velocity was employed.

Syngas conversion change with time and/or process conditions during run SB–20601 is shown in Figure 29a. During the first 80 hours of testing at baseline conditions (260 °C, 2.1 MPa, 3.3 Nl/g-Fe/h) the syngas conversion increased with time reaching 85 %. After reaching the maximum conversion, the catalyst started to deactivate, and at 224 hours on stream the syngas conversion was 72 %. Upon increasing gas space velocity to 5 Nl/g-Fe/h the conversion decreased as expected, and the catalyst continued to deactivate between 225 and 280 hours on stream. Between 280 and 334 hours, the conversion was fairly stable (43–44 %). After returning to the baseline conditions at 335 h, the syngas conversions was about 60 %, but the activity continued to decrease with time and at the end of the run (384 h) the conversions was about 48 %. The average loss in syngas conversion (catalyst deactivation rate) between 80 and 224 hours was 0.09 %/hour, whereas the average conversion loss for the time period between 80 and 384 hours was 0.145 %/hour (3.84 %/day). This shows that catalyst deactivation was faster during the latter portion of the test.

As can be seen in Figure 29b the syngas conversion increased with time on stream during the first 53 h of testing at 260 °C, 2.1 MPa and 3.1 Nl/g-cat/h, and reached the maximum value of 86.5 %. During the next 150 h (53–203 h) of testing, the conversion declined slowly and reached 78 % at 204 h. During the next 40 hours the conversion was significantly lower, about 66%, probably due to reduced stirring rate, followed by an electric motor malfunction, which resulted in suspension of the test at 247 h due to complete stoppage of the stirrer. During the test interruption, the catalyst was kept in N_2 atmosphere at 120°C for 30 days. After the motor was repaired, the test was resumed, and the initial conversion was similar to that observed at 204 h, i.e. before the problem with electric motor arose. Thus, the exposure of catalyst to N_2 atmosphere over a 30-day period did not result in any loss of activity. However, the catalyst activity continued to decrease with time reaching 60 % at the end of the test (449 h). The average rate of catalyst activity loss between 53–449 h was 0.0676 %/h (1.62 %/day), which is significantly lower than that observed in Run SB–20601.

Both catalysts exhibited very high WGS activity. Selectivity to CO_2 increased quickly with time reaching a stable value of about 49 %. The WGS activity remained stable throughout the test, even though the F–T activity decreased with time.

Hydrocarbon selectivities (CH_4 and C_5^+) were similar in both tests (Fig. 30). Methane selectivity decreased during the first 150 h of testing, reaching a stable value of 2.0±0.2 %. Methane selectivity was not affected by changes in conversion and/or process conditions (Run SB–20601). Selectivity of C_5^+ hydrocarbons (liquids and wax) was high in both tests. It increased to 84–86 % during the first 130 hours of testing (Figure 30b), and then remained fairly stable. Liquid plus wax selectivity (fraction of C_5+ hydrocarbons among total hydrocarbons on carbon atom basis) was also independent of conversion level and/or process conditions.

Run SB–11102 was conducted using a catalyst with nominal composition 100 Fe/3 Cu/4 K/16 SiO_2, which was synthesized and spray-dried at HU. Precipitated catalyst of the same composition was synthesized and tested at TAMU during previous DOE contracts, and its performance (activity, selectivity and stability) was better than that of the state-of-the art iron F–T catalysts [18–20]. Results from this test are shown in Figures 31 and 32, together with results from two tests with TAMU's precipitated catalyst of the same composition. Pretreatment conditions in runs SB–11102 and SA–09496 were the same, whereas a slightly different procedure was employed in run SB–21896 (CO/He = 1/10, 280 °C for 8 h). Initial process conditions were the same in all three tests (260 °C, 1.5 MPa, 3.9 Nl/g-Fe/h, H_2/CO = 2/3).

Syngas conversion in all three tests increased with time reaching a steady state value after 40–80 h. The steady state conversion in run SB–11102 (spray-dried HU catalyst) was lower (~73 %) than that in tests with precipitated TAMU catalyst (~78 %). The conversion in run SB–11102 was stable up to 160 h, and then decreased to 70 % (160–210 h), whereas the catalyst activity in run SA–21896 remained stable up to 210 h. The activity of the CO pretreated TAMU catalyst (SA–09496) was the same as that of the catalyst pretreated in CO/He (SA–21896). At about 140 h, the space velocity in run SA–09496 was decreased to 3.1 Nl/g-Fe/h (while keeping the other conditions unchanged) and the syngas conversion increased to 80 % (not shown in Figure 31). In runs SB–11102 and SA–21896 at about 210 h, the gas space velocity and reaction pressure were increased to 5.8 Nl/g-Fe/h and 2.2 MPa, respectively. At these conditions the spray-dried catalyst started to deactivate at about 260 h, and the syngas conversion was 64 % at the end of the run (450 h). On the other hand, the activity of precipitated TAMU catalyst (SA–21896) continued to increase slightly with time, and the conversion reached 83 % at 500 h. The CO pretreated TAMU catalyst (SA–09496) was tested at 2.2 MPa and 4.4 Nl/g-Fe/h between 230 and 440 h, and its activity also increased slightly with time (not shown). The syngas conversion was 81 % at 440 h on stream.

Hydrocarbon selectivity trends are shown in Figure 32. In all three tests methane selectivity was low (2.2–3.8 %) and C_5^+ selectivity was high (72–86 %). Also, in all three tests methane selectivity was lower and C_5^+ selectivity higher during testing at 2.2 MPa, compared to the corresponding values obtained during testing at 1.5 MPa. Methane and C_5^+ selectivities were similar in tests with TAMU's precipitated catalyst (Runs SA–09496 and SA–21896). In general, methane selectivity was higher, and C_5^+ selectivity lower in the test with the spray-dried catalyst, in comparison to the corresponding values obtained in two tests with the precipitated TAMU's catalyst.

Comparison of Performance

Selected activity and selectivity data from three tests with spray-dried catalysts synthesized at Hampton University are shown in Table 4. Results from run SA–21896 with the precipitated TAMU's catalyst are also included for comparison.

Spray-dried catalysts containing 1.1 SiO_2 (binder SiO_2) and 11 SiO_2 (precipitated SiO_2) have excellent selectivity characteristics (low methane and high C_5^+ yields), but their activity and stability (deactivation rate) need to be improved significantly. Selectivity of these two catalysts is slightly better than that of TAMU's precipitated catalyst (lower methane), but their activity and productivity are significantly lower relative to TAMU's catalyst.

Spray dried catalyst containing 16 SiO_2 (precipitated SiO_2) produced more methane and less C_5^+ hydrocarbons than the other two spray-dried catalysts and the TAMU's precipitated catalyst of the same composition. Its activity and stability were better than those of the other two spray-dried catalysts synthesized at HU, but inferior in comparison to the TAMU's catalyst.

STSR tests of precipitated iron catalysts synthesized at TAMU

Run SB–19102 with PPS3516–1 catalyst

This catalyst was prepared using a modified TAMU's procedure for synthesis of a precipitated catalyst with potassium silicate as a source of SiO_2 as described earlier in this report (Catalyst Synthesis and Characterization). In this case potassium (K) was added to wet slurry of 100 Fe/3 Cu/16 SiO_2 precursor, whereas according to our standard procedure the addition of K is by IWI of a vacuum dried precursor.

Syngas conversion changes with time and/or process conditions are shown in Figure 33. Initially, during testing at baseline conditions of 260 °C, 1.5 MPa and 4 Nl/g-Fe/h, the conversion increased with time reaching 56 % at 125 h, and then remained stable for another 70 hours. Upon increasing reaction pressure to 2.2 MPa, while keeping other conditions unchanged, it started to decrease rapidly, reaching a stable value of ~40 % at 255 h. Between 256 and 311 h the catalyst activity was relatively stable. Upon returning to the baseline conditions (1.5 MPa) the conversion decreased to ~32 % (315–350 h). At this point the catalyst was regenerated with H_2 at 0.8 MPa, 260 °C and 4 Nl/g-Fe/h for 24 h. After H_2 regeneration, the F–T synthesis was resumed at the baseline conditions and the syngas conversion increased from 26.8 % to 34.6 % during the next 20 h (382–402 h). Another attempt to improve the catalyst activity was made by using CO regeneration for 24 h (under the same conditions employed during the H_2 regeneration). As can be seen the catalyst activity was further improved after 24 h CO regeneration. Syngas conversion increased from 13 % to 39 % between 429 and 482 h, and the rejuvenated catalyst activity was maintained during the next 20h of time on stream. These results show that the catalyst activity can be partially restored with regeneration, and that CO is more efficient regeneration agent than H_2.

Table 4. Performance of spray-dried and precipitated catalysts in STSR tests.

Catalyst Run No.	Spray-dried 11 SiO_2 (P) HU SB–20601	Spray-dried 1.1 SiO_2 (B) HU SB–34701	Spray-dried 16 SiO_2 (P) HU SB–11102	Precipitated 16 SiO_2 TAMU SA–21896
SV (Nl/g-Fe/h)[a]	3.3	3.1	5.8	5.8
Syngas Conversion (%)	70 – 85	63 – 86	66 – 70	80
TOS (h)	50 – 220	50 – 400	260 – 440	300 – 450
Hydrocarbon Selectivity (C% basis)				
CH_4	2.1	2.1	2.6	2.4
C_2–C_4	13.9	14.9	18.4	14.6
C_5^+	84.0	83.0	79.0	83.0
Activity/Productivity				
g HC/g-Fe/h	0.46 – 0.56	0.37 – 0.53	0.76 – 0.81	0.93
Apparent rate constant (mmol H_2+CO/g-Fe/MPa/h)	200 – 300	130 – 250	280 – 350	430
Deactivation rate (% loss in conversion/day)	2.33	1.41	0.46	0.00

(a) Other process conditions: 260 ^oC, 2.1–2.2 MPa, H_2/CO = 2/3

B = Binder SiO_2; P = Precipitated SiO_2

During the first 198 h of F–T synthesis, the steady state CO_2 selectivity was about 44 % (Figure 33b). During testing at 2.2 MPa the CO_2 selectivity started to decrease with time (198 to 255 h) and stabilized at ~38 %. Upon returning to the baseline conditions at 312 h, the CO_2 selectivity increased to ~40 %, which is lower than the steady state value during the first 198 of testing. This is the result of lower conversion, which favors the primary hydrocarbon synthesis reaction. After H_2 and CO regenerations, the CO_2 selectivity increased with time, reaching 49 % at the end of the test.

Methane selectivity, decreased from about 5.3 % to 3.8 % during the first 53 hours of testing (Figure 34a). Between 54 and 198 h, CH_4 selectivity was fairly stable (3.8±0.2 %). It decreased to ~3.0 % when the reaction pressure was increased to 2.2 MPa (199–311 h). Upon returning to the baseline conditions, methane selectivity increased to 4.4 %. Unfortunately, both H_2 and CO regenerations were accompanied by significant increase in methane selectivity (7.6–8.0 % after 382 h).

Selectivity of C_5^+ hydrocarbons (liquids and wax) on the catalyst increased with time during the first 66 h. After that, it was stable at about 70 % until 198 h (Figure 34b). During testing at 2.2 MPa (200–310 h) the C_5^+ selectivity remained unchanged, but it decreased to 63 % upon returning to the baseline pressure of 1.5 MPa. These results show that catalyst deactivation had an adverse effect on hydrocarbon selectivity (more methane and less C_5^+ products). Liquid plus wax (C_5^+ products) selectivity decreased after the catalyst regeneration with H_2 and CO.

Overview

Performance of precipitated 100 Fe/3 Cu/5 K/16 SiO_2 catalyst synthesized following procedures similar to those used previously in our laboratory was significantly inferior in comparison to that of 100 Fe/3 Cu/4 K/16 SiO_2 catalyst used in runs SA–09496 and SA–21896 (Figures 31 and 32). Syngas conversion (i.e., catalyst activity) in run SB–19102, at the baseline conditions, was substantially lower than that in runs SA–09496 and SA–21896 (56 % vs. 77 %). Also, the catalyst used in run SB–19102 had relatively poor selectivity (more methane and less C_5^+ hydrocarbons) in comparison to the catalyst synthesized previously in our laboratory.

It seems that relatively poor performance of this catalyst is caused by some unknown errors made during its synthesis. In order to check this hypothesis another catalyst of the same composition was synthesized (PPS3516–2) according to our standard procedure, and it was tested in run SB–04803. Results from this test are described in the next section.

Run SB–04803 with PPS3516–2 catalyst

Selected activity and selectivity data from run SB–04803 with the PPS3516–2 catalyst are shown in Figures 35 and 36. Results from run SA–09496 with 100 Fe/3 Cu/4 K/16 SiO_2 (designated as PPS3416–4), which have been reported earlier [31], are also included for comparison. Both catalysts were pretreated under the same conditions (CO at 280 °C and 0.8 MPa for 8 h), and tested at baseline process conditions of 260 °C, 1.5 MPa, 3.9–4.0 Nl/(g-Fe/h)

and $H_2/CO = 2/3$. The catalysts were also tested at other process conditions, but these results are not shown in Figures 35 and 36.

In both tests, during the first 50–80 h on stream, the syngas conversion increased with time reaching 77–81 % (Fig. 35). After this induction period, which is typical for CO pretreated Fe catalysts; the conversion was fairly stable in both tests. The intrinsic activities of these two catalysts were similar, which is as expected (both catalysts were prepared by the same procedure and their compositions are the same, except for slightly higher K content of the PPS3516–2 catalyst). Both catalysts exhibited very high WGS activity. Selectivity to CO_2 increased quickly and stabilized at about 46–49 % (not shown).

Hydrocarbon selectivities (CH_4 and C_5^+) were similar in both tests (Fig. 36). Methane selectivity (carbon atom basis) decreased during the first 150 h of testing, reaching ~ 2.9 %. In run SB–04803, between 150 and 200 h, methane selectivity was about 2.7 %. Selectivity of C_5^+ hydrocarbons (liquids and wax) was high in both tests. After 130–150 hours of testing it was ~82 % (Fig. 36b).

Both catalysts were also tested at a higher reaction pressure of 2.2 MPa, but the gas space velocities used were not the same in both tests, which prevents one from making comparisons of activities in terms of syngas conversions. During testing at 2.2 MPa the PPS3416–4 catalyst (run SB–09496) did not deactivate with time, whereas the PPS3516–2 (run SB–04803) catalyst deactivated rapidly. In run SB–04803 at 203 h on stream, the reaction pressure was increased to 2.2 MPa and gas space velocity to 5.9 Nl/g-Fe/h, while keeping the feed composition and reaction temperature at their baseline values. After about 60 h at these process conditions the syngas conversion decreased from 78.5 % (at 202 h) to 45.8 % (at 264 h). After that the syngas conversion continued to decrease with time, but much more slowly; reaching 40 % at 364 h. On the other hand, the catalyst selectivity in run SB–04803 continued to improve during testing at 2.2 MPa. At the end of the test methane selectivity was 1.9 %, and C_5^+ selectivity was 85.5 %.

Performance of the PPS3516–2 catalyst at the baseline process conditions was excellent (high single pass conversion, high C_5^+ selectivity and catalyst productivity, and low methane selectivity) and similar to that of the PPS3416–4 catalyst, which has been tested extensively at TAMU [19,20,31]. The latter catalyst had the highest intrinsic activity and catalyst productivity among high α catalysts, and is ideally suited for production of high-quality diesel fuels (via hydrocracking of the F–T wax product) and $C_2 - C_4$ olefins [19,20]. Rapid catalyst deactivation that was observed in run SB–04803 upon increasing reaction pressure and gas space velocity to 2.2 MPa and 5.9 Nl/g-Fe/h, respectively, is attributed to small capacity of gas purification traps. This problem (rapid deactivation upon simultaneous increase of reaction pressure and gas space velocity) was also observed in several other tests (e.g. SB–19102, SB–30702 and SB–33802). Before commencement of the STSR test SB–09703 we installed larger gas purification traps and the deactivation rate during testing at 2.2 MPa was much slower as described later in this report.

STSR tests with spray-dried catalysts synthesized at TAMU from dry precursors

Three tests were conducted using precipitated catalyst precursors, which were synthesized previously at TAMU during DOE Contract DE−AC22−94PC93069 (catalysts 4 and 5 in Table 1).

Run SB−16502 with DPS5624−2 catalyst

Spray-dried 100 Fe/5 Cu/6 K/24 SiO_2 catalyst was tested in run SB−16502 and results are shown in Figures 37 and 38. Results from run SB−25397 with precipitated 100 Fe/5 Cu/6 K/24 SiO_2 catalyst (batch 3) are included for comparison. The precipitated catalyst was pretreated using CO/He = 1/10 at 280 °C, 0.8 MPa, 5500 cm^3/min for 8 h, whereas the spray-dried catalyst was pretreated with pure CO at 660 cm^3/min (the other conditions being the same as for the precipitated catalyst).

Syngas conversion increased with time in both tests reaching 49 % at 100 h in run SB−16502, and 70 % at 20 h in run SB−25397 (Fig. 37). In this case the observed values of conversions can't be used directly for comparison of catalyst activities, due to differences in gas space velocities employed in two tests (4 Nl/g-Fe/h in run SB−16502 vs. 3.3 Nl/g-Fe/h in run SB−25397). However, it is clear that the precipitated catalyst is more active than the spray-dried one, since the syngas conversion is 40 % higher with the former, whereas the gas space velocity is only 20 % smaller. Upon increasing simultaneously the reaction pressure and gas space velocity, while keeping gas residence time constant, the syngas conversions did not change markedly during testing at 2.2 MPa (Figure 37). The syngas conversion decreased slightly to ~36 % in run SB−16502 (161−295 h), whereas it increased slightly to ~74 % in run SB−25397 (117−295 h). Catalyst stability at a higher reaction pressure was good in both tests.

Methane selectivity on the spray-dried catalyst was about 5 % during testing at 1.5 MPa, and ~4.5 % during testing at 2.2 MPa. The corresponding values of methane selectivity on the precipitated catalyst were lower: ~3.9 % at 1.5 MPa and 3 % at 2.2 MPa (Figure 38a). Selectivity to C_5^+ hydrocarbons was markedly higher on the precipitated catalyst (run SB−25397) at both 1.5 MPa and 2.2 MPa (Fig. 38b).

In summary, precipitated 100 Fe/5 Cu/6 K/24 SiO_2 catalyst (from batch 3) was more active, and had markedly better selectivity (less methane and more C_5+ hydrocarbons) than spray-dried catalyst of the same composition (prepared from batch 5). While batch to batch differences and slight differences in catalyst pretreatments may have had some effect on the catalyst performance, we believe that the major differences in performance were due to steps introduced during spray drying of the catalyst used in run SB−16502. We suspect that this is mainly due to presence of impurities in the spray-dried catalyst. We collected 128 g of material from the bottom of cyclone separator, but obtained only 66 g after calcination at 300 °C for 5 h. Obviously, the spray drying chamber and/or the line connecting the chamber with the cyclone had a residual material left from the previous use. This material is partially volatile, but some impurities may have been retained on the catalyst even after calcination at 300 °C, and this may have had an adverse effect on the catalyst performance.

Runs SB–22102 and SB–28402 with DPS3616 catalyst

Run SB–22102 with spray-dried 100 Fe/3 Cu/6 K/16 SiO_2 catalyst was terminated after only 57 h on stream. No meaningful data were obtained during the test due to problems with fluctuating tail gas flow rate and faulty mass flow meter (vide infra). After the test it was found that the backpressure regulator was clogged with liquid (waxy) products resulting in flow fluctuations, whereas the mass flow meter did not function properly giving wrong values for feed gas flow rate.

The same catalyst was tested again in the STSR test SB–28402. Syngas conversion increased with time, reaching 63 % at 80 h, and then remained stable up to 100 h (Fig. 39). However, it declined from 62.7 % to 53.2 % during the next 10 h. This may have been caused by N_2 back-flushing of the wax filter, to facilitate wax removal from the reactor. After that the conversion increased to about 60 % at 134 h, and it remained at this value until the test was terminated at 170 h. The reason for relatively early run termination was the fact that we were unable to withdraw any wax from the reactor. We attribute the latter to particle breakup and blocking of a metal porous filter.

Methane selectivity on the catalyst was very low, and fairly stable after 100 h on stream (~2.2 %). Also, the C_5^+ selectivity on this catalyst was high (80–83 %), and was relatively stable during 170 h of testing (Fig. 40).

Catalyst activity at the baseline process conditions (i.e., synthesis conversion of 61.3%) was not as high as that on the precipitated Fe catalyst of similar composition tested in run SB–04803 (Fig. 35). Thus, spray drying of a dry precursor seems to yield a lower catalyst activity, which was also observed in run SB–16502 with the DPS35624–2 catalyst. On the other hand, the catalyst selectivity of the spray-dried catalyst was slightly better (lower methane and higher C_5^+) than the corresponding selectivity of the PPS3516–2 catalyst used in run SB–04803.

As can be seen from a SEM micrograph (Fig. 4a) the DPS3516 catalyst had a very large number of small particles after spray drying. A median size of this catalyst at TOS = 0 h was about 30 μm, and about 18 % of particles were smaller than 10 μm in diameter. The presence of a large number of small particles had caused plugging of a metal porous filter of nominal pore size of 2 μm during the STSR test SB–28402.

<u>STSR tests with spray-dried catalysts synthesized at TAMU from wet precursors</u>

Catalysts WCS3516–1, WTO3516–1 and WPS3516–4 were spray-dried at TAMU from wet slurries having the same composition (100 Fe/3 Cu/5 K/16 SiO_2) but were prepared using different sources of silica (Table 1). Results illustrating catalyst activity and selectivity in STSR tests of these three catalysts are shown in Figures 41 to 44. Results from run SB–04803 with a precipitated (not spray-dried) Fe catalyst PPS3516–2 of the same composition are included for comparison. Catalysts PPS3516–2 and WPS3516–4 were prepared from the same wet precursor (100 Fe/3 Cu/16 SiO_2).

Syngas conversion at the baseline process conditions (260 °C, 1.5 MPa, 4 Nl/g-Fe/h) increased initially with time in all four tests (Fig. 41). After reaching a maximum value (50–70 h on stream) it either stabilized (SB–30702) or started to slowly decrease with time. As can be seen from Fig. 41, the precipitated (not spray-dried) catalyst in run SB–04803 was the most active (maximum conversion of 80 %) whereas in three tests with the spray-dried catalysts the maximum conversion was between 71 % (SB–09703) and 76 % (SB–33802).

Methane and C_5^+ selectivities at the baseline conditions are shown in Fig. 42. General trend is that methane selectivity decreased whereas C_5^+ selectivity increased with time, before reaching a steady state value. The best selectivity (the least amount of methane and the maximum amount of C_5^+ products) was obtained in run with the spray-dried catalyst in run SB–09703. However, it is to be noted that selectivity was excellent in all four tests, methane selectivity ranged from 2.2 to 3.5 %, whereas that of C_5^+ products was between 78 and 86 % (both on C–atom basis).

All four catalysts were also evaluated at a higher reaction pressure (2.2 MPa) and gas space velocity of 5.9 Nl/g-Fe/h (to keep the gas residence time constant), and results are shown in Figures 43 and 44. Upon increasing reaction pressure, in three of the four tests (i.e., runs SB–30702, SB–33802 and SB–04803), the syngas conversion decreased rapidly during the first 30 h, and then either stabilized or continued to decrease slowly with time (Fig. 43). A different trend (i.e., no rapid deactivation upon increasing reaction pressure to 2.2 MPa) was observed in run SB–09703 with spray-dried WPS3516–4 catalyst. We believe that rapid catalyst deactivation in these three tests (with catalysts prepared by different methods) was not the result of intrinsic instability of these three catalysts at high reaction pressure, but that it was caused by inefficient gas purification traps. Prior to commencement of the STSR test SB–09703, in which we did not observe a rapid catalyst deactivation during testing at 2.2 MPa, we installed a larger trap for iron carbonyl removal, and replaced trap material in all other gas purification traps.

Methane and C_5^+ selectivities at 2.2 MPa and gas space velocity of 5.9 Nl/g-Fe/h are shown in Fig. 44. By comparing data at different reaction conditions (Figs. 42 and 44) we note that selectivity improved during testing at 2.2 MPa in runs SB–04803 and SB–09703. For example, in run SB–09703 methane selectivity was very low 1.8 %, whereas selectivity of C_5^+ products was as high as 87 % at the end of the test. In run SB–30702 the selectivities at 2.2 MPa were initially better than those at 1.5 MPa, but towards the end C_5^+ selectivity started to decrease (from 81 % to 77 %), whereas methane selectivity increased from 2.4 % to 2.9 %. However, the latter value is still lower than that obtained during testing at 1.5 MPa (about 3.5 % - Fig. 42). On the other hand, during testing at 2.2 MPa in run SB–33802 the selectivity started to shift towards lighter products (more methane and less liquid + wax products). At the end of the run methane selectivity was 2.8 % and C_5^+ selectivity was 75 %. In this case, the catalyst deactivation had a negative impact on hydrocarbon product distribution.

In summary the catalyst productivity on spray-dried catalysts was about 5–10 % lower, than that on the precipitated (not spray-dried) catalyst of the same composition. Spray-dried WPS3516–4 catalyst (K_2SiO_3 as the source of silica) had the best selectivity toward high molecular weight hydrocarbons. Unfortunately, the attrition strength of this catalyst (as well as that of WTO3516–1 catalyst) could not be quantified due to inability to completely remove residual

hydrocarbon wax from the catalyst particles at the end of run SB−09703. Spray-dried WCS3516−1 catalyst (run SB−30702) had excellent attrition strength, but it produced less high molecular weight products.

Conclusions

Attrition strength of various types of iron F−T catalysts was studied under reaction conditions in a stirred tank slurry reactor. The attrition behavior was evaluated on the basis of observed changes in morphological properties (via SEM), and changes in particle size distribution after F−T synthesis in the STSR. In the latter case, PSD measurements were performed using the Coulter Counter Multisizer. The catalysts used in this study can be classified in the following four groups: (1) precipitated (not spray-dried) catalysts; (2) spray-dried catalysts prepared from vacuum dried precursors; (3) spray-dried catalysts prepared from wet precursors at TAMU; and (4) spray-dried catalysts synthesized at Hampton University. First we'll summarize our findings on the attrition strength of these four groups of catalysts, and then provide concluding remarks on their catalytic performance.

The attrition properties of precipitated catalysts with nominal compositions 100 Fe/3 Cu/5 K/16 SiO_2 (catalysts PPS3516−1 and PPS3516−2) and 100 Fe/5 Cu/4.2 K/25 SiO_2 (commercial Ruhrchemie catalyst) were evaluated in STSR tests SB−19102, SB−04803 and SB−32901. In all three tests the particle size reduction due to fracture was moderate, whereas attrition by erosion was small. All three precipitated Fe F−T catalysts have had relatively high attrition strength, under reaction conditions in the STSR reactor after 364−497 h of testing. The observed reductions in the volume moment diameter were 14.3−18.6 %, whereas the increase in fraction of particles smaller than 10 μm was between 2.6 and 7.8 %. It is obvious that precipitated silica, which was used as a binder, provides strong interlocking forces between the primary particles. The observed increase in fraction of fine particles is similar to that observed in tests with spray dried catalysts (HU1112 and HU3471) synthesized at Hampton University (Table 2).

Spray-dried catalyst particles, prepared from vacuum dried Fe/Cu/K/SiO_2 precursors, were largely of irregular shape (SEM micrographs) except for small particles, which were nearly spherical (Figure 4). Particle morphology and attrition strength of spray-dried DPS5624−2 catalyst (100 Fe/5 Cu/6 K/24 SiO_2) tested in run SB−16502 were similar to those of precipitated (not spray-dried). After 295 h of testing, the observed reduction in the volume moment was 16.1 %, whereas the increase in fraction of fine particles was 2.3 % (Table 2). The attrition strength of DPS3616 catalyst tested in run SB−28402 was not determined quantitatively. However, this test had to be terminated prematurely after 170 h on stream, due to clogging of a porous metal filter used for wax withdrawal from the reactor. This fact implies that the catalyst particles had disintegrated, and is an indication of poor attrition strength. Thus, spray drying of dry precursors did not impart any additional strength, at least not under conditions employed in the present study.

Spray-dried catalysts prepared from wet precursors at TAMU had excellent sphericity and smooth external surfaces (Figures 5 and 6). The particle size distribution was rather broad

ranging from 5 μm to 40 μm in diameter, regardless of the source of silica used. The observed morphology of spray-dried catalysts (APV Anhydro Lab S1 unit) is ideally suited for use in slurry reactors, but the particles were smaller than intended (30–70 μm) due to limitations of small-scale equipment used for spray drying. Catalysts WCS3516–1, WTO3516–1 and WPS3516–4 were spray-dried from wet slurries having the same composition (100 Fe/3 Cu/16 SiO_2) but were prepared from different silica sources. Colloidal silica, TEOS and potassium silicate, respectively, were used as sources of silica in preparation of these three catalysts. All three catalysts were impregnated with potassium by incipient wetness impregnation after spray drying, and were tested in STSR runs SB–30702, SB–33802 and SB–09703 (300–364 h on stream).

WCS3516–1 catalyst (prepared from colloidal silica) had the highest attrition strength among all catalysts studied during the course of this project. After 345 h of testing in the STSR the catalyst morphology remained practically unchanged (Fig. 20) and PSD measurements showed small reductions in the volume mean diameter (5.4 %) and very small increase in the fraction of fine particles (0.7 %). After testing in the STSR WTO3516–1 and WPS3516–4 catalysts lost their sphericity due to attrition and agglomeration effects (Figures 23 and 26). The presence of large irregularly shaped particles has been attributed to micro-spherical particle breakup and encapsulation by residual wax. The attempts to remove the wax through multiple washings with hot Varsol 18, CS_2, n-hexane followed by Soxhlet extraction (with xylenes for 48 h, followed by 48 h of extraction with MEK) were only partially successful. In spite of the absence of reliable results from PSD measurements with WTO3516–1 and WPS3516–4 catalysts, it is clear that the spray dried WCS3516–1 was more attrition resistant than the other two spray-dried catalysts. However, we do not feel that generalization of these findings (i.e., colloidal silica is a better binder than silica from TEOS or potassium silicate) would be justified at this point. We performed spray drying with small amounts of wet precursors, and have not optimized the spray drying conditions for any of these three types of catalysts.

Three spray-dried catalysts prepared at HU were tested in the STSR for 380–450 hours. Catalysts HU2061 and HU1112 contain 11 and 16 parts of precipitated silica (from TEOS), respectively, whereas catalyst HU3471 contains 1.1 parts of silica binder per 100 parts of Fe. Mechanical integrity of catalysts HU2061, HU1112 and HU3471 was markedly dependent upon their morphological features. The attrition strength of catalysts made out of largely spherical particles (HU1112 and HU3471) was considerably higher than that of the HU2061 catalyst consisting of irregularly shaped particles (i.e. plate-like particles). The latter catalyst experienced large changes in Sauter mean and volume moment diameters (85 and 65.7 %, respectively) after 380 h of testing in the STSR. The inferior attrition strength of this catalyst is also reflected in considerable generation of fine particles (less than10 μm in diameter) during the STSR test (62.5 %). Both HU1112 and HU3471 catalysts lost their sphericity after ~450 hours in the STSR (Figures 8b and 9b). However, the generation of fine particles was relatively small (6.7 and 3.7 %). HU1112 and HU3471 had similar reductions in their Sauter mean diameters (32.7 and 40.1 %, respectively) after testing in the STSR. On the other hand, the change in volume moment diameter for these two catalysts showed an unexpected behavior. The volume moment diameter of HU1112 catalyst decreased by 5.7 % only (Table 2), whereas that of HU3471 catalyst increased by 2.2 % (listed as -2.2 % in Table 2). This has been attributed to

agglomeration of particles in the presence of residual wax, which was not completely removed during washing with hot Varsol 18 solvent.

In order to assess catalytic performance of the catalysts tested in this study, we have used TAMU's precipitated catalysts of similar compositions as benchmarks. TAMU's precipitated catalyst PPS3416–4 (100 Fe/3 Cu/4 K/16 SiO_2) was found to have the highest intrinsic activity and catalyst productivity, among high alpha iron F–T catalysts, as well as excellent selectivity (low methane and high yield of C_5^+ hydrocarbons) as reported earlier [19,20,31].

Catalytic performance of precipitated (not spray-dried) TAMU's catalyst PPS3516–2 at baseline process conditions (260 °C, 1.5 MPa, 4 Nl/g-Fe/h and H_2/CO = 2/3) was excellent (syngas conversion of 81 %, methane selectivity of 2.7 %, and C_5^+ selectivity of 82 %). This is quite similar to the performance of PPS3416–4 catalyst (Figs. 35 and 36). Catalytic performance of the other precipitated catalysts (PPS3516–1, Ruhrchemie catalyst) and spray-dried catalysts prepared from dry precursors (DPS3616 and DPS5624–2) was very good, but their productivity was lower and their selectivity less favorable (more light hydrocarbon products) in comparison to that of the PPS3416–4 catalyst.

Spray-dried catalysts, synthesized at Hampton University, with compositions 100 Fe/5 Cu/4.2 K/11 (P) SiO_2 and 100 Fe/5 Cu/4.2 K/1.1 (B) SiO_2 had excellent selectivity characteristics (methane selectivity of 2 %, and C_5^+ selectivity of about 85 %) but their activity and stability (deactivation rate) need to be improved significantly. Spray-dried HU1112 catalyst (100 Fe/3 Cu/4 K/16 (P) SiO_2) produced more methane (3.5 %) and less C_5^+ hydrocarbons (77 %) than the other two spray-dried catalysts and the TAMU's precipitated catalyst of the same composition. Its productivity and stability were better than those of the other two spray-dried catalysts synthesized at HU, but inferior in comparison to the PPS3416–4 catalyst (Table 4 and Figure 31).

Catalytic performance of catalysts WCS3516–1, WTO3516–1 and WPS3516–4, prepared by spray drying from wet slurries of the same composition (100 Fe/3 Cu/4 K/16 SiO_2), at the baseline process conditions was excellent (Figs. 41 and 42). Syngas conversion was between 71 and 76 %, whereas methane selectivity was between 2.2 and 3.5 % and that of C_5^+ hydrocarbons was between 78 and 86 % (all selectivities are on C–atom basis). Catalyst productivities were 5–12 % lower than that of precipitated (not spray-dried) PPS3516–2 catalyst of the same composition, whereas hydrocarbon selectivities were similar. Spray-dried WCS3516–1 catalyst (run SB–30702) had the most superior strength but it produced more light hydrocarbons than the other two spray-dried catalysts.

The primary project objectives have been achieved. We were successful in synthesizing both precipitated and spray-dried iron F–T catalysts with adequate attrition strength and desirable F–T activity and selectivity for use in SBCR for converting coal-derived synthesis into liquid fuels.

Acknowledgements

The continuing financial support from the US DOE of our research on conversion of coal-derived synthesis gas to transportation fuels is gratefully acknowledged. We thank Mr. Donald Krastman, DOE Project Manager, for his continuing interest in this project. Also, we are grateful to: Drs. S. Koseoglu and S. Gregory (Food and Protein Research Center at TAMU) for allowing us to use spray driers, Professor Adeyinka Adeyiga (Department of Chemical Engineering at Hampton University) for providing several spray-dried catalysts, Professor Jim Bonner (Department of Civil Engineering at TAMU) for use of the Coulter Counter Multisizer, and Microscopy and Imaging Center at TAMU for assistance with SEM measurements.

References

[1] H. Kölbel and M. Ralek, *Catal. Rev. - Sci. Eng.* 21 (1980) 225.
[2] B. Jager and R. Espinoza, *Catal. Today* 23 (1995) 17.
[3] B. Jager, P. Van Berge and A. P. Steynberg, *Stud. Surf. Sci. Catal.* 136 (2001) 63.
[4] B. L. Bhatt, E. S. Schaub, E. C. Hedorn, D. M. Herron, D. W. Studer and D. M. Brown, in: *Proc. of Liquefaction Contractors Review Conference*, eds. G. J. Stiegel and R. D. Srivastava, U. S. Department of Energy, Pittsburgh, 1992, p. 403.
[5] D. S. Kalakkad, M. D. Shroff, S. Kohler, N. Jackson and A. K. Datye, *Appl. Catal. A* 133 (1995) 335.
[6] A. K. Datye, M. D. Shroff, Y. Jin, R. P. Brooks, M. S. Harrington, A. G. Sault and N. B. Jackson, *Stud. Surf. Sci. Catal.* 101 (1996) 1421.
[7] R. Srinivasan, L. Xu, R. L. Spicer, F. L. Tungate and B. H. Davis, *Fuel Sci. Technol. Int.* 14 (1996) 1337.
[8] H. N. Pham, J. Reardon and A. K. Datye, *Powder Technol.* 103 (1999) 95.
[9] R. Zhao, J. G. Goodwin Jr. and R. Oukaci, Appl. Catal. A 189 (1999) 99.
[10] H. N. Pham, A. Viergutz, R. J. Gormley and A. K. Datye, *Powder Technol.* 110 (2000) 196.
[11] R. J. O'Brien, L. Xu, S. Bao, A. Raje and B. H. Davis, *Appl. Catal. A* 196 (2000) 173.
[12] R. Zhao, J. G. Goodwin Jr., Jothimurugesan, K., Gangwal, S.K. and Spivey, J.J., *Ind. Eng. Chem. Res.* 40 (2001) 1065.
[13] R. Zhao, J. G. Goodwin Jr., Jothimurugesan, K., Gangwal, S.K. and Spivey, J.J., *Ind. Eng. Chem. Res.* 40 (2001) 1320.
[14] D. Wei, Goodwin Jr., J.G., R. Oukaci and A. H. Singleton, *Appl. Catal. A* 210 (2001) 137.
[15] K. Sudsakorn, J. G. Goodwin Jr., K. Jothimurugesan and A. A. Adeyiga, *Ind. Eng. Chem Res.* 40 (2001) 4778.
[16] H. N. Pham, L. Nowicki, J. Xu, A. K. Datye, D. B. Bukur and C. Bartholomew, *Ind. Eng. Chem. Res.* 42 (2003) 4001.
[17] W. Pietsch, *Chem. Eng. Prog.* 92 (1996) 185.
[18] D. B. Bukur, L. Nowicki and X. Lang, *Chem. Eng. Sci.* 49 (1994) 4615.
[19] D. B. Bukur and X. Lang, *Stud. Surf. Sci. Catal.* 119 (1998) 113.
[20] D. B. Bukur and X. Lang, *Ind. Eng. Chem. Res.,* 38 (1999) 3270.
[21] D. B. Bukur, X. Lang, J. A. Rossin, W. H. Zimmerman, M. P. Rosynek, E. B. Yeh and C. Li, *Ind. Eng. Chem. Res.* 28 (1989) 1130.

[22] D. B. Bukur, X. Lang, D. Mukesh, W. H. Zimmerman, M. P. Rosynek and C. Li, *Ind. Eng. Chem. Res*. 29 (1990) 1588.
[23] K. Jothimurugesan, J. J. Spivey, S. K. Gangwal and J. G. Goodwin Jr., *Stud. Surf. Sci. Catal.,* 119 (1998) 215.
[24] K. Jothimurugesan, J. G. Goodwin Jr., S. K. Gangwal and J. J. Spivey, *Catal. Today*, 58 (2000) 335.
[25] D. B. Bukur, S. Patel and X. Lang, *Appl. Catal.* 61 (1990) 329.
[26] D. B. Bukur, L. Nowicki and S. A. Patel, *Canadian J. Chem. Eng*. 74 (1996) 399.
[27] D. B. Bukur, *Final Report* for U. S. DOE Contract No. DE-AC22-94PC93069, July 1999.
[28] D. B. Bukur, V. Carreto−Vazquez, L. Nowicki, A. K. Datye and H. N. Pham, *AIChE Annual Meeting*, San Francisco, CA, Nov. 16-21, 2003, Paper 505f.
[29] D. B. Bukur, L. Nowicki, R. K. Manne and X. Lang, X., *J. Catal*., 155 (1995) 366.
[30] D. B. Bukur, L. Nowicki and X. Lang, X., *Stud. Surf. Sci. Catal.*, 107 (1997) 163.
[31] D. B. Bukur, X. Lang and Y. Ding, *Appl. Catal.* A 186 (1999) 255.

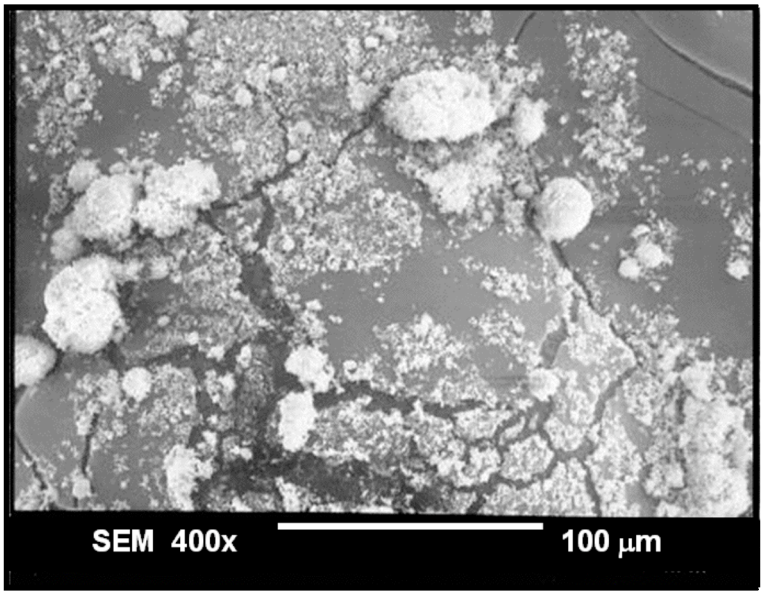

Figure 1a. SEM image of spray-dried Fe_2O_3 (from Bayer). The resulting powder consists of small irregularly shaped agglomerates

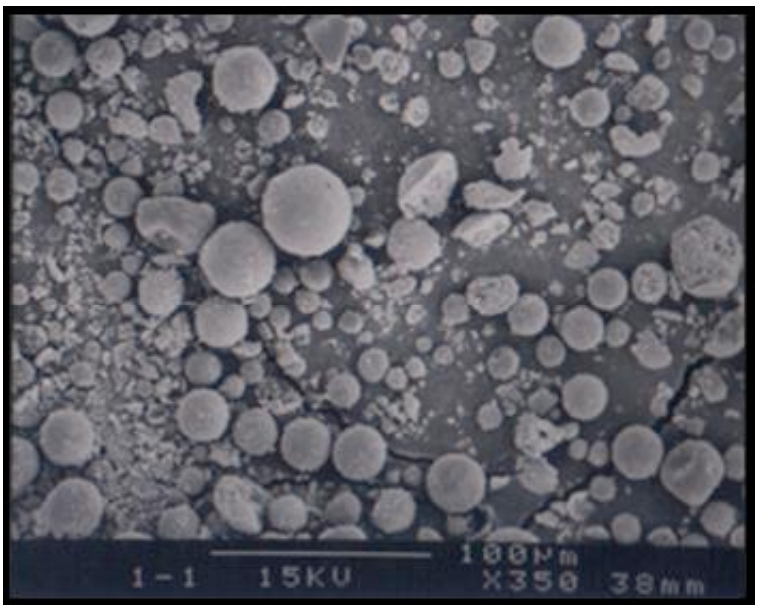

Figure 1b. SEM image of spray-dried Fe_2O_3 / silica binder. Addition of silica binder results in formation of largely spherical agglomerates with smooth external surface

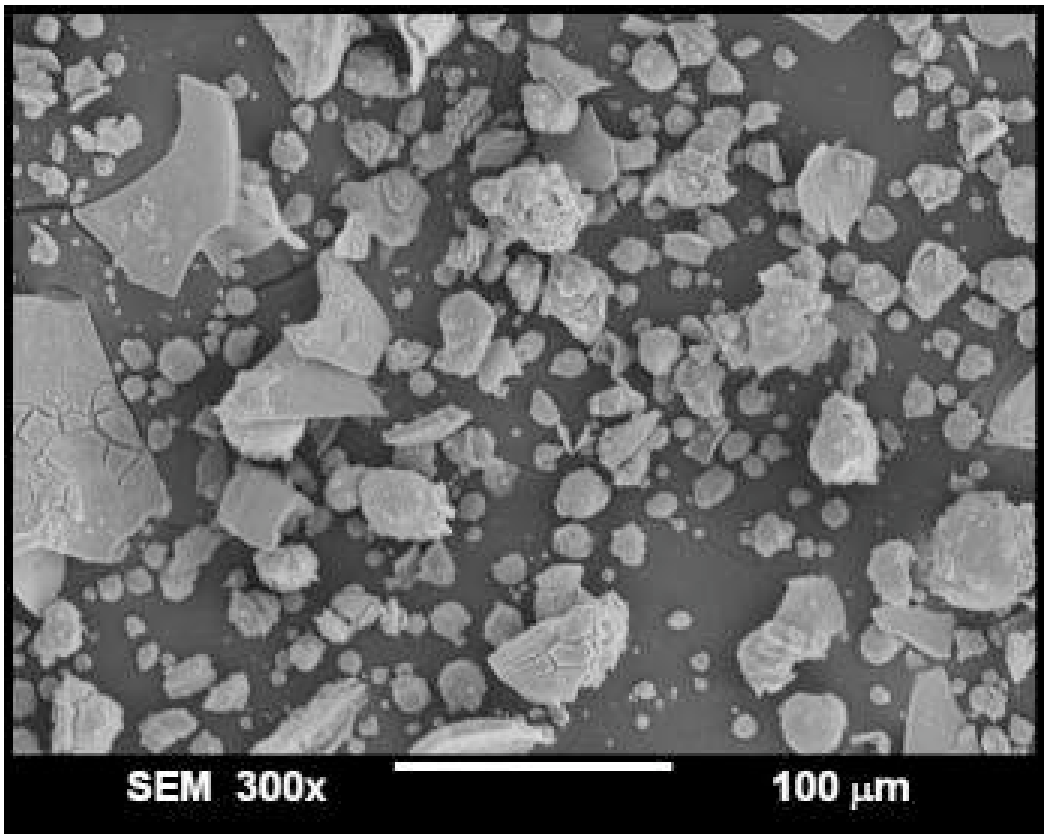

Figure 2. SEM image of spray-dried 100 Fe/5 Cu/4.2 K/11 (P) SiO_2 catalyst prepared at HU. Smaller particles (5-10 μm) are nearly spherical, whereas larger particles are of irregular shape, including some plate-like particles.

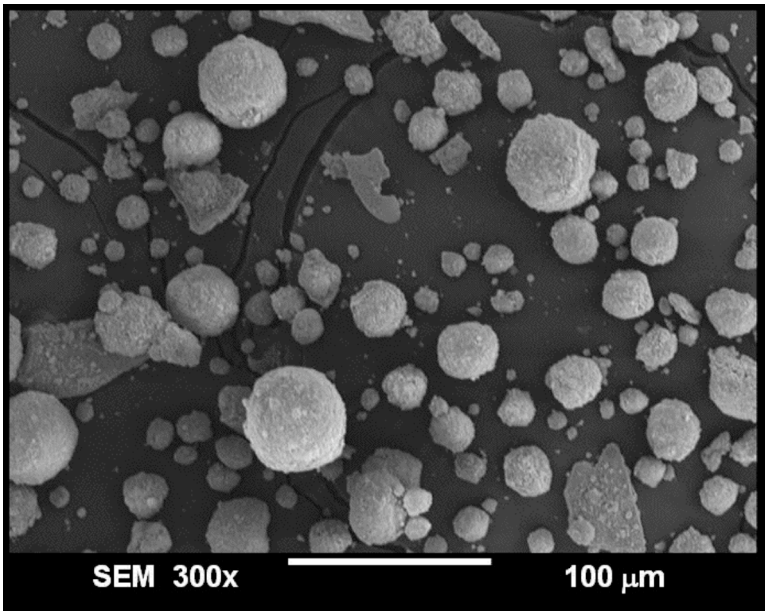

Figure 3a. SEM image of spray-dried 100 Fe/5 Cu/4.2 K/1.1 (B) SiO_2 catalyst prepared at HU.

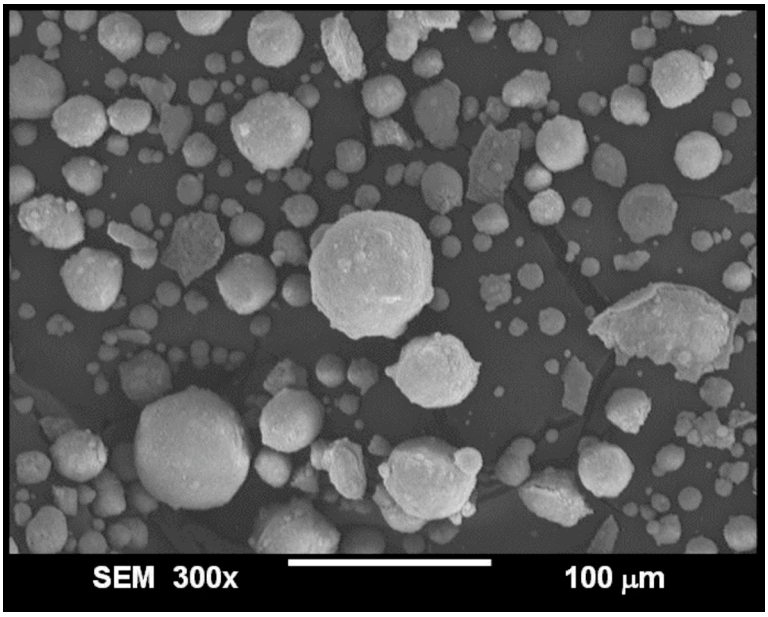

Figure 3b. SEM image of spray-dried 100 Fe/3 Cu/4 K/16 (P) SiO_2 catalyst prepared at HU. Majority of particles are nearly spherical, but external surfaces are relatively rough and smaller particles are attached to the surface.

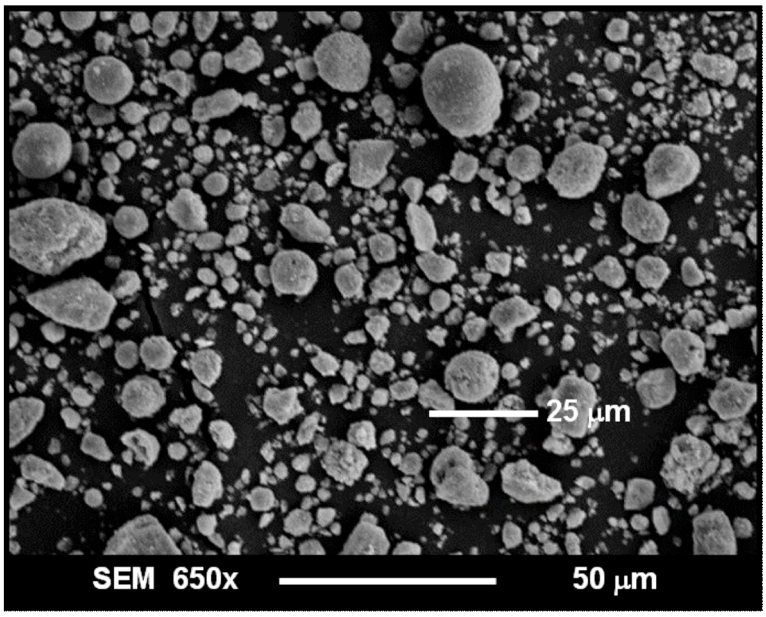

Figure 4a. SEM image of spray-dried TAMU catalyst (100 Fe/3 Cu/6 K/16 SiO_2 + 3wt % SiO_2 from Bindzil) prepared from vacuum dried precursor.

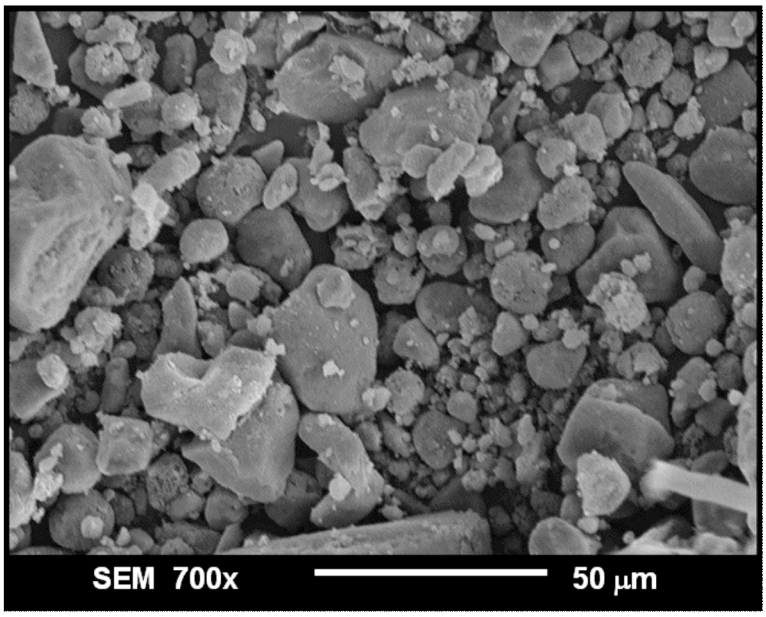

Figure 4b. SEM image of spray-dried TAMU catalyst (100 Fe/5 Cu/6 K/24 SiO_2) prepared from vacuum dried precursor.

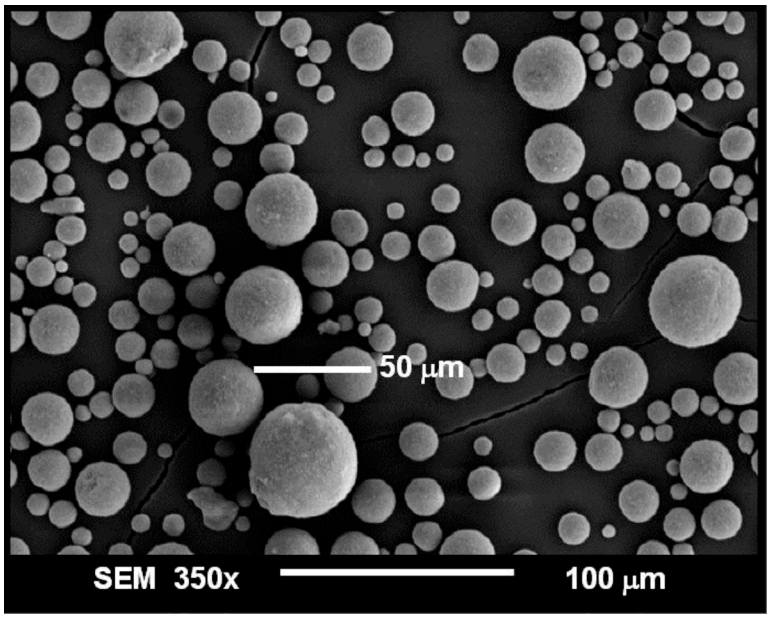

Figure 5a. SEM image of spray-dried TAMU catalyst (100 Fe/3 Cu/5 K/16 SiO_2 + 3wt % SiO_2 from Bindzil) prepared from wet precursor (No. 8 in Table 1).

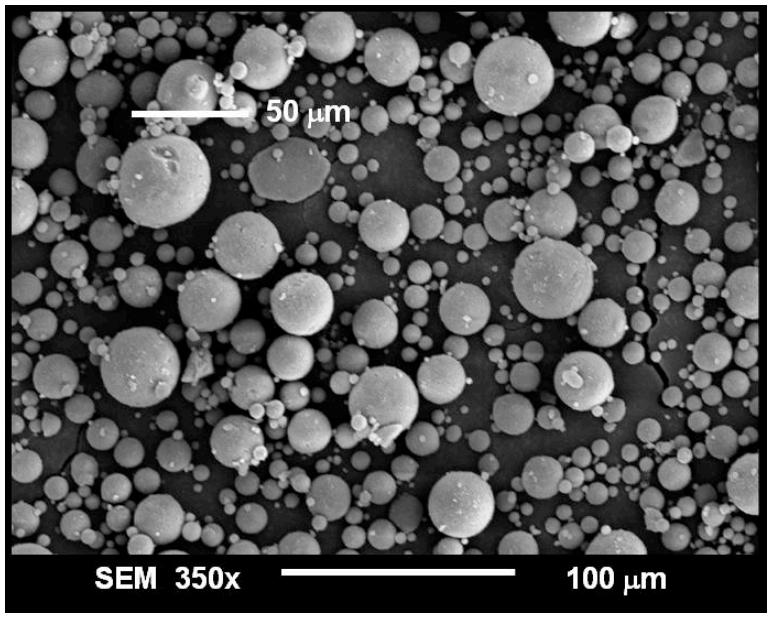

Figure 5b. SEM image of spray-dried TAMU catalyst No. 12 in Table 1 prepared from wet precursor using colloidal silica. The catalyst was impregnated with potassium after spray-drying, and particles have excellent sphericity and smooth external surfaces.

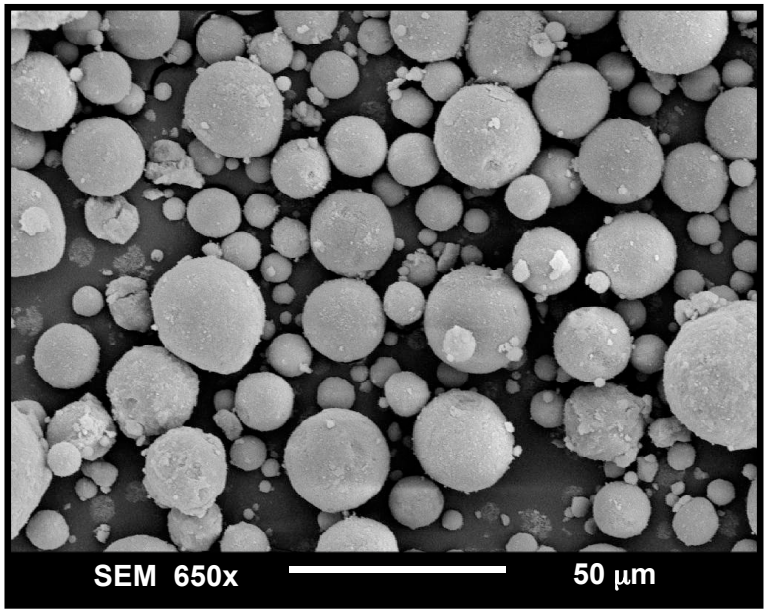

Figure 6a. SEM image of WPS3516-4 catalyst (No. 11 in Table 1) prepared by spray drying. Potassium was added by IWI after spray drying.

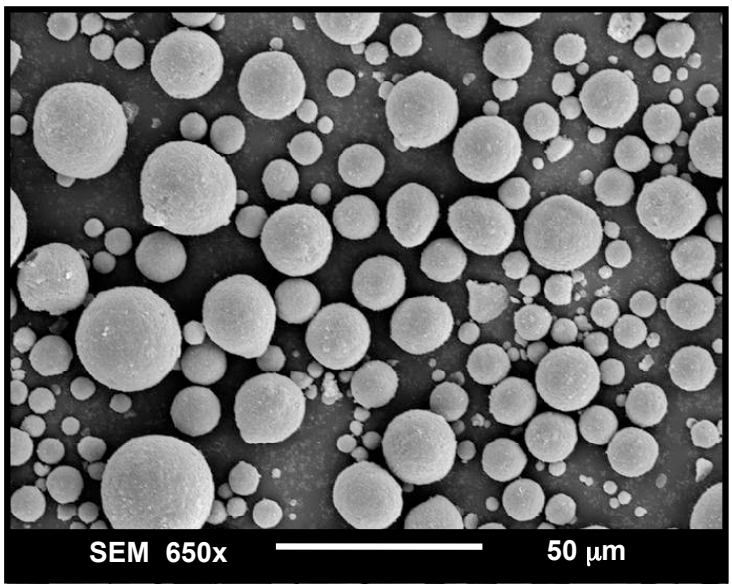

Figure 6b. SEM image of WTO3516-1 catalyst (No. 14 in Table 1) prepared by spray drying. Potassium was added by IWI after spray drying.

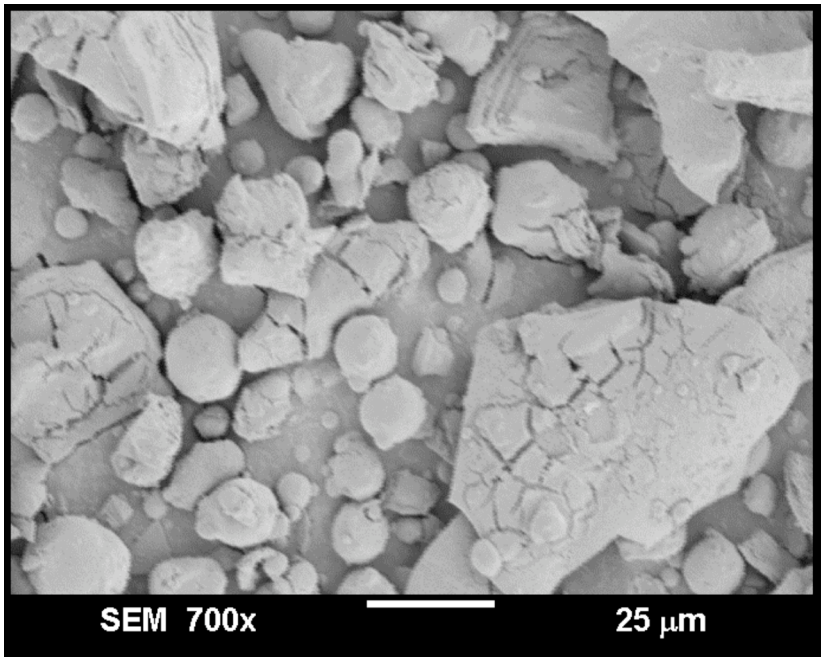

(a) TOS = 0 h

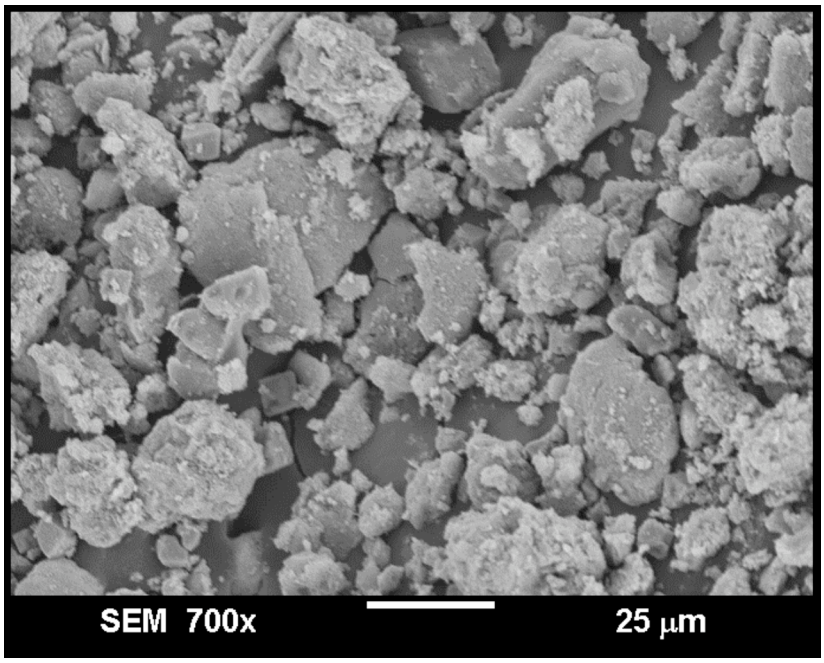

(b) TOS = 380 h

Figure 7. SEM images of spray-dried 100 Fe/5 Cu/4.2 K/11 (P) SiO_2 catalyst used in STSR test SB-20601.

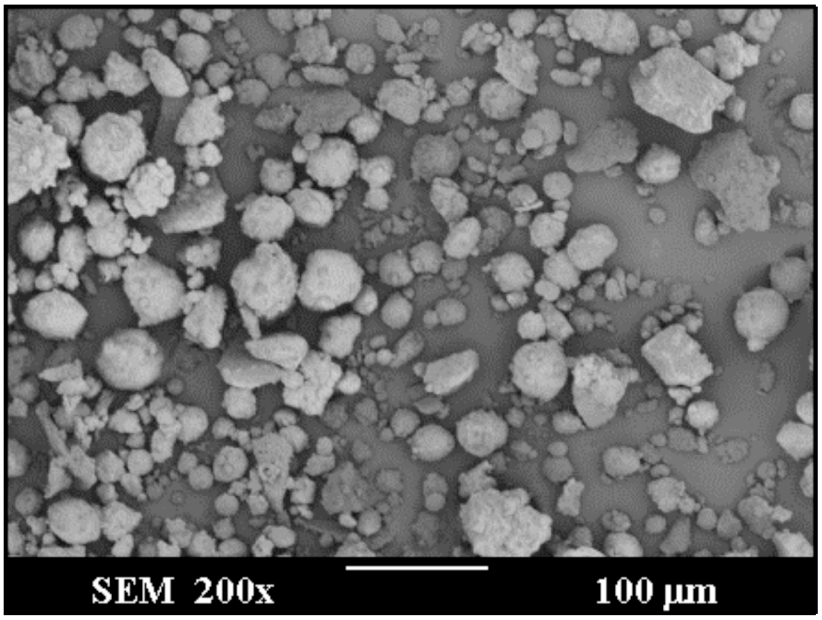

(a) TOS = 0 h

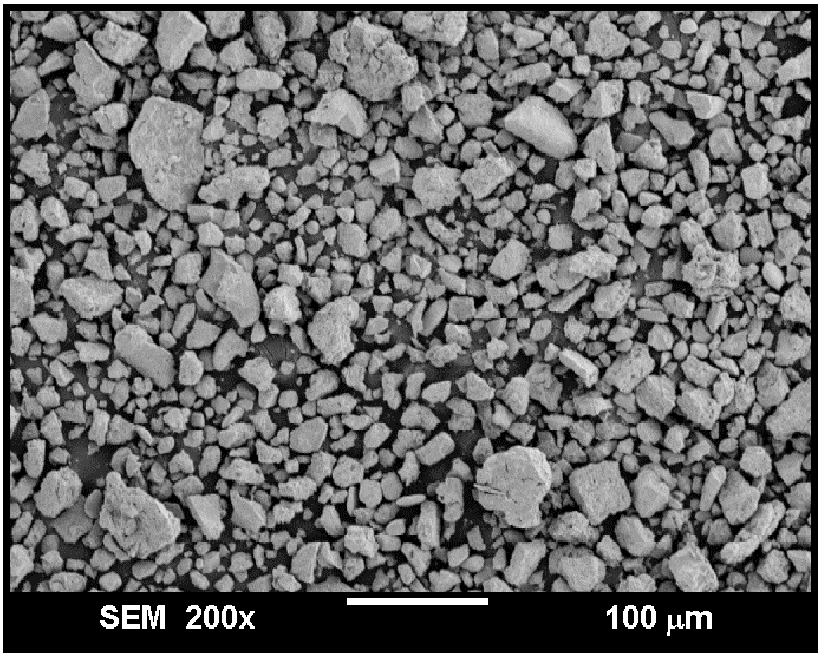

(b) TOS = 449 h

Figure 8. SEM images of spray-dried 100 Fe/5 Cu/4.2 K/1.1 (B) SiO_2 catalyst used in STSR test SB-34701.

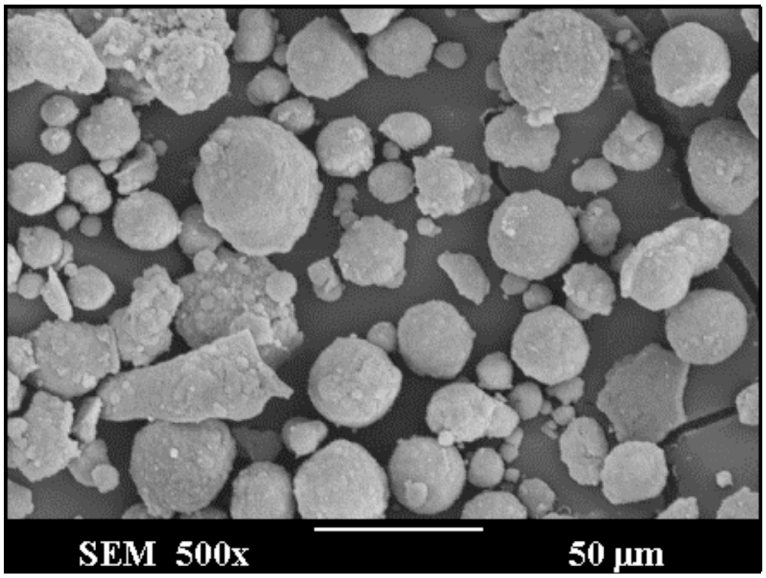

(a) TOS = 0 h

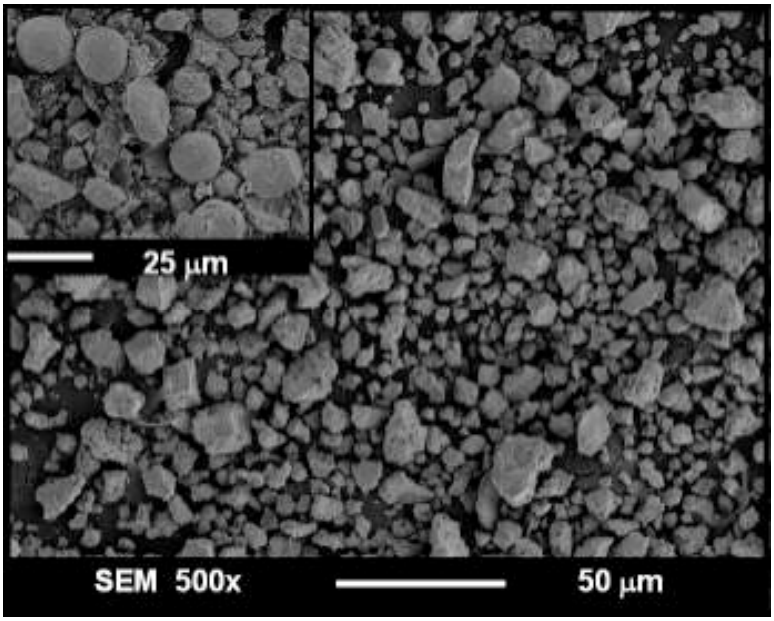

(b) TOS = 450 h

Figure 9. SEM images of spray-dried 100 Fe/3 Cu/5 K/16 (P) SiO_2 catalyst used in STSR test SB-11102.

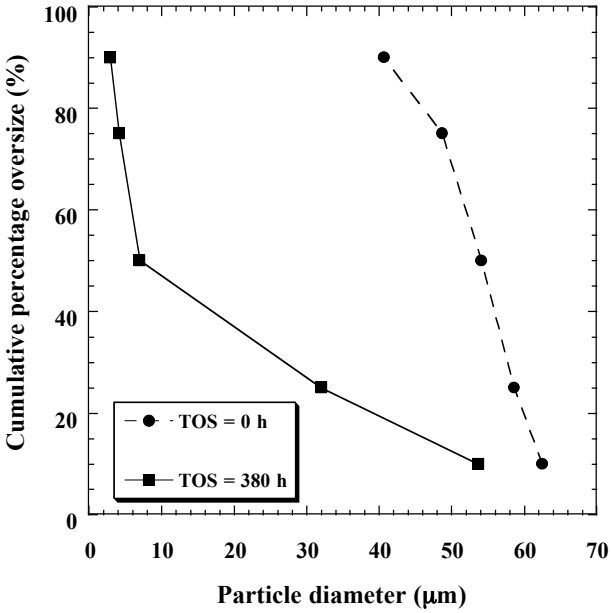

(a) SB-20601

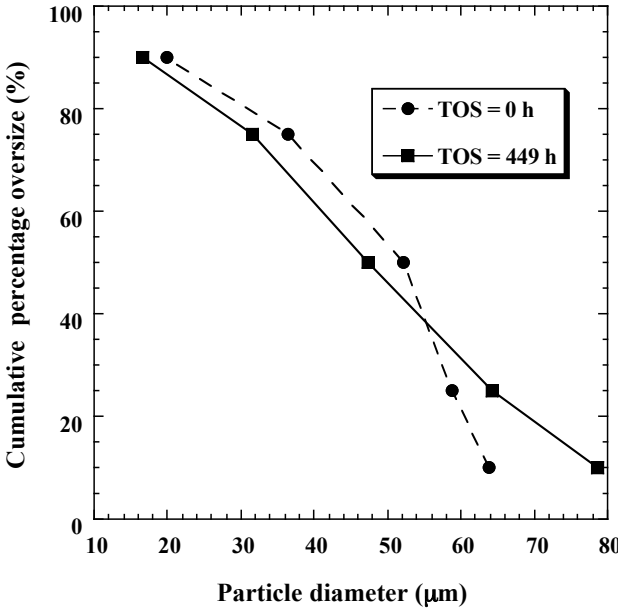

(b) SB-34701

Figure 10. Changes in PSD of HU2061 and HU3471 catalysts during F-T synthesis in STSR tests SB-20601 and SB-34701.

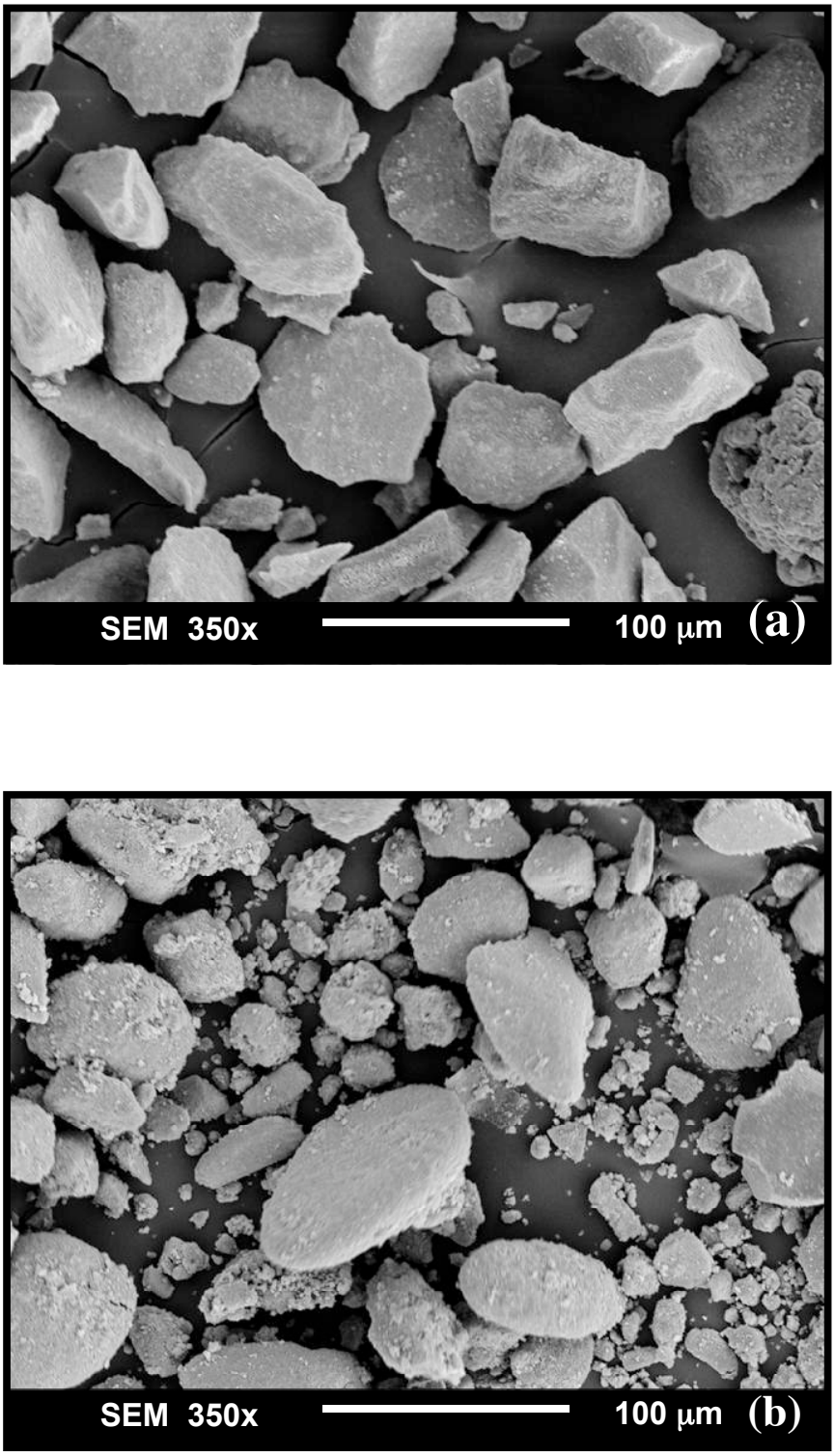

Figure 11. SEM image of PPS3516-1 (100 Fe/3 Cu/5 K/16 SiO_2 catalyst): (a) before F-T synthesis; (b) after 497 h of F-T synthesis in the STSR (run SB-19102).

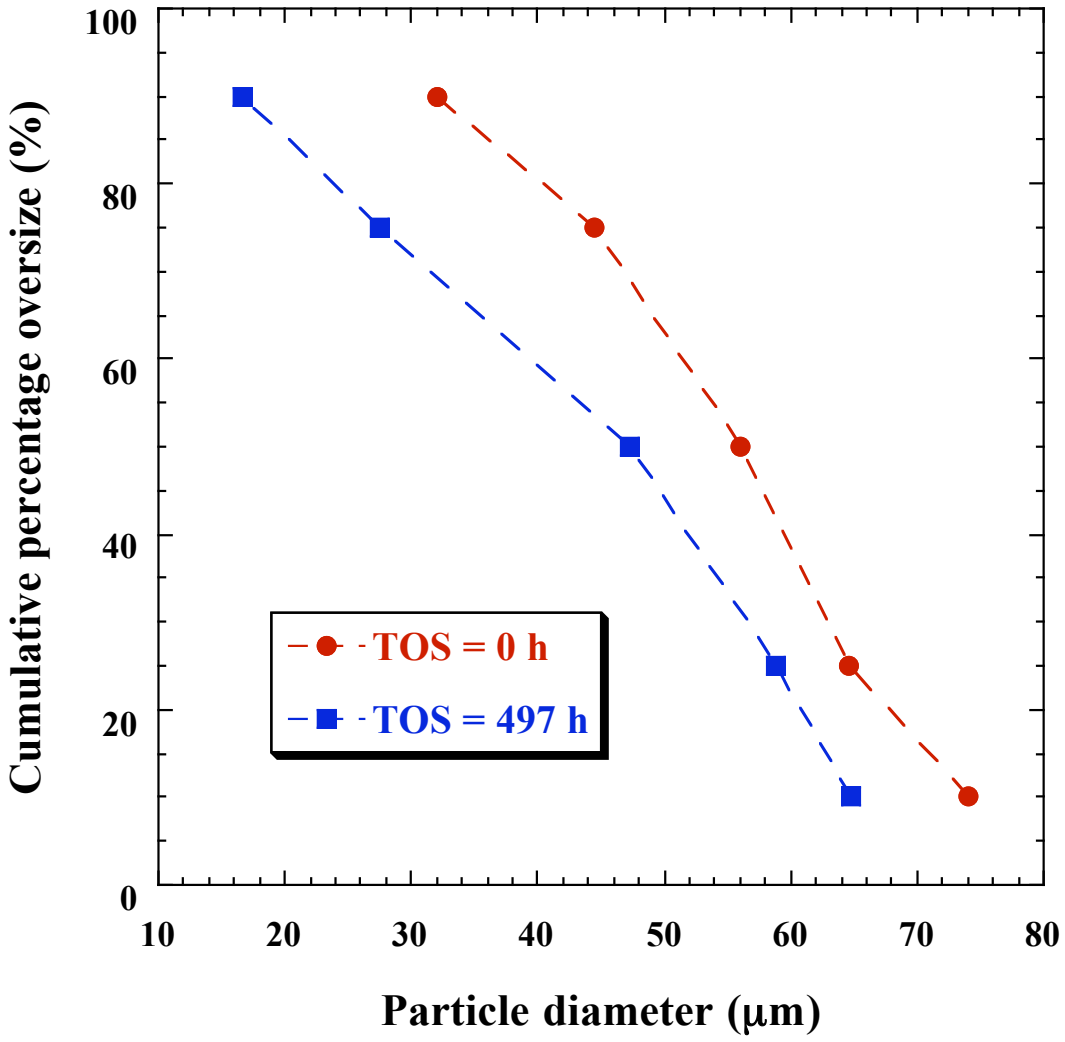

Figure 12. PSD of 100 Fe/3 Cu/5 K/16 SiO_2 catalyst (PPS3516-1) before and after F-T synthesis in the STSR test SB-19102.

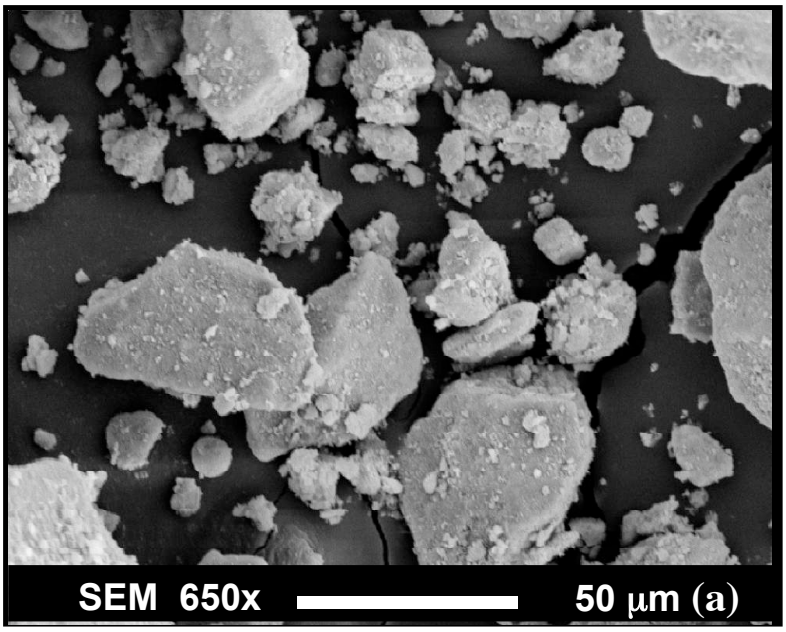

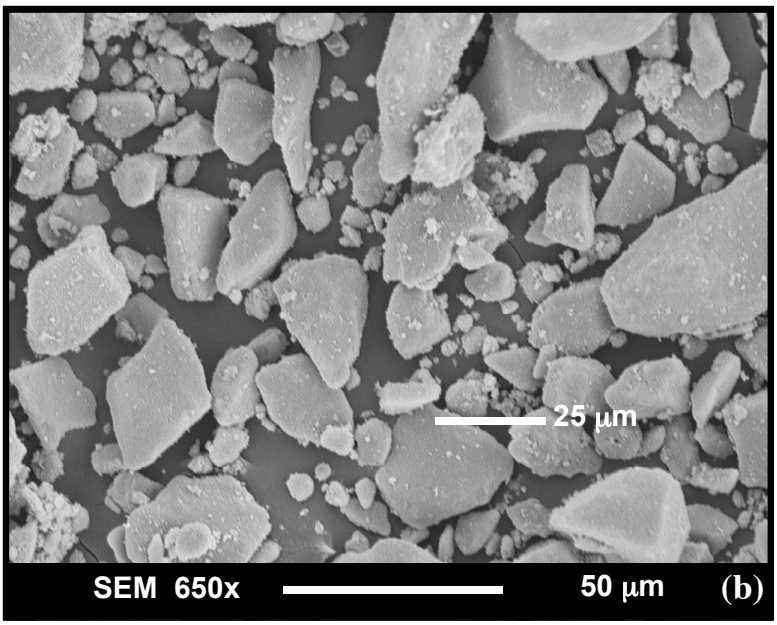

Figure 13. SEM image of PPS3516-2 (100 Fe/3 Cu/5 K/16 SiO_2) catalyst: (a) before F-T synthesis; (b) after 364 h of F-T synthesis in the STSR test SB-04803.

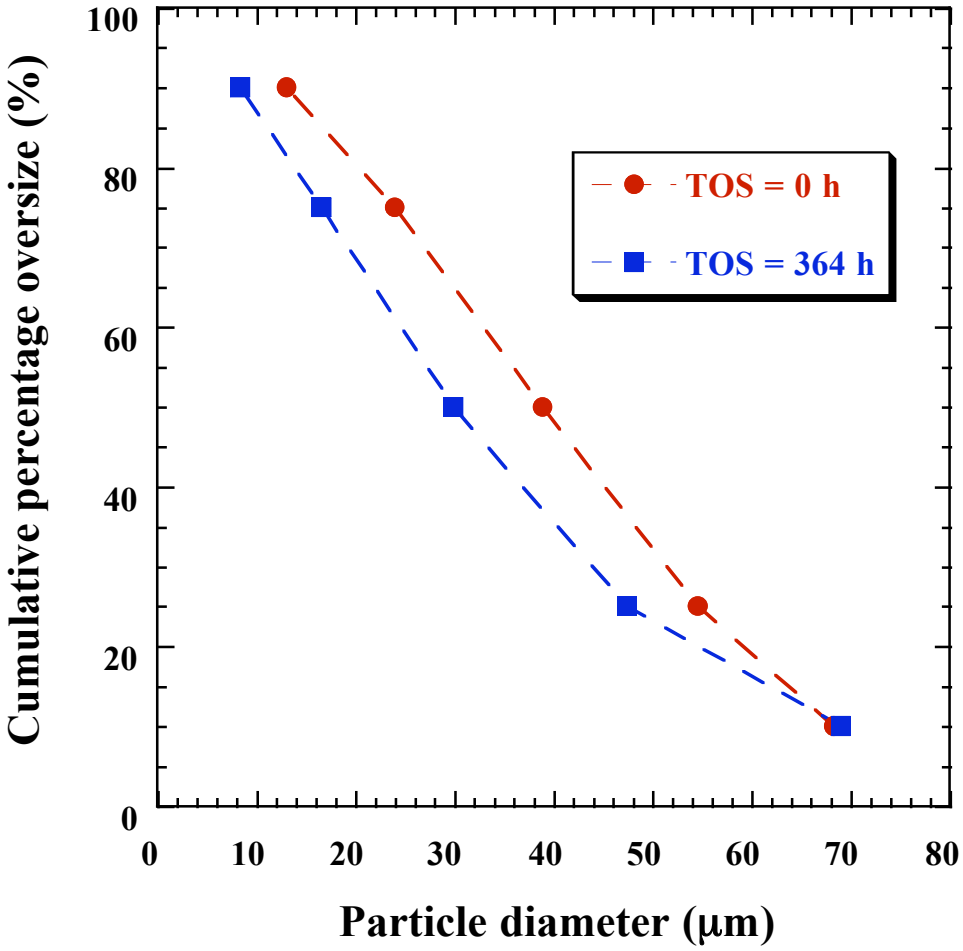

Figure 14. PSD of PPS3516-2 (100 Fe/3 Cu/5 K/16 SiO_2) catalyst before and after F-T synthesis in the STSR (run SB-04803).

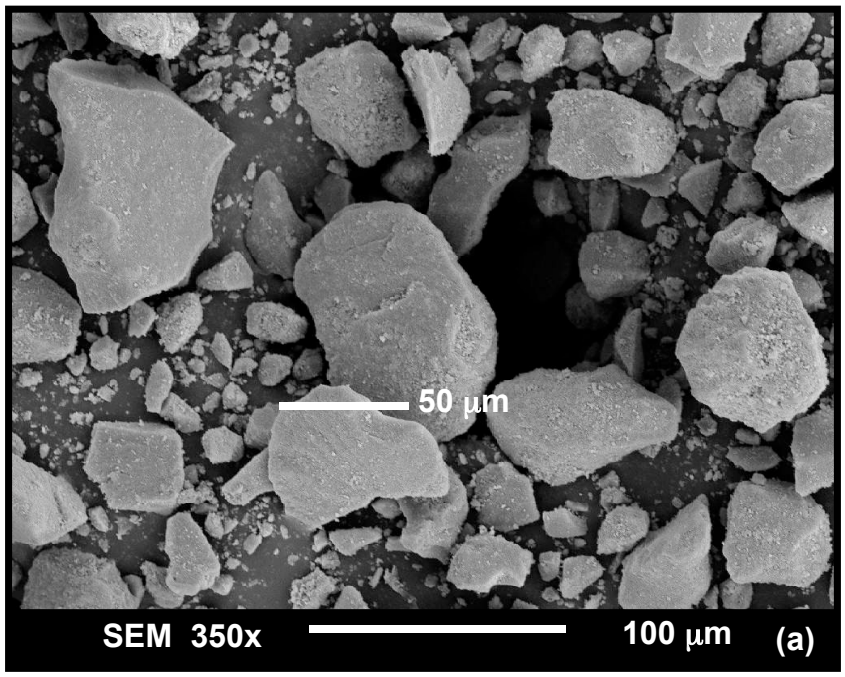

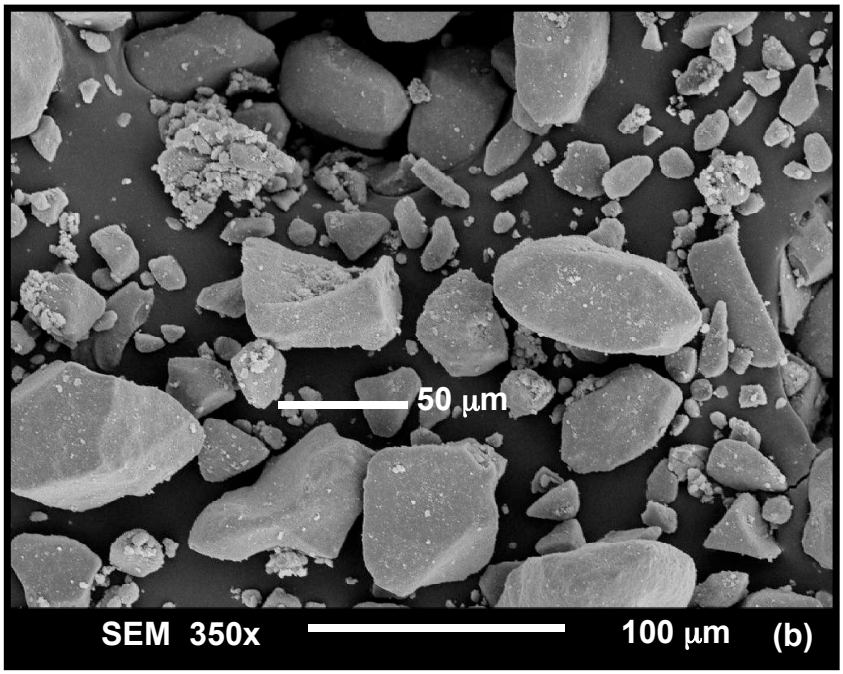

Figure 15. SEM image of the Ruhrchemie catalyst (100 Fe/5 Cu/4.2 K/25 SiO_2): (a) before F-T synthesis; (b) after 428 h of F-T synthesis in the STSR test SB-32901.

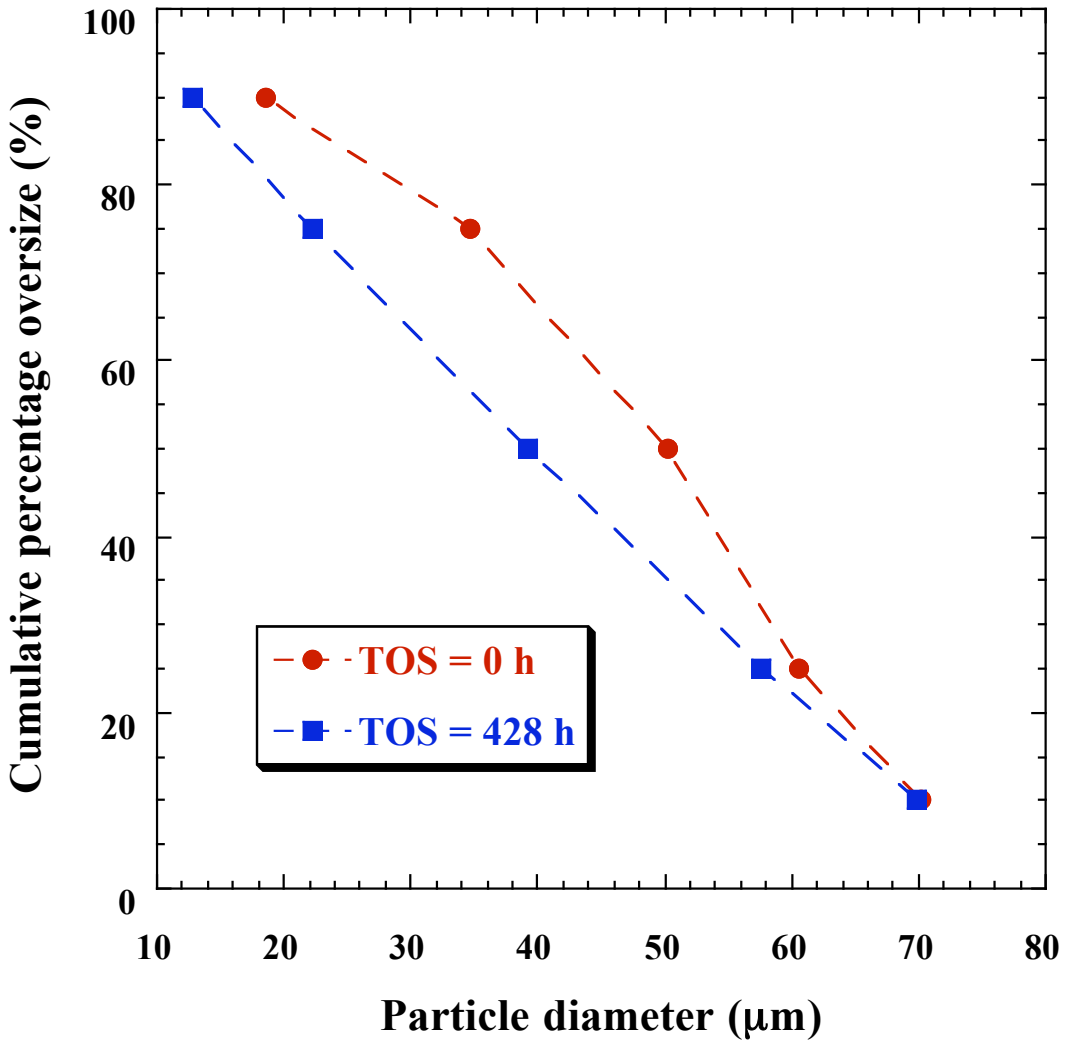

Figure 16. PSD of the Ruhrchemie catalyst (100 Fe/5 Cu/4.2 K/25 SiO_2) catalyst before and after F-T synthesis in the STSR test SB-32901.

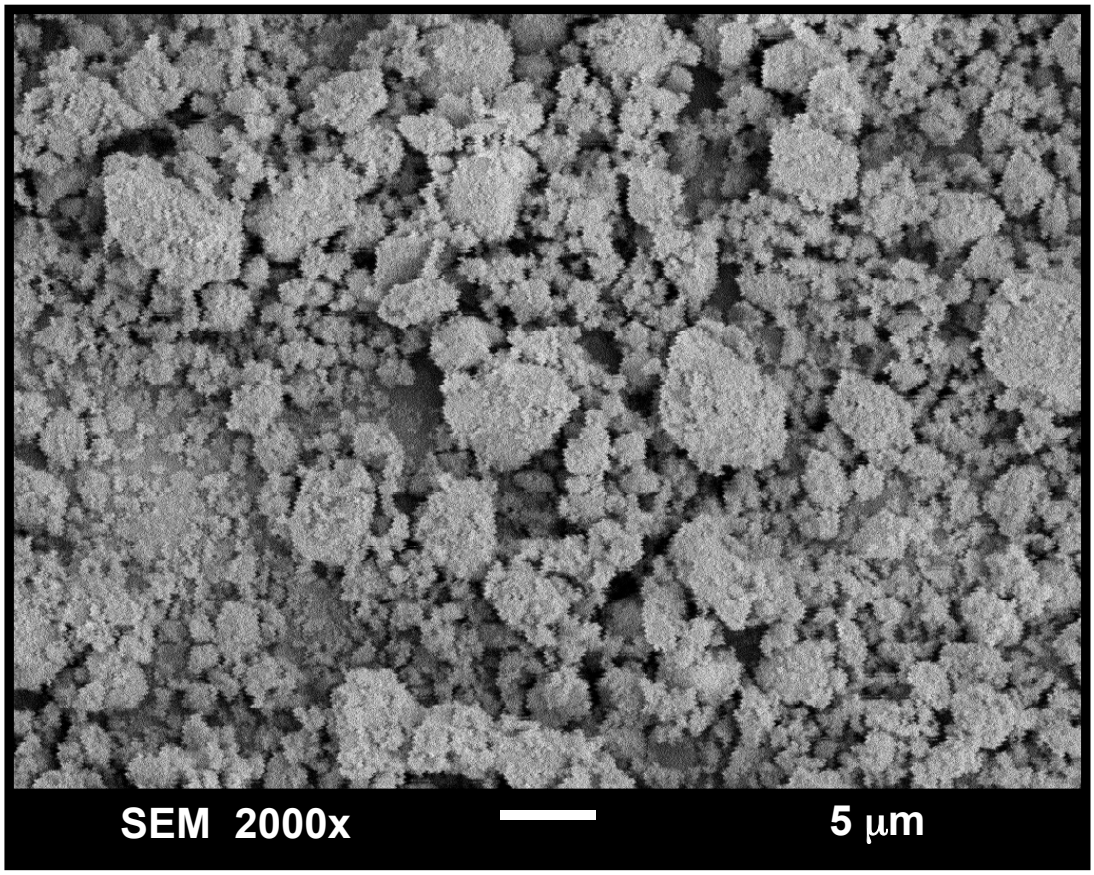

Figure 17. SEM image of calcined DPS-5624-2 (100 Fe/5 Cu/6 K/24 SiO_2) catalyst after size reduction in a tumbler and ultrasonication.

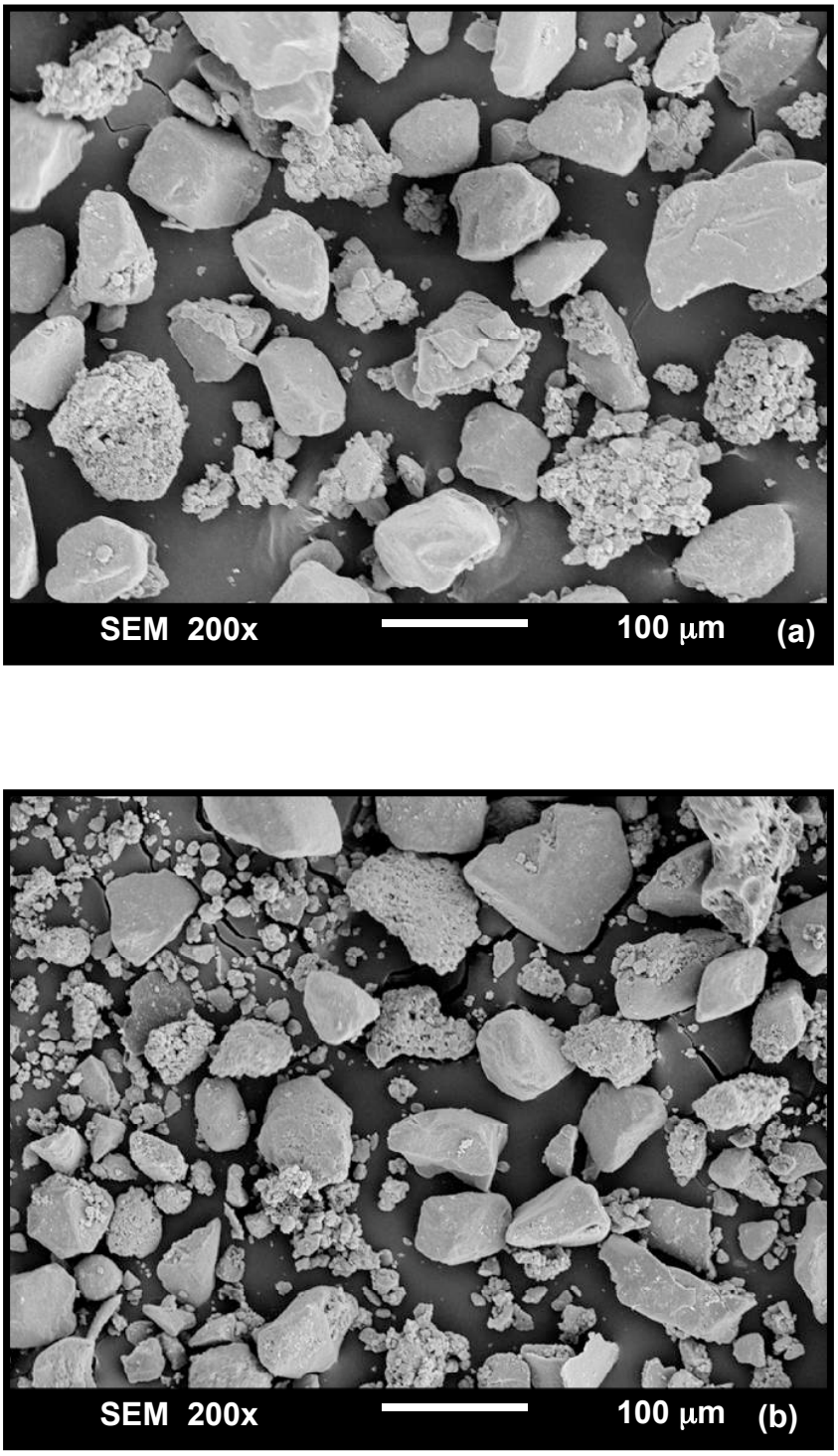

Figure 18. SEM image of spray-dried DPS5624-2 (100 Fe/5 Cu/6 K/24 SiO_2) catalyst:
(a) before F-T synthesis; (b) after 295 h of F-T synthesis in the STSR test SB-16502.

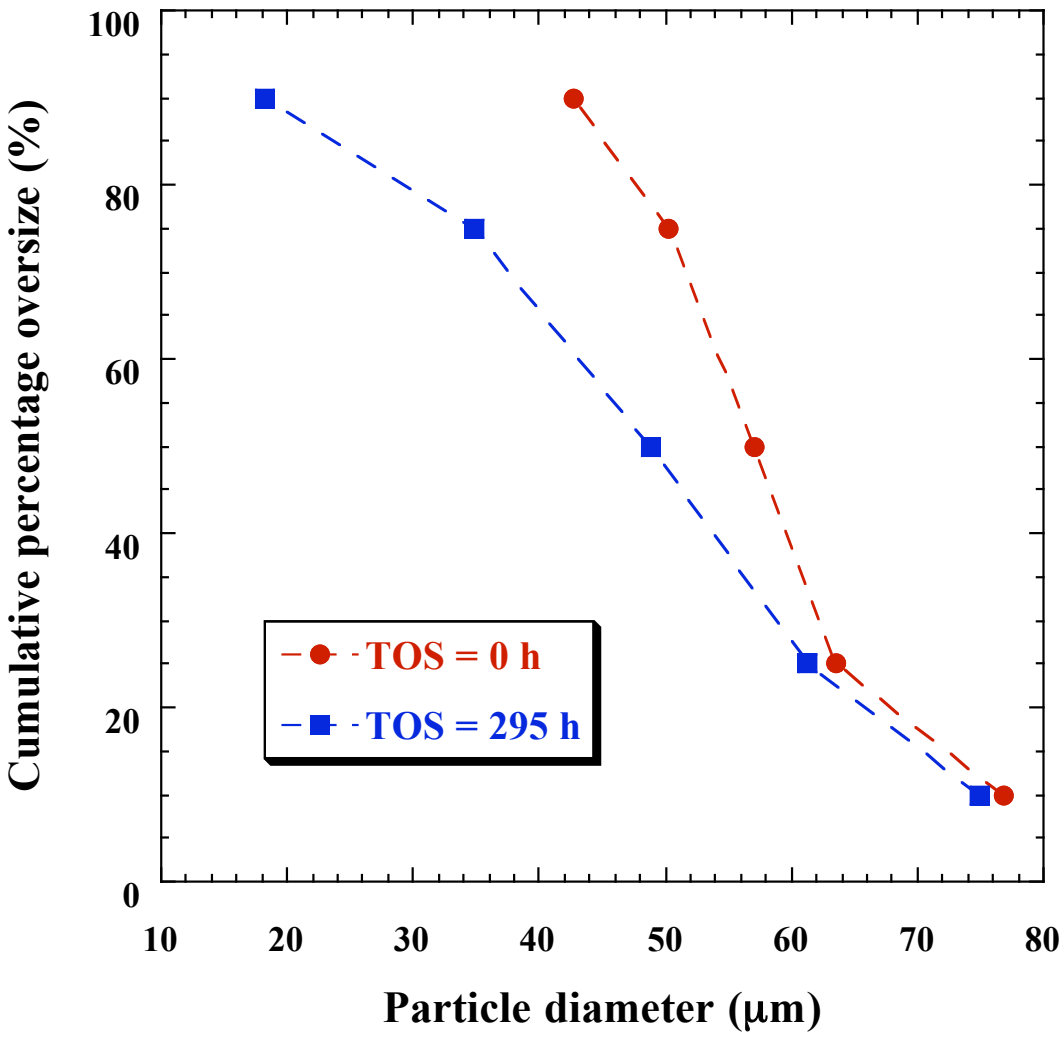

Figure 19. PSD of spray-dried DPS5624-2 (100 Fe/5 Cu/6 K/24 SiO_2) catalyst before and after F-T synthesis in the STSR test SB-16502.

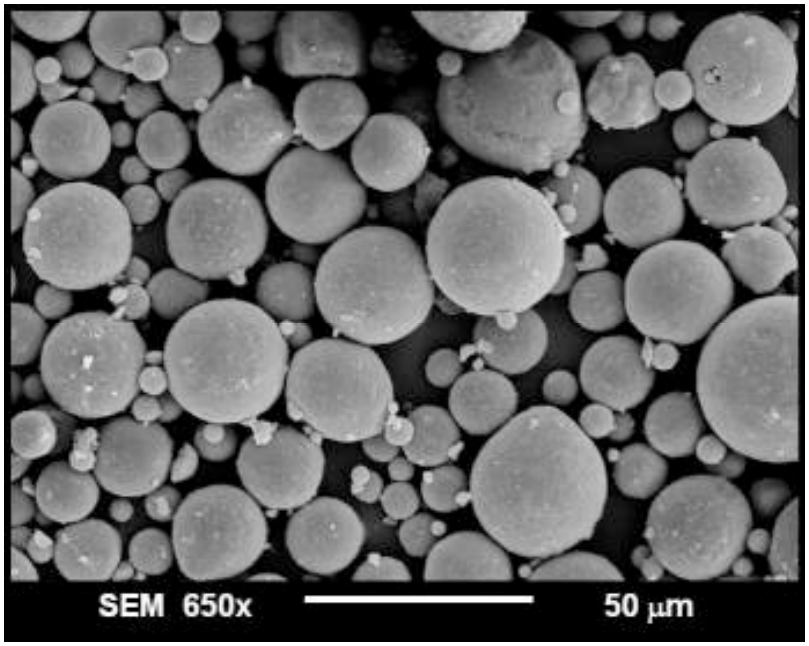

(a) TOS = 0 h

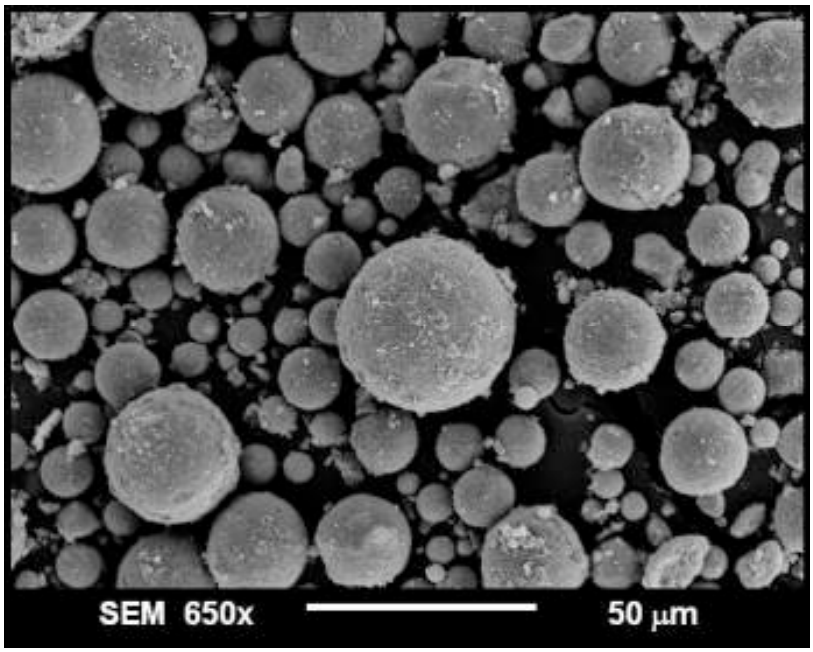

(b) TOS = 345 h

Figure 20. SEM image of spray-dried WCS3516-1 (100 Fe/3 Cu/5 K/16 SiO_2) catalyst: (a) before F-T synthesis; (b) after 345 h of F-T synthesis in the STSR test SB-30702.

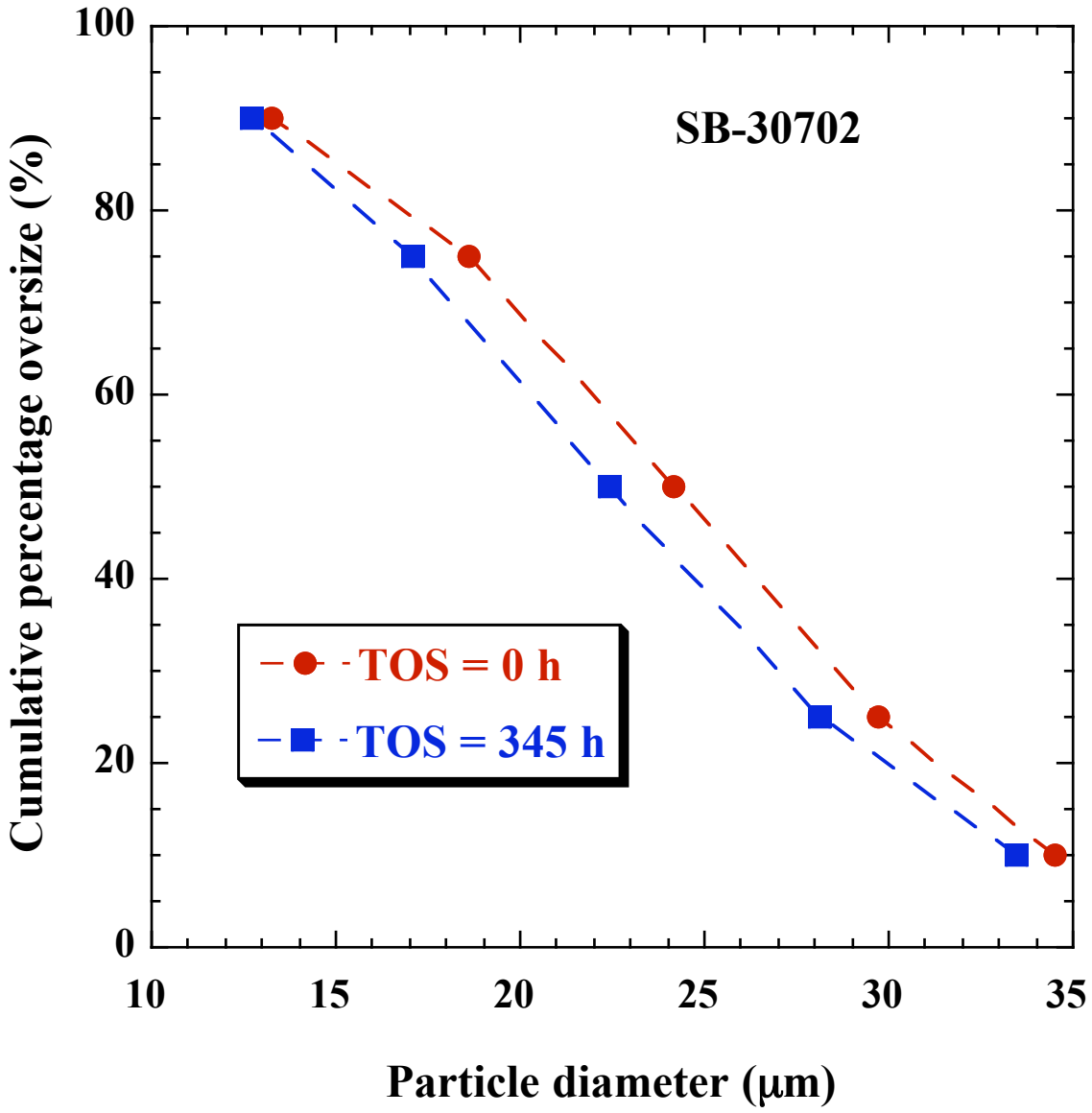

Figure 21. PSD of spray-dried WCS3516-1 (100 Fe/3 Cu/5 K/16 SiO_2) catalyst before and after F-T synthesis in the STSR test SB-30702.

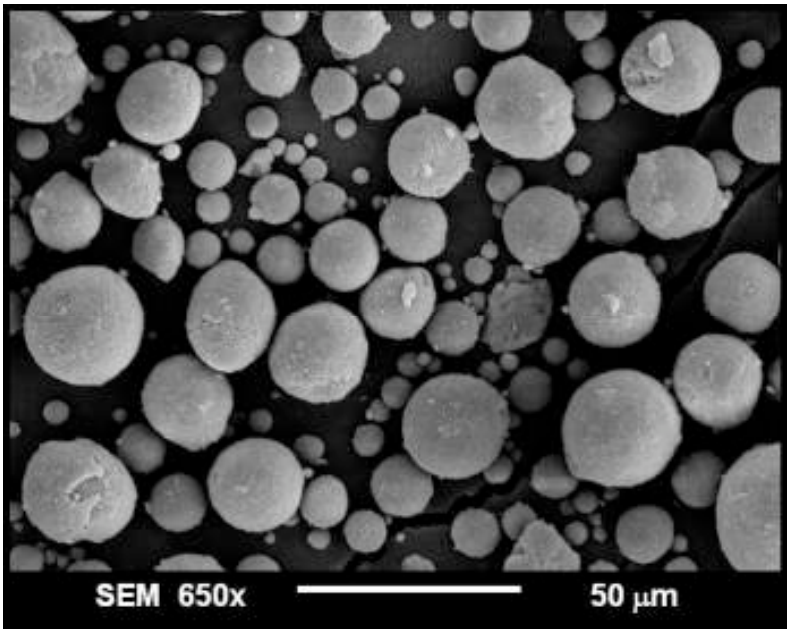

(a) TOS = 0 h

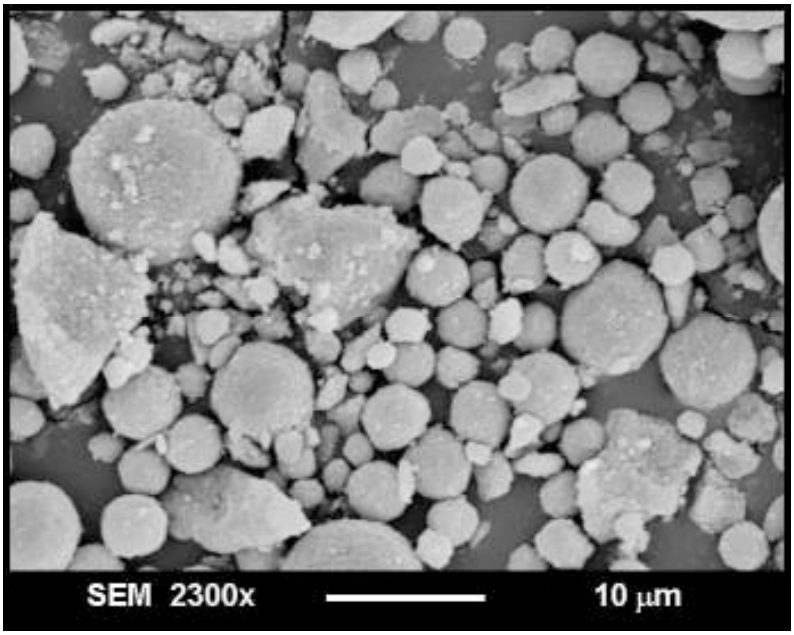

(b) TOS = 0 h

Figure 22. SEM images of WTO3516-1 (100 Fe/3 Cu/5 K/16 SiO_2) catalyst withdrawn from STSR (run SB-33802) at TOS = 0 h.

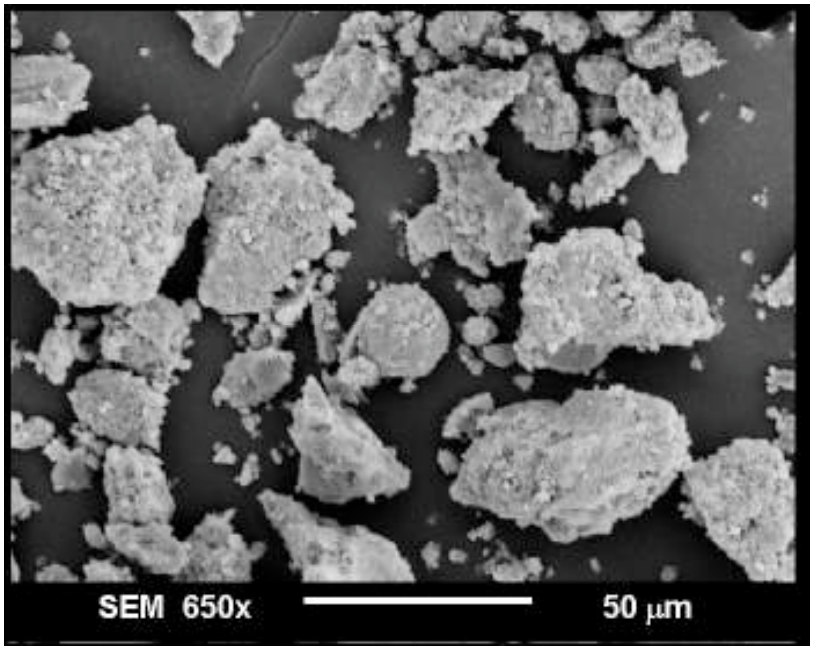

(a) EOR sample (TOS = 299 h) after first washing

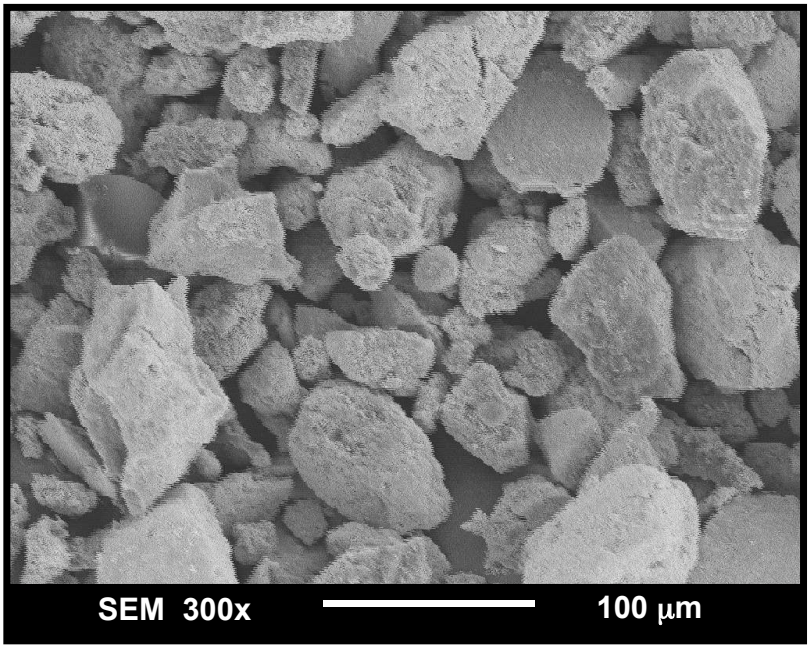

(b) EOR sample (TOS = 299 h) after Soxhlet extraction

Figure 23. SEM images of WTO3516-1 (100 Fe/3 Cu/5 K/16 SiO_2) catalyst at the end of STSR run SB-33802 after (a) washing with Varsol 18; (b) Soxhlet extraction.

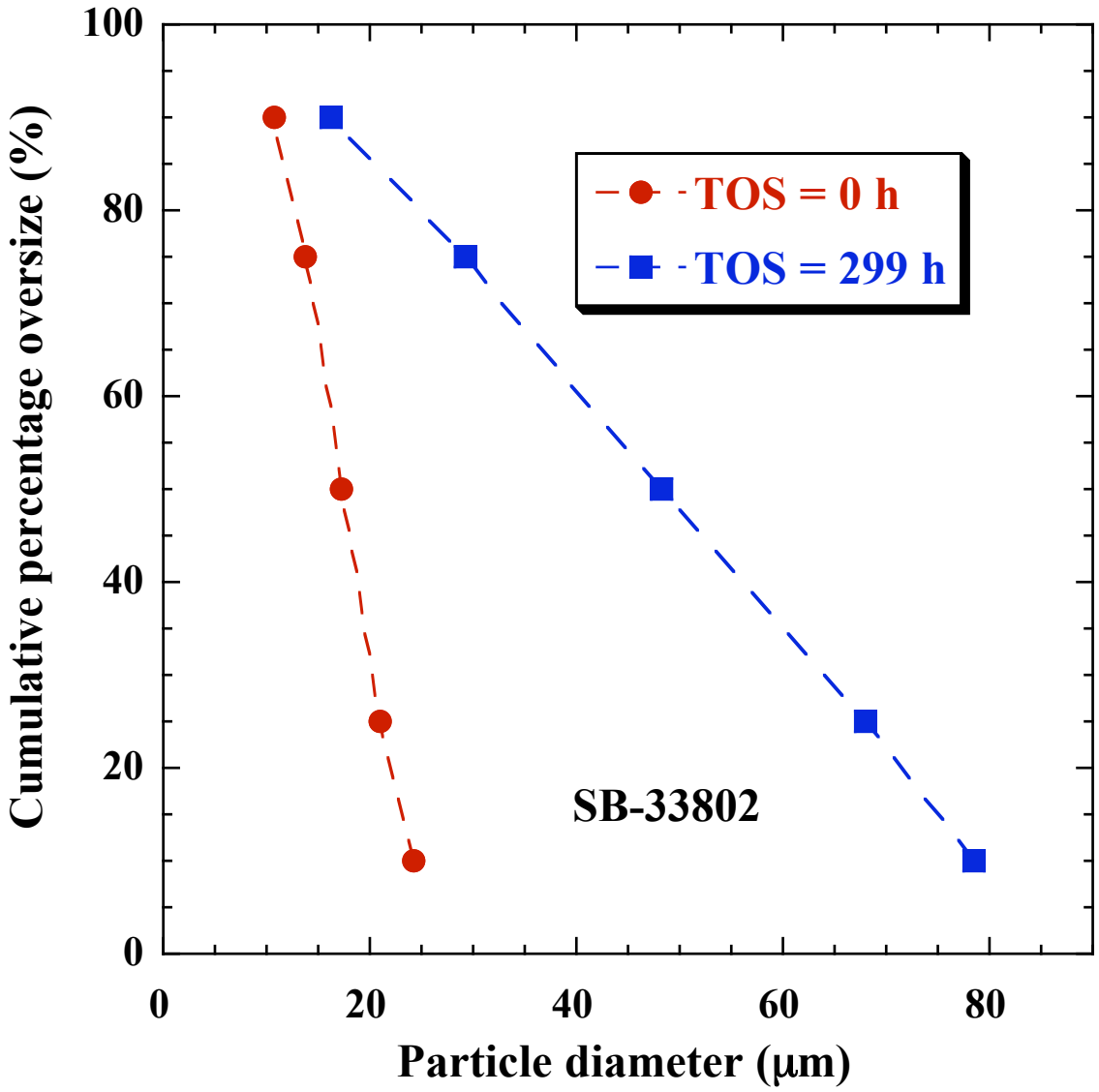

Figure 24. PSD of spray-dried WTO3516-1 (100 Fe/3 Cu/5 K/16 SiO_2) catalyst before and after F-T synthesis (EOR sample after first washing) in the STSR test SB-33802.

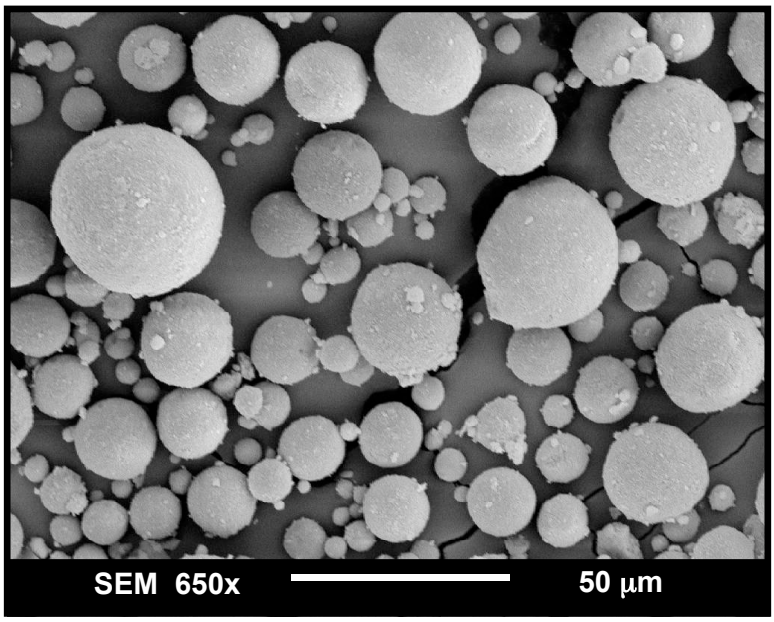

(a) TOS = 0 h

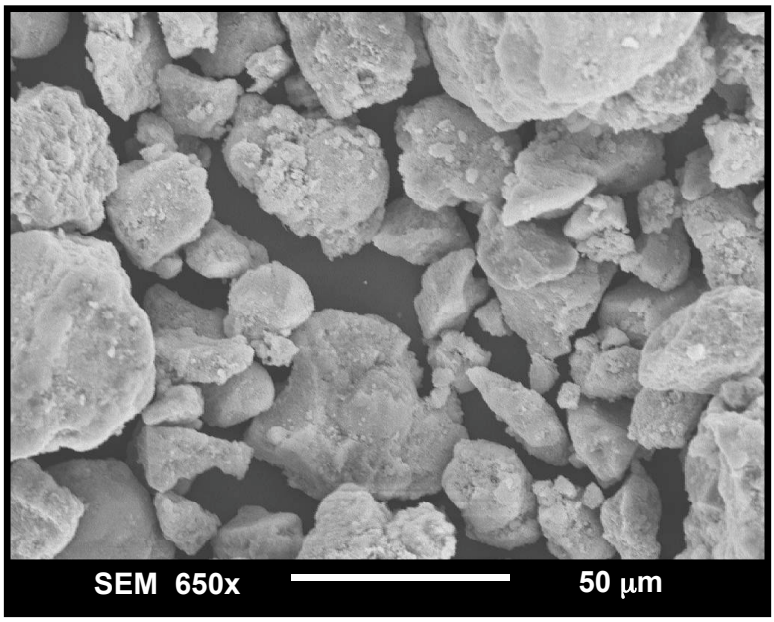

(b) EOR sample (TOS = 364 h) after the first washing

Figure 25. SEM images of WPS3516-4 (100 Fe/3 Cu/5 K/16 SiO_2) catalyst (a) before F-T synthesis; (b) after 364 h of F-T synthesis in the STSR test SB- SB-09703.

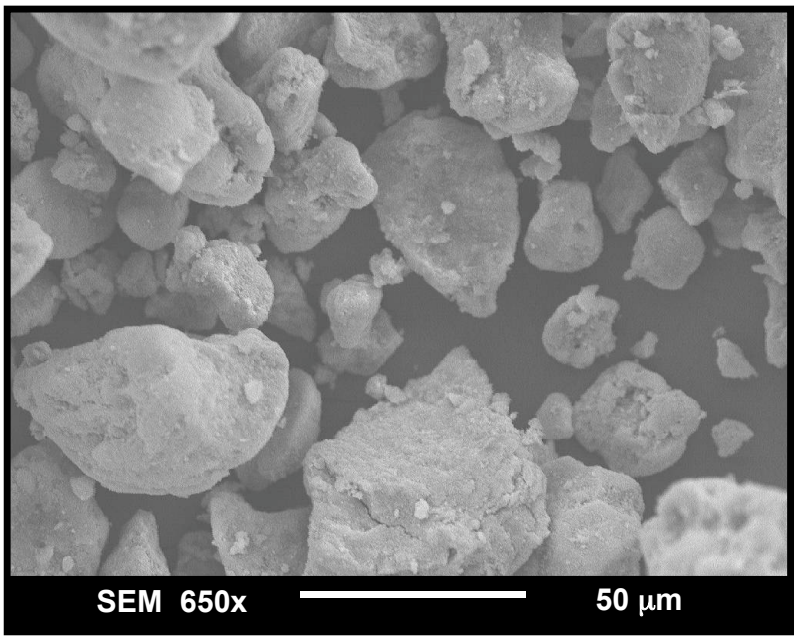

(a) EOR sample (TOS = 364 h) after multiple washings

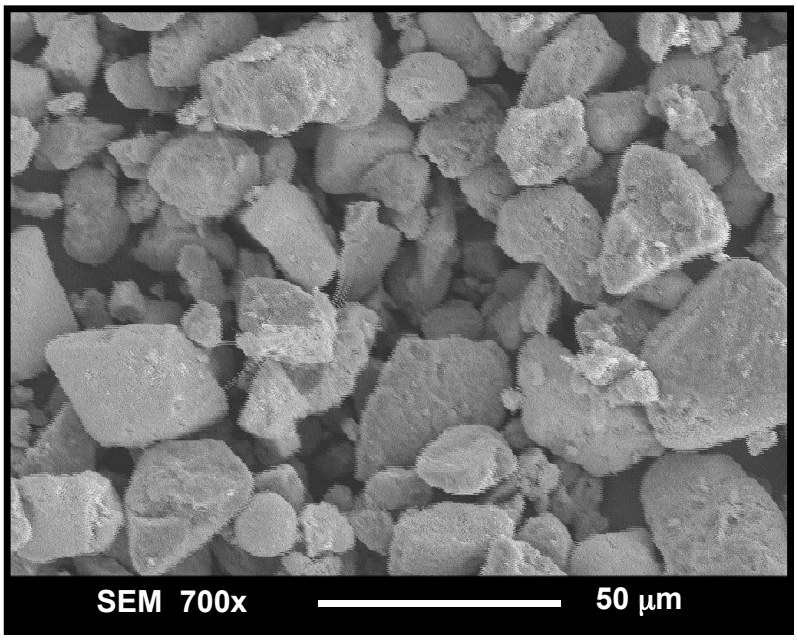

(b) EOR sample (TOS =364 h) after Soxhlet extraction

Figure 26. SEM images of WPS3516-4 (100 Fe/3 Cu/5 K/16 SiO_2) catalyst at the end of STSR run SB-09703 after (a) multiple washings; (b) Soxhlet extraction.

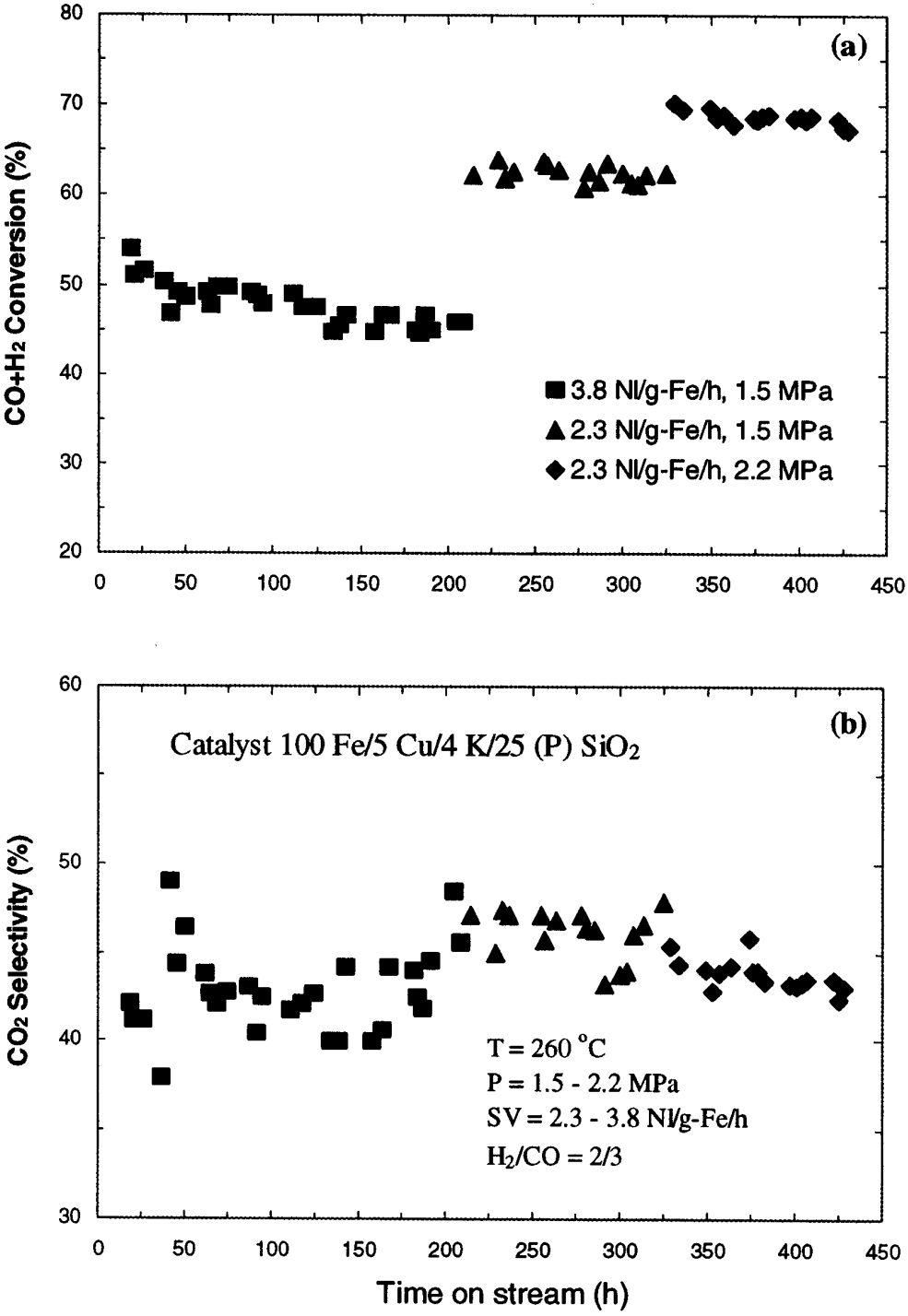

Figure 27. Syngas conversion (a) and CO_2 selectivity (b) as a function of time for STSR test SB-32901 of the Ruhrchemie catalyst (100 Fe/5 Cu/4 K/25 (P) SiO_2).

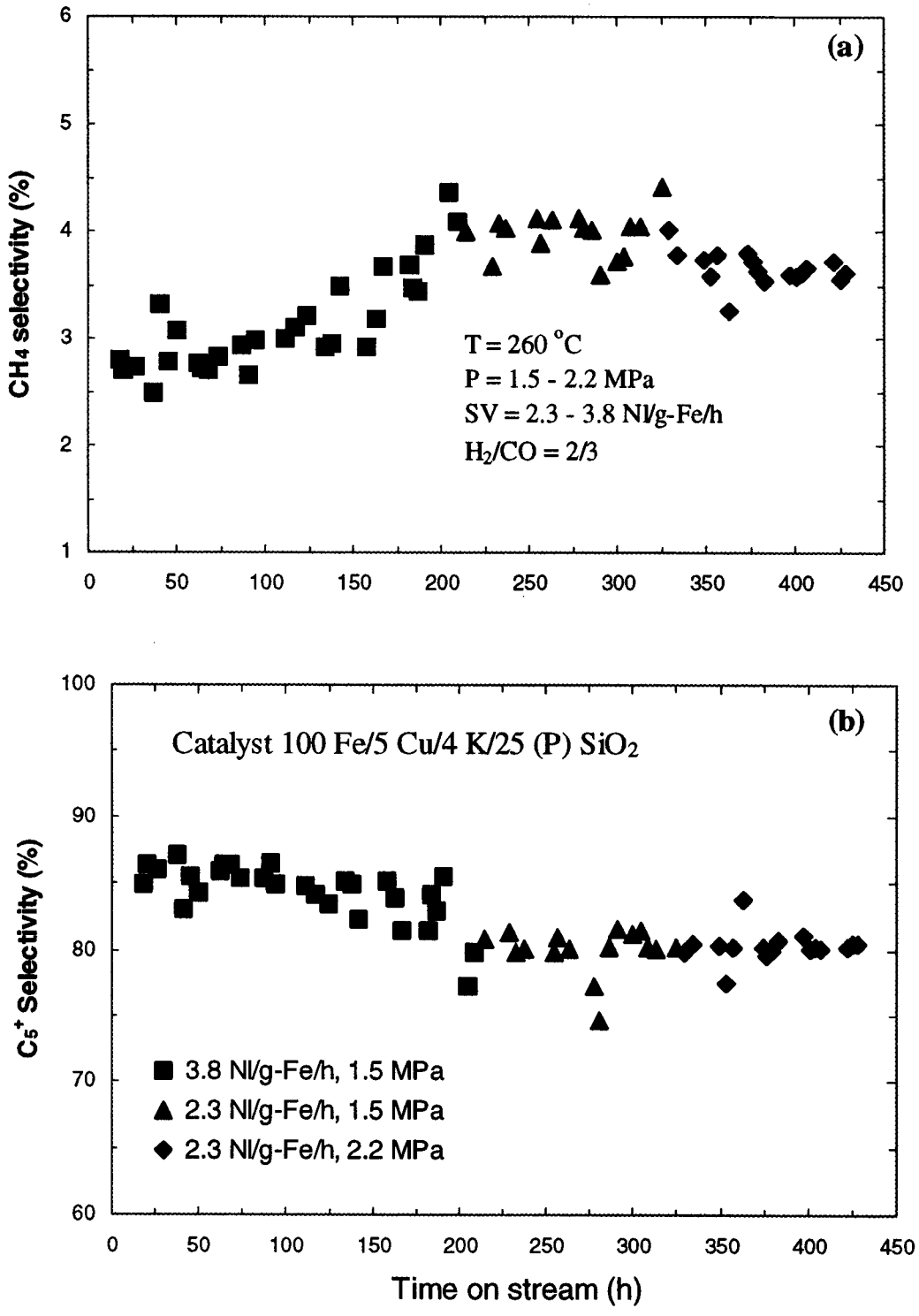

Figure 28. CH_4 selectivity (a) and C_5^+ selectivity (b) as a function of time for STSR test of the Ruhrchemie catalyst (100 Fe/5 Cu/4 K/25 (P) SiO_2).

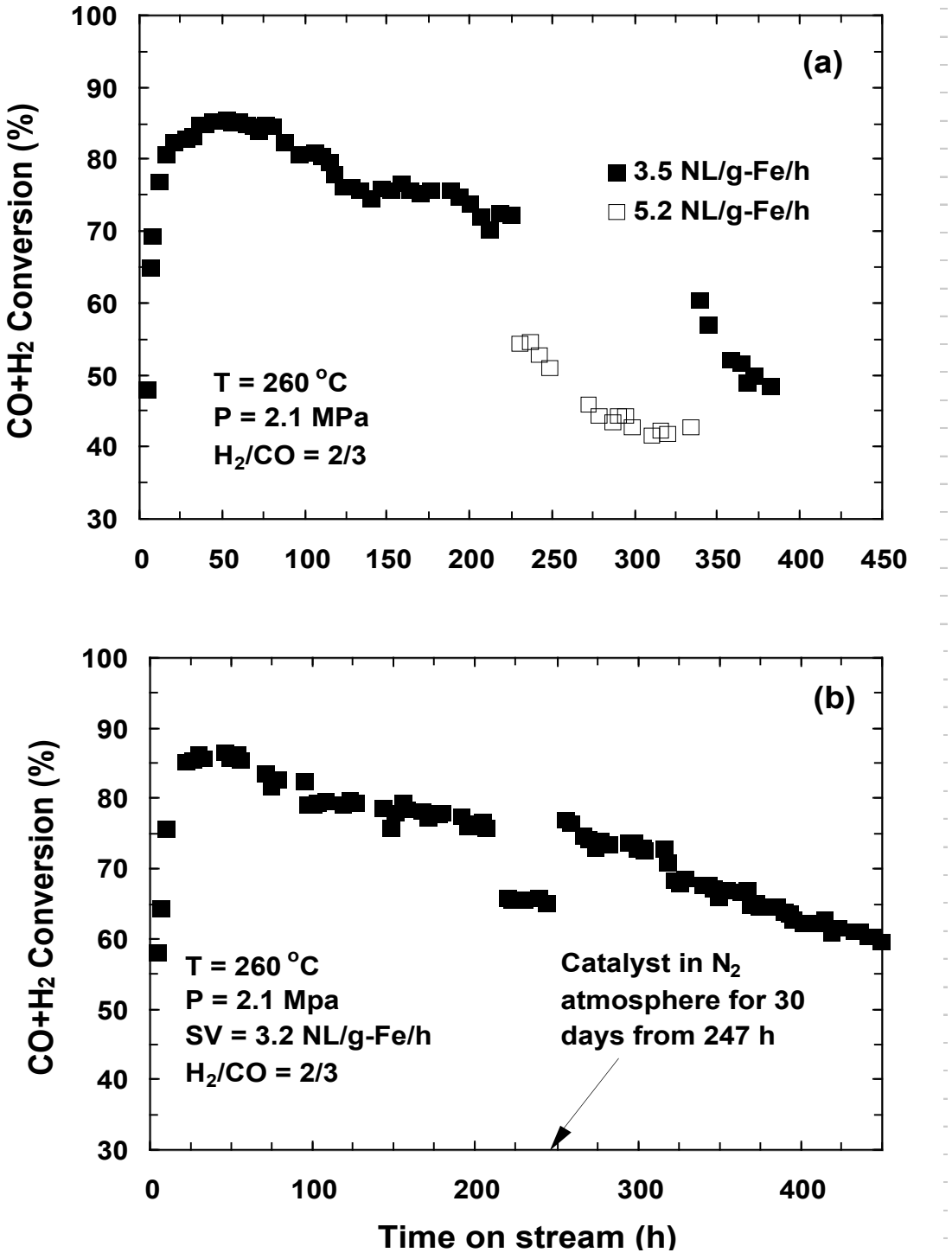

Figure 29. Syngas conversion as a function of time for STSR tests of spray-dried catalysts
(a) 100 Fe/5 Cu/4.2 K/11 (P) SiO_2 (SB-20601)
(b) 100 Fe/5 Cu/4.2 K/1.1 (B) SiO_2 (SB-34701).

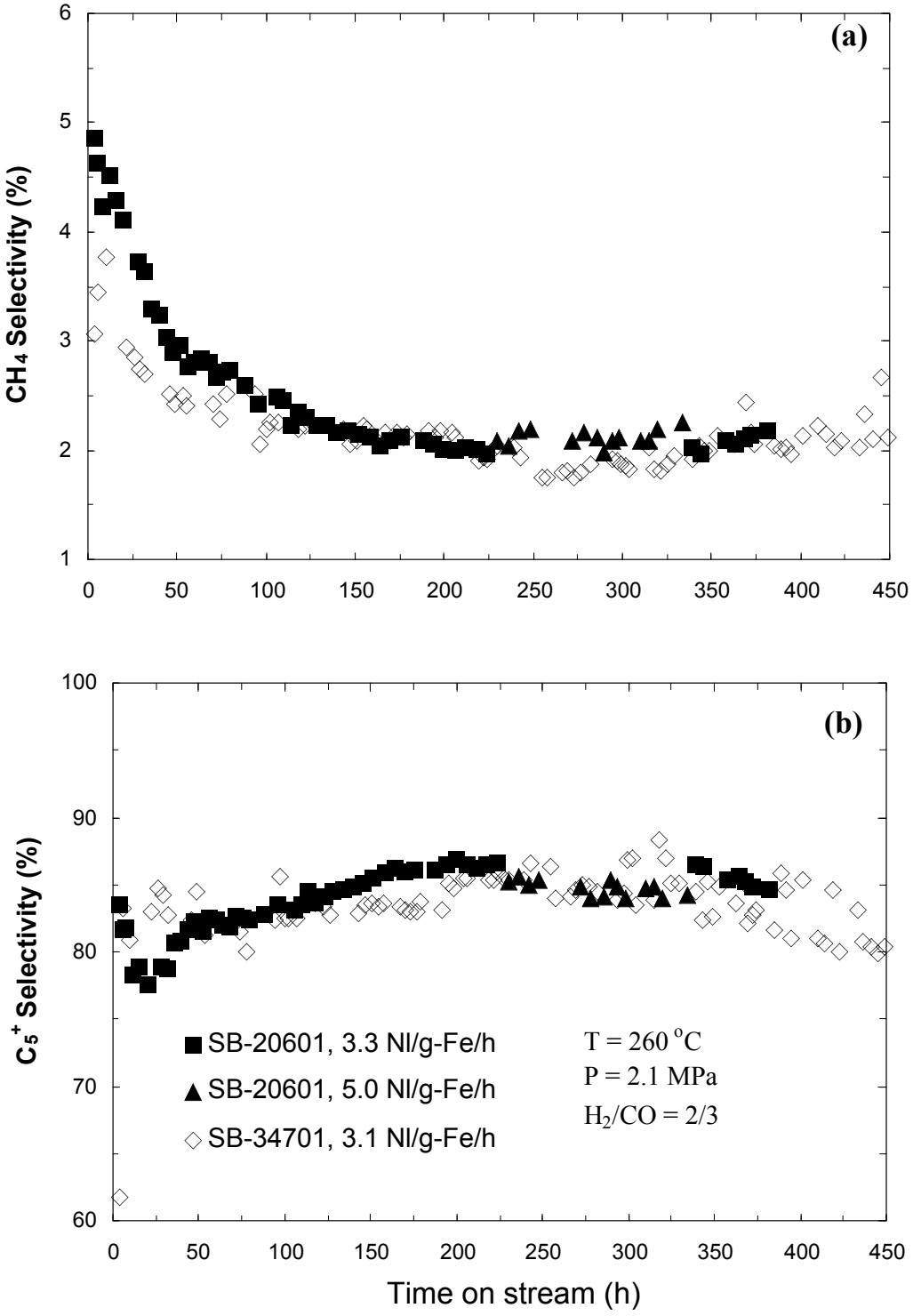

Figure 30. Change in CH_4 selectivity (a) and C_5^+ selectivity (b) with time and process conditions in STSR tests of spray-dried catalysts: 100 Fe/5 Cu/4.2 K/11 (P) SiO_2 (SB-20601) and 100 Fe/5 Cu/4.2 K/1.1 (B) SiO_2 (SB-34701).

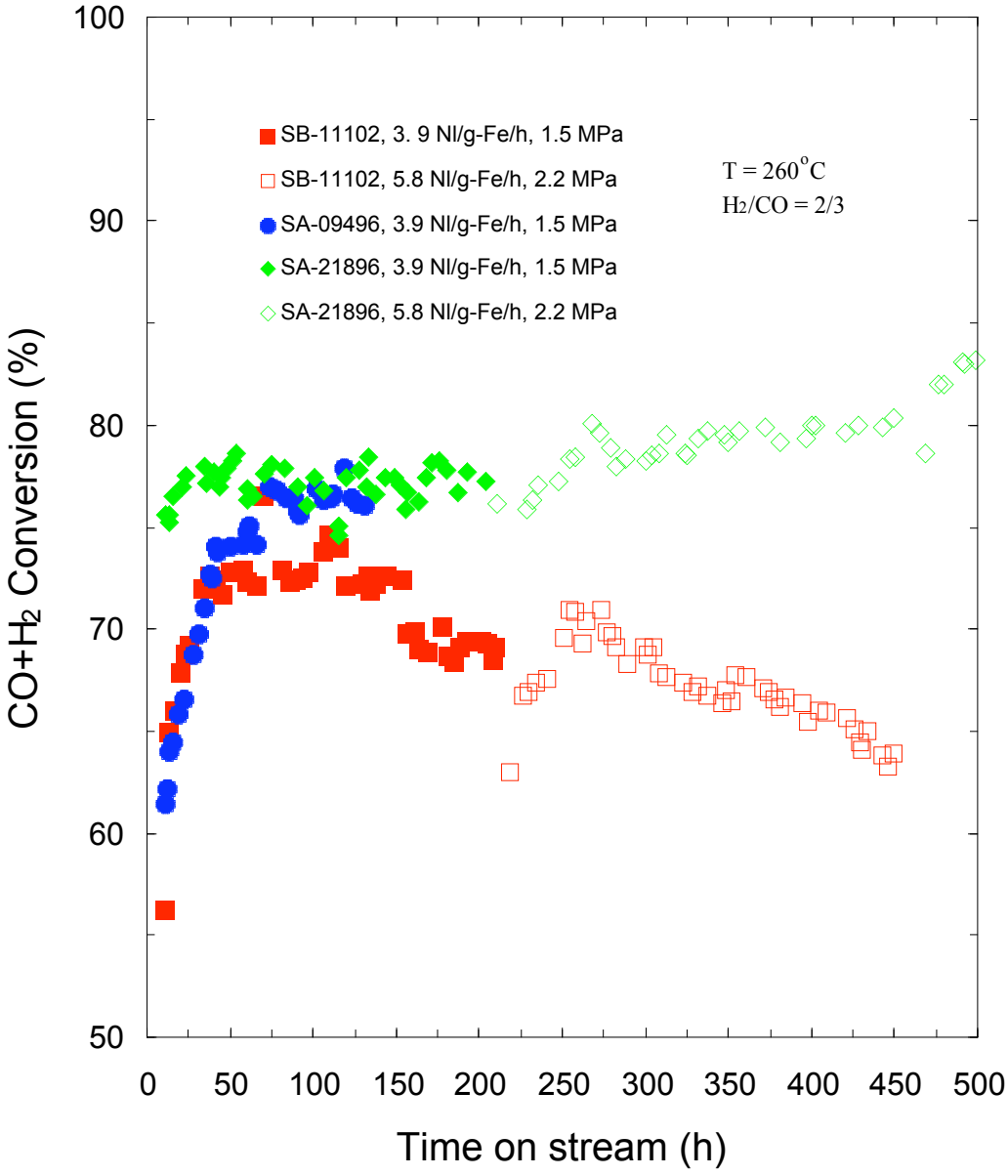

Figure 31. Change in syngas conversion with time and process conditions in STSR tests of precipitated (SA-09496 and SA-21896) and spray-dried (SB-11102) 100 Fe/3 Cu/4 K/16 (P) SiO_2 catalysts.

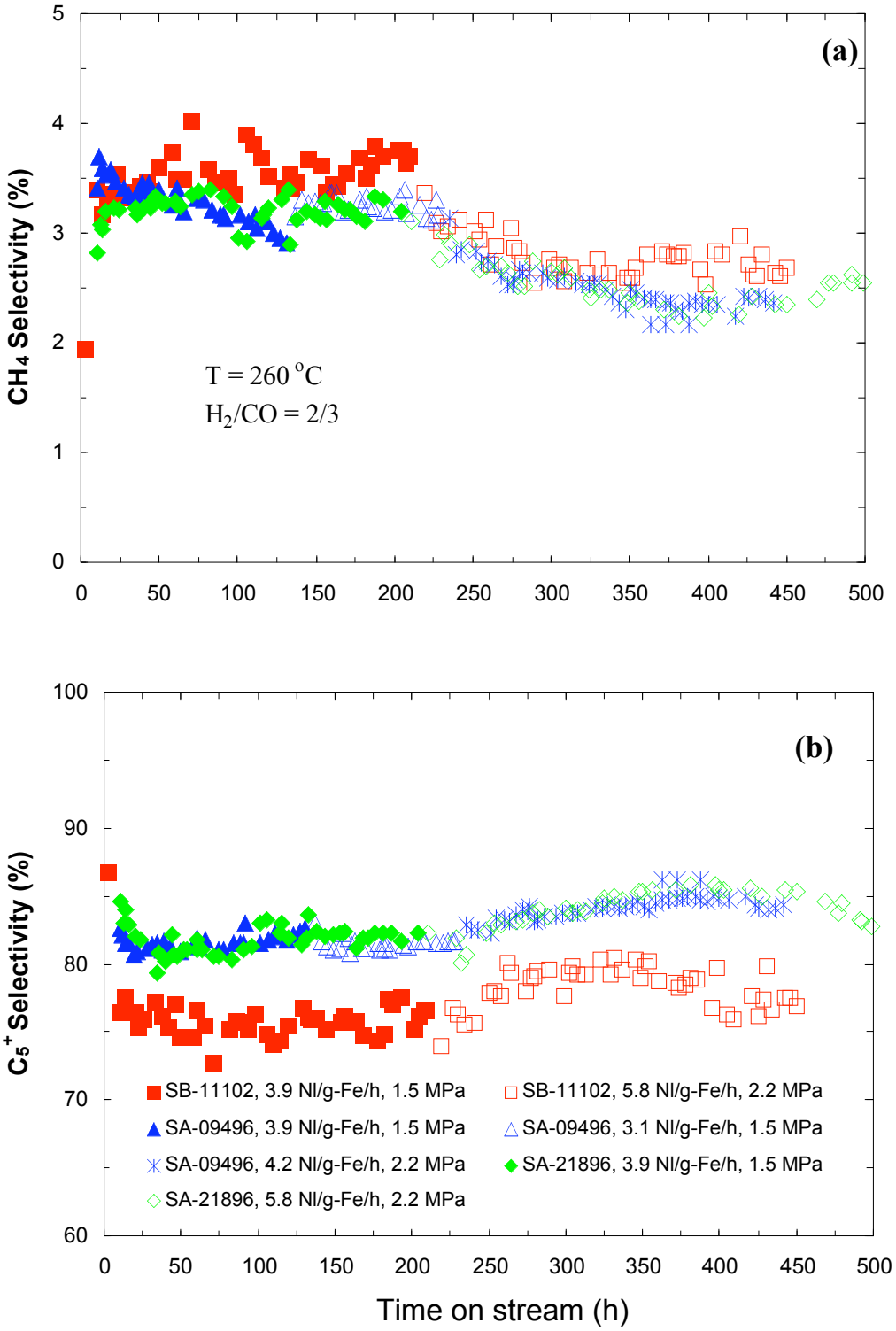

Figure 32. Change in CH_4 selectivity (a) and C_5^+ selectivity (b) with time and process conditions in STSR tests of precipitated (SA-09496 and SA-21896) and spray-dried (SB-11102) 100 Fe/3 Cu/4 K/16 (P) SiO_2 catalysts.

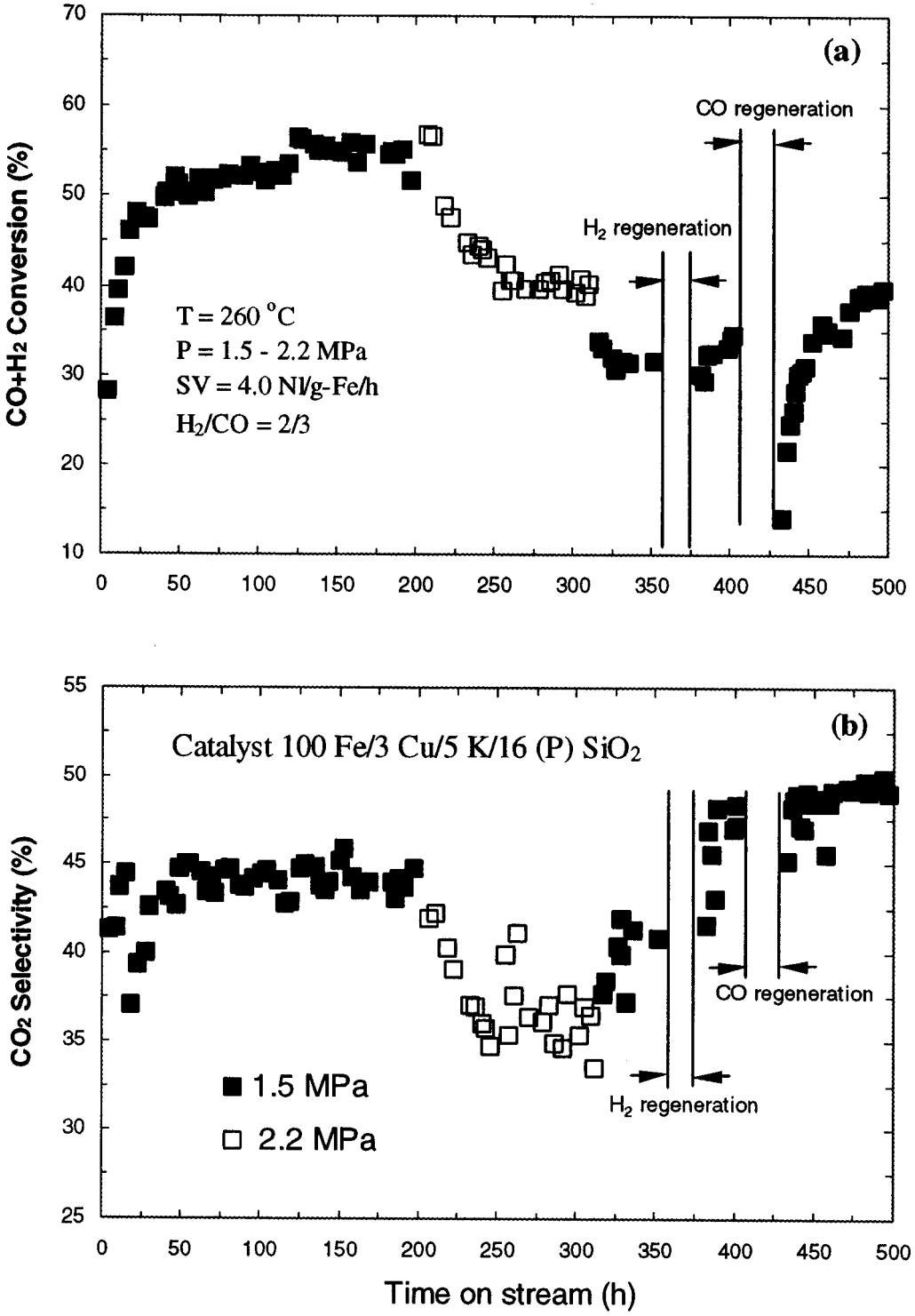

Figure 33. Syngas conversion (a) and CO_2 selectivity (b) as a function of time for STSR test of precipitated 100 Fe/3 Cu/5 K/16 (P) SiO_2 catalyst (SB-19102).

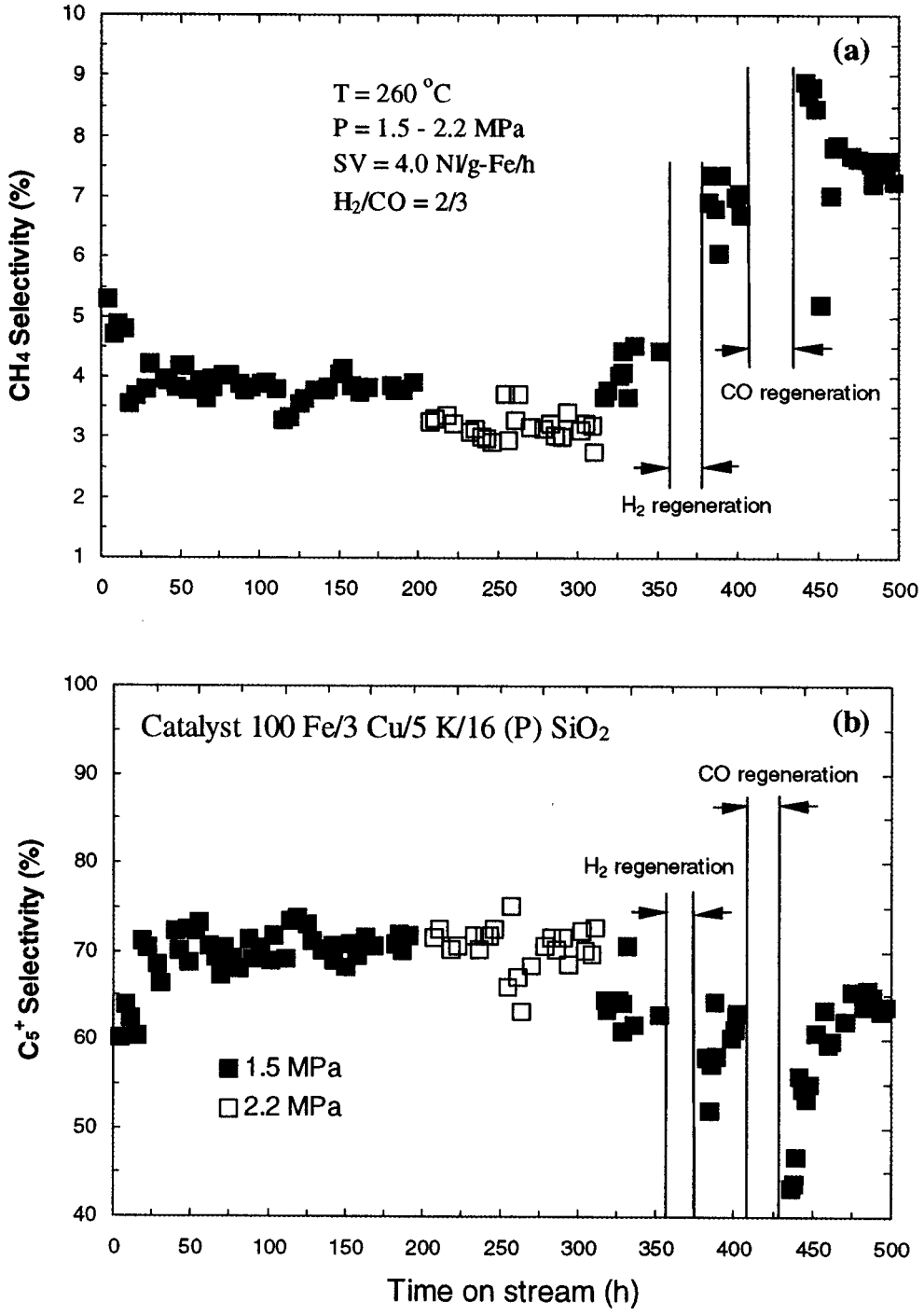

Figure 34. CH_4 selectivity (a) and C_5^+ selectivity (b) as a as a function of time for STSR test of precipitated 100 Fe/3 Cu/5 K/16 (P) SiO_2 catalyst (SB-19102).

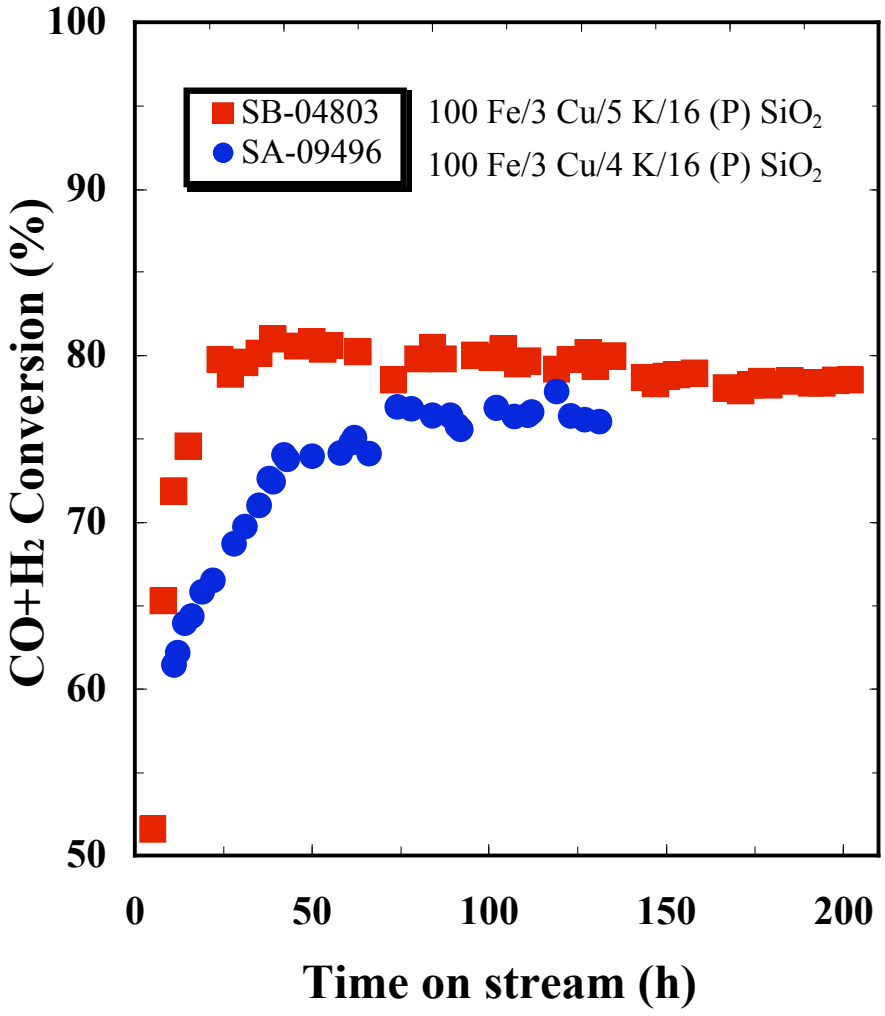

Figure 35. Comparison of syngas conversions of two precipitated Fe catalysts at baseline process conditions (260°C, 1.5 MPa, 3.9 - 4 Nl/g-Fe/h, $H_2/CO = 2/3$).

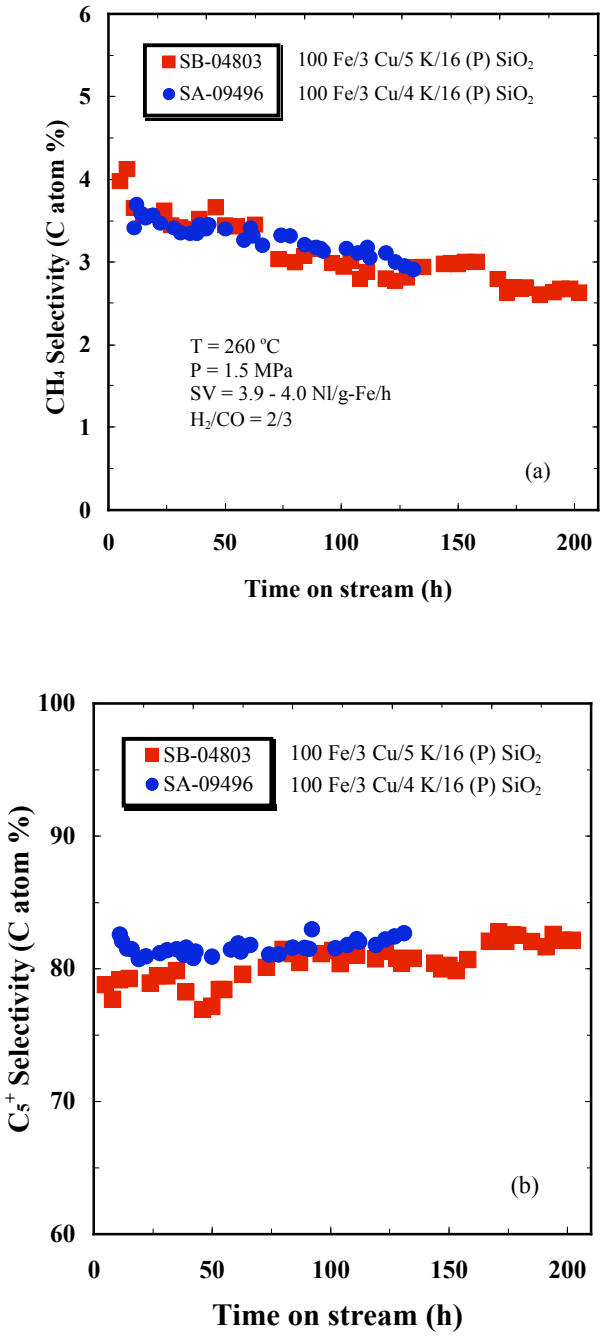

Figure 36. Comparison of hydrocarbon selectivities of two precipitated Fe catalysts in STSR tests at baseline process conditions.

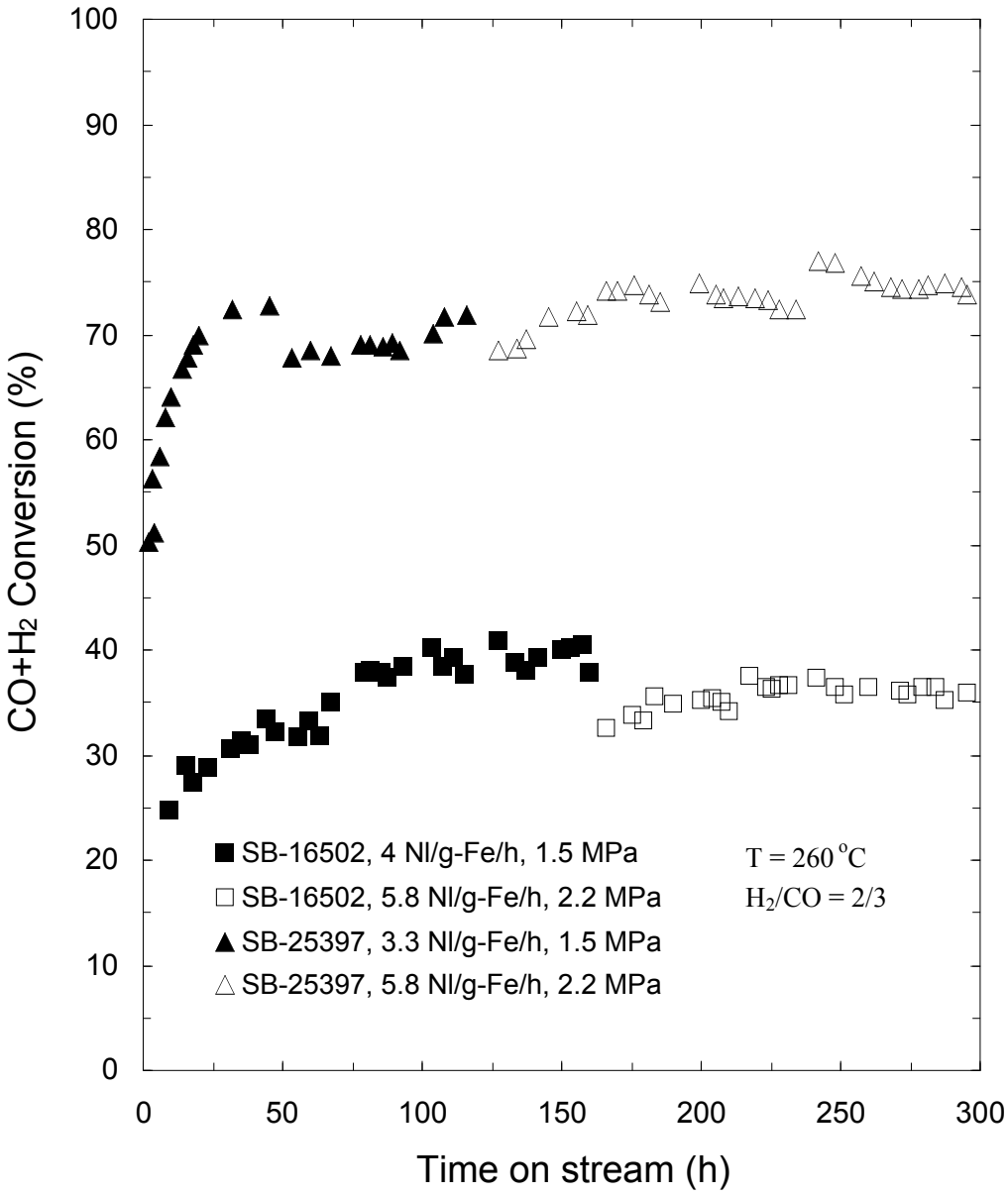

Figure 37. Change in syngas conversion with time and process conditions in STSR tests of precipitated (SB-25397) and spray-dried (SB-16502) catalysts.

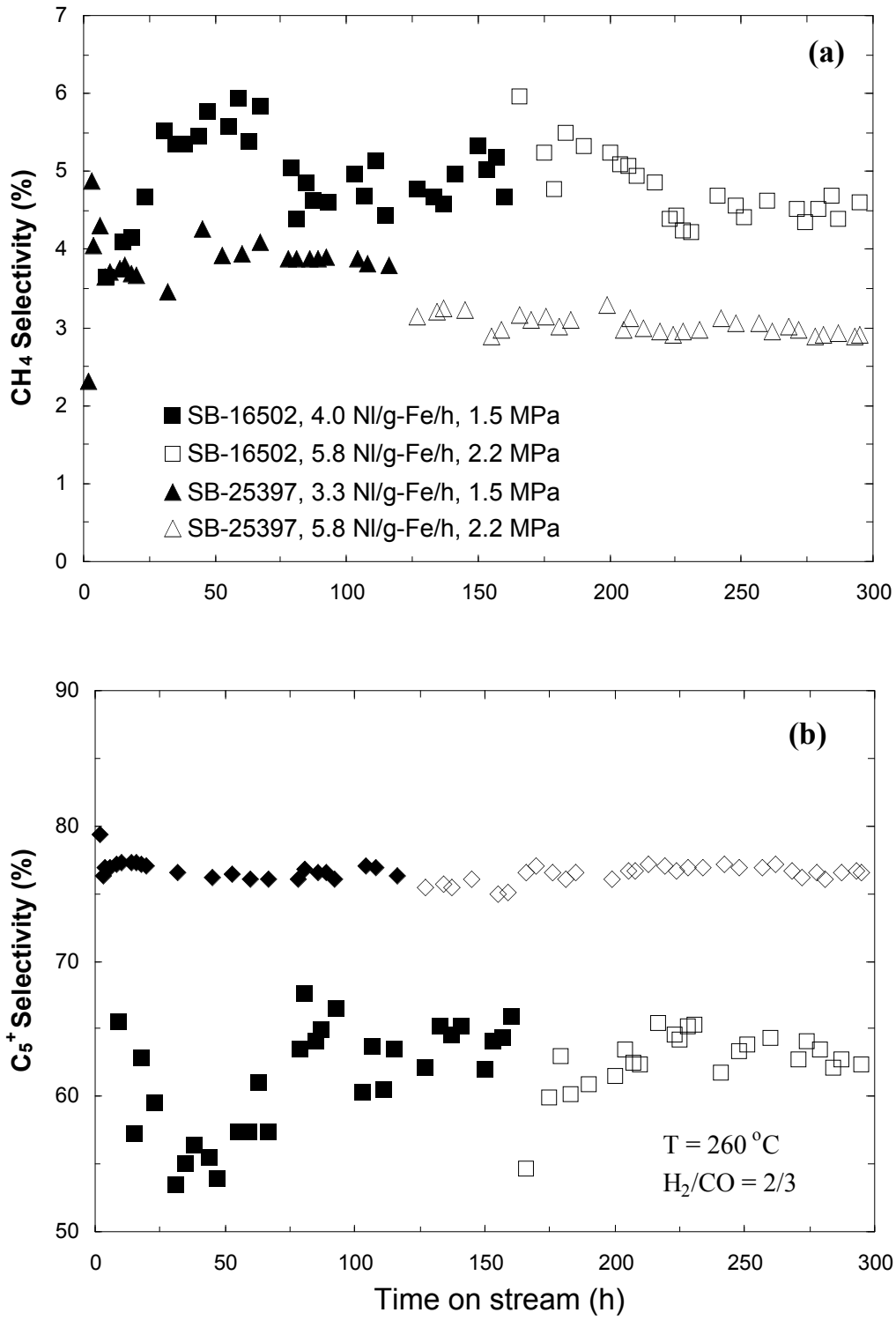

Figure 38. Change in CH_4 selectivity (a) and C_5^+ selectivity (b) with time and process conditions in STSR tests of precipitated (SB-25397) and spray-dried (SB-16502) catalysts of the same composition (100 Fe/5 Cu/6 K/24 (P) SiO_2).

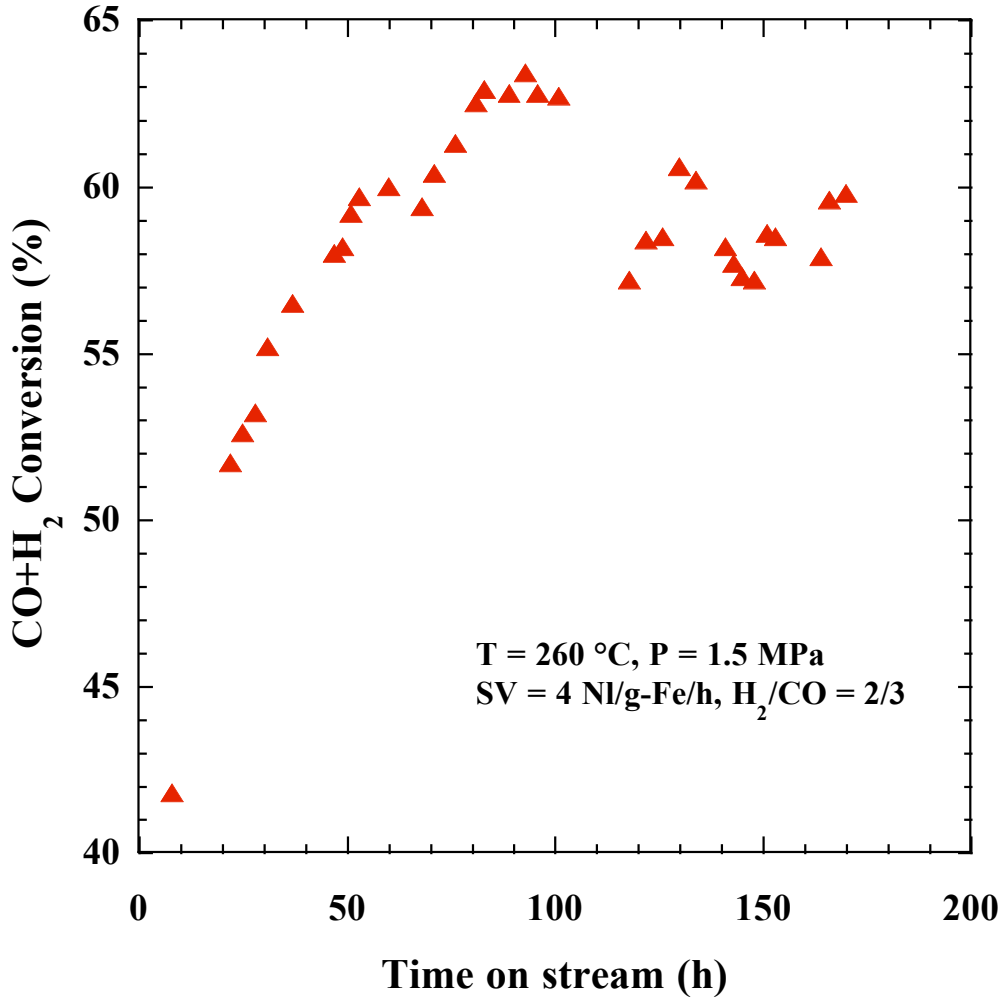

Figure 39. Change of syngas conversion with time of spray-dried DPS3616 catalyst during STSR test SB-28402.

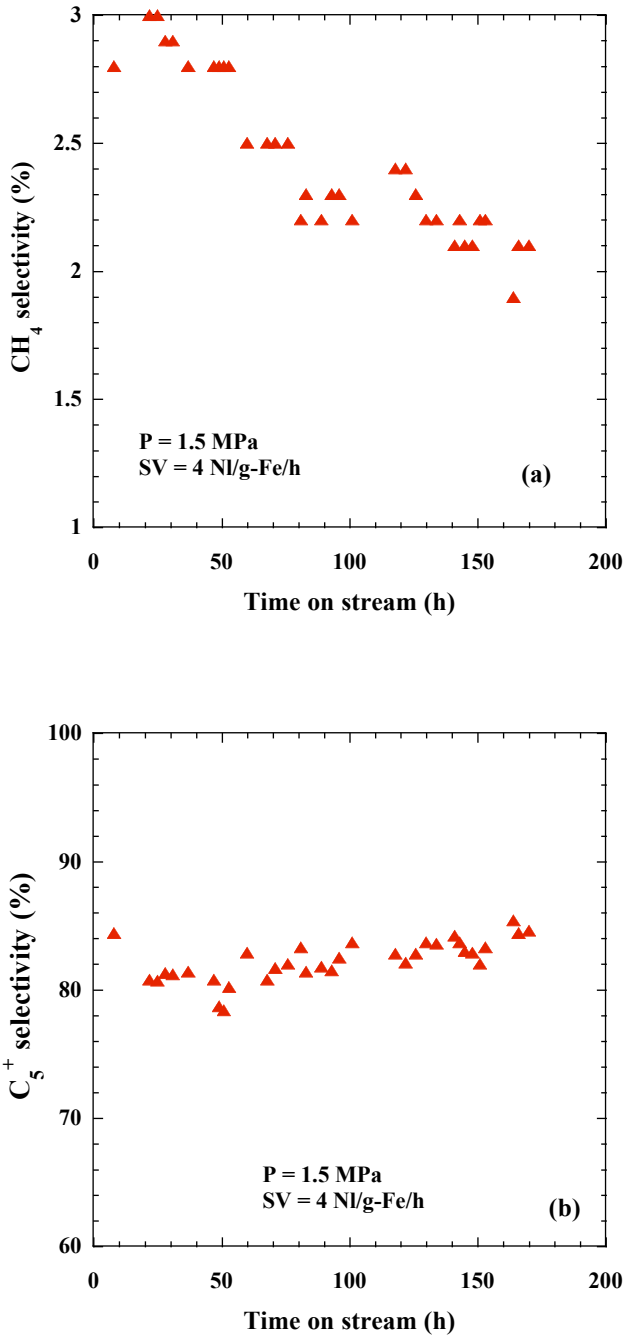

Figure 40. Methane selectivity (a) and C_5^+ selectivity (b) as a function of time in STSR test SB-24802 with spray-dried DPS3616 catalyst.

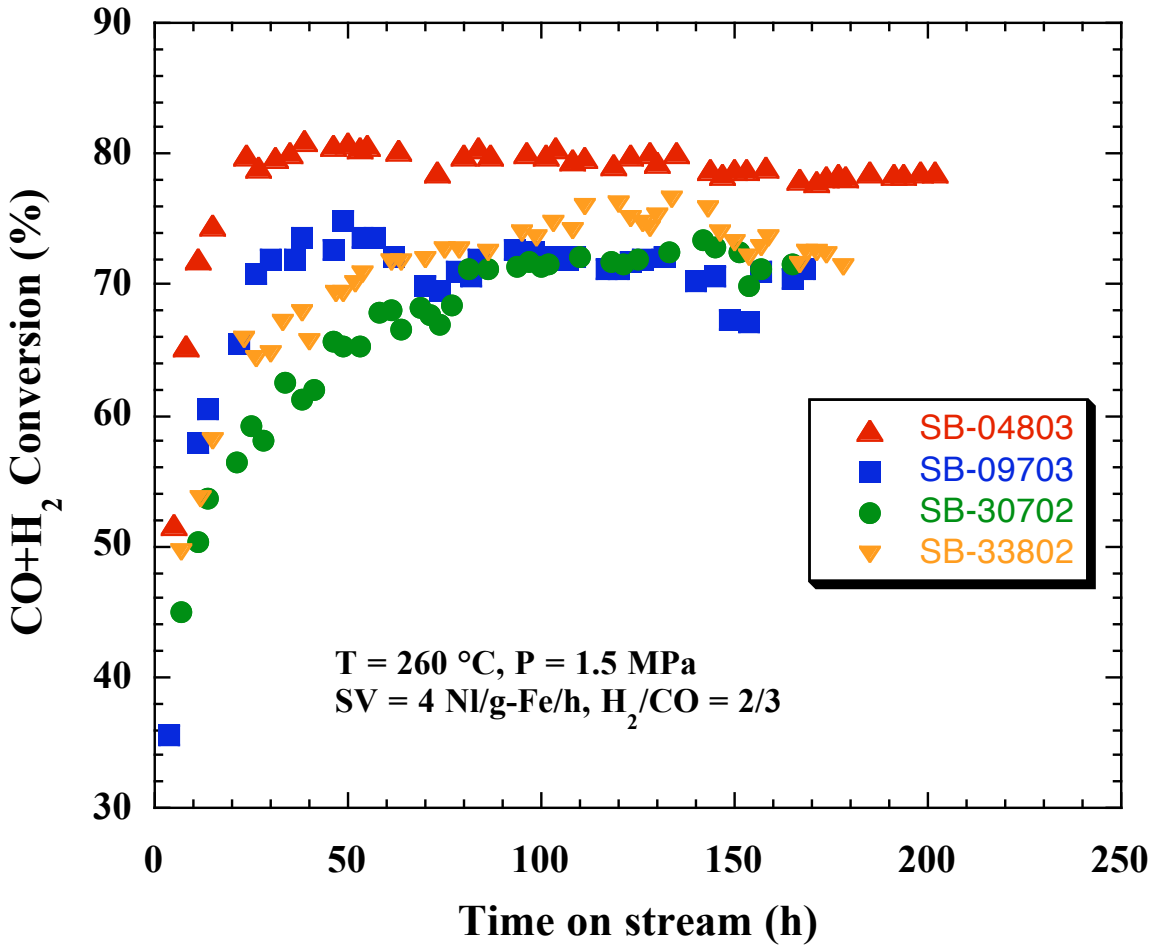

Figure 41. Changes in syngas conversion with time in STSR tests of spray-dried and precipitated Fe catalysts of the same nominal composition (100 Fe/3 Cu/5 K/16 SiO_2).

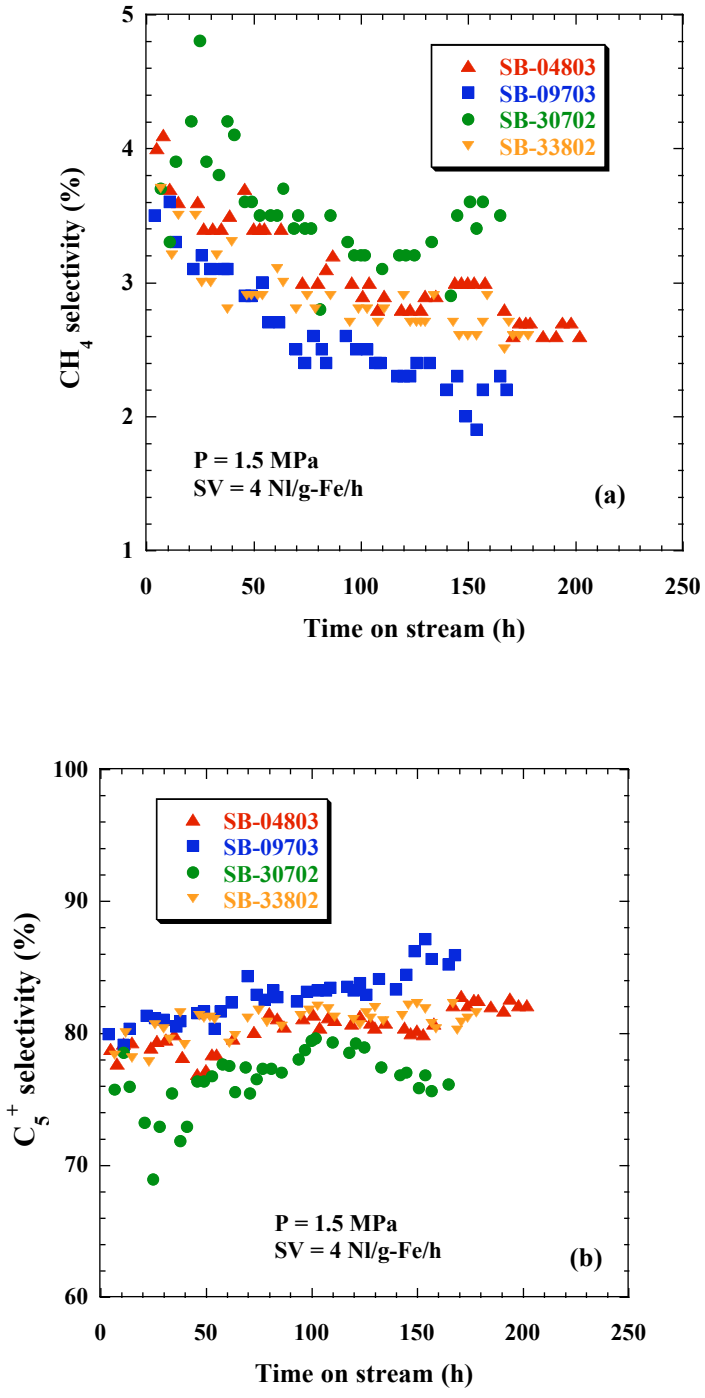

Figure 42. Changes in methane (a) and C_5^+ selectivity (b) with time in STSR tests of spray-dried and precipitated Fe catalysts of the same nominal composition (100 Fe/3 Cu/5 K/16 SiO_2).

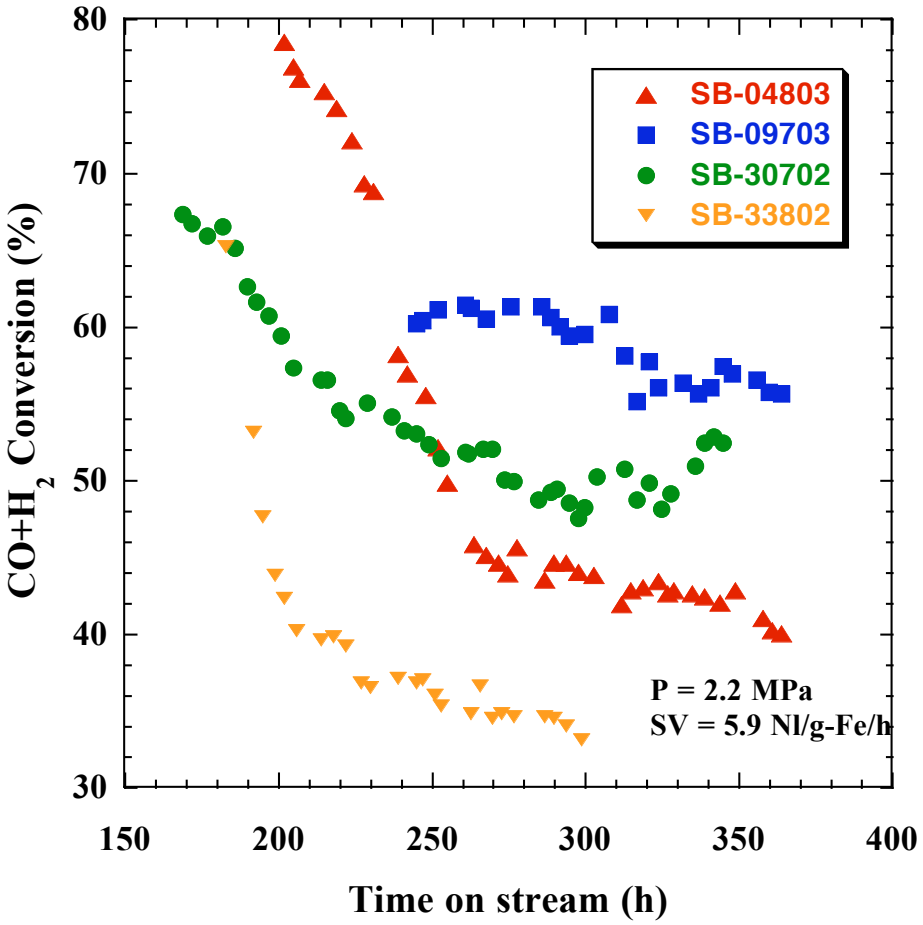

Figure 43. Changes in syngas conversion with time in STSR tests of spray-dried and precipitated Fe catalysts of the same nominal composition (100 Fe/3 Cu/5 K/16 SiO_2).

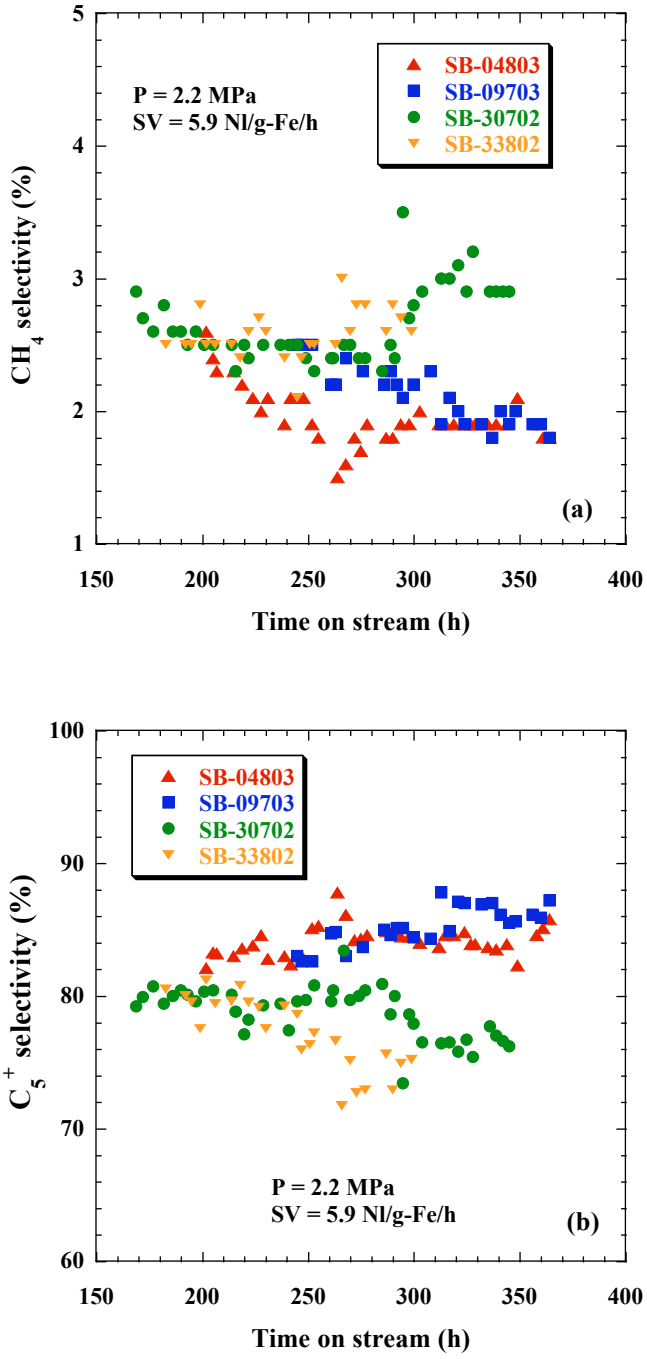

Figure 44. Changes in methane (a) and C_5^+ selectivity (b) with time in STSR tests of spray-dried and precipitated Fe catalysts of the same nominal composition (100 Fe/3 Cu/5 K/16 SiO_2).